Prepared in cooperation with the Department of Energy, National Nuclear Security Administration Nevada Site Office, Office of Environmental Management under Interagency Agreement, DE-NA0001654

Hydraulic Characterization of Volcanic Rocks in Pahute Mesa Using an Integrated Analysis of 16 Multiple-Well Aquifer Tests, Nevada National Security Site, 2009–14

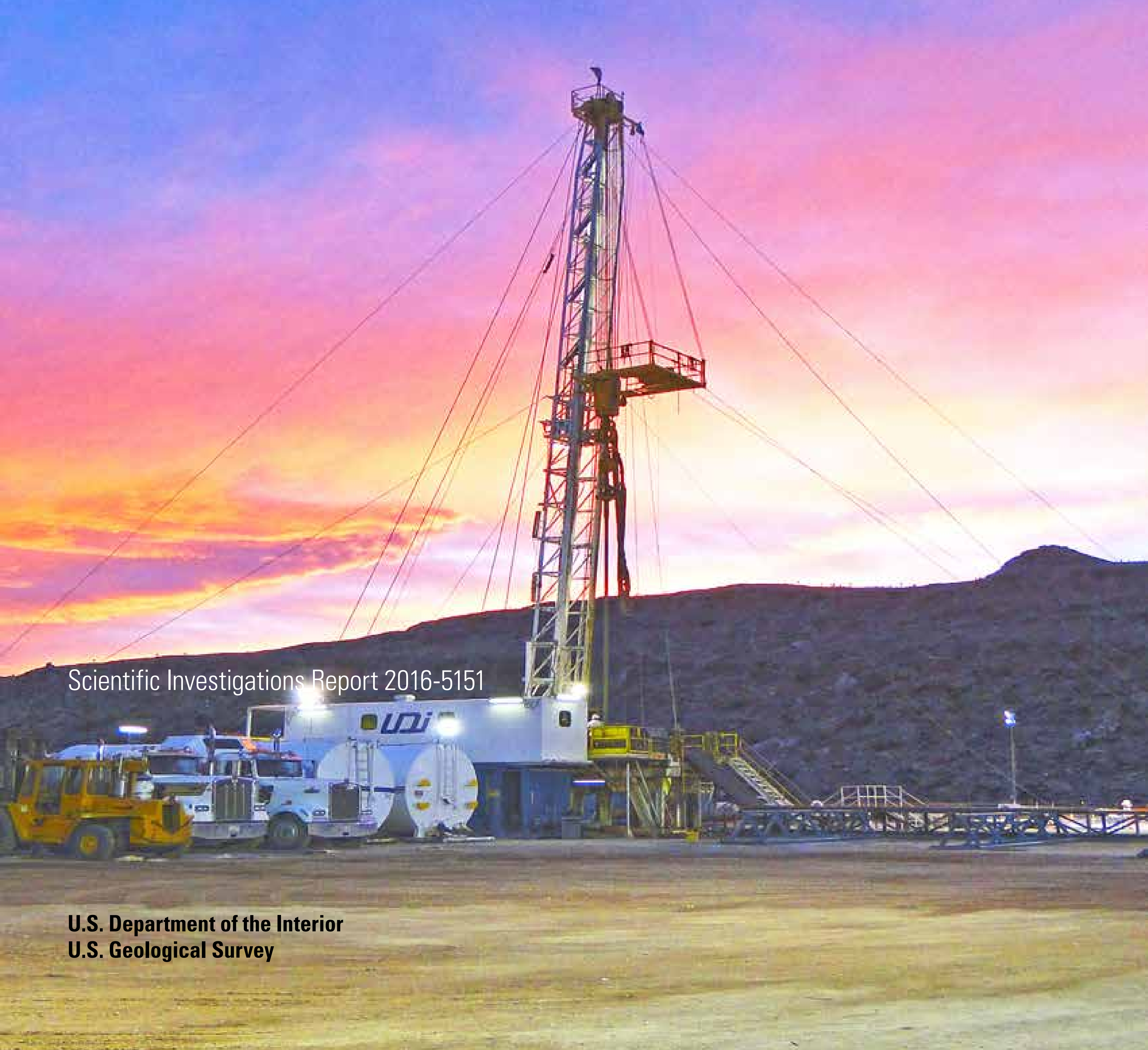

Scientific Investigations Report 2016-5151

U.S. Department of the Interior
U.S. Geological Survey

Cover photograph: Drill rig at the ER-EC-15 well site at Pahute Mesa, looking west, within 2 miles of the western Nevada National security Site and Area 20 boundary. Photograph by Robert B. Goodwin, Navarro, November 2010.

Hydraulic Characterization of Volcanic Rocks in Pahute Mesa Using an Integrated Analysis of 16 Multiple-Well Aquifer Tests, Nevada National Security Site, 2009–14

By C. Amanda Garcia, Tracie R. Jackson, Keith J. Halford, Donald S. Sweetkind, Nancy A. Damar, Joseph M. Fenelon, and Steven R. Reiner

Prepared in cooperation with the Department of Energy, National Nuclear Security Administration Nevada Site Office, Office of Environmental Management under Interagency Agreement, DE-NA0001654

Scientific Investigations Report 2016–5151

U.S. Department of the Interior
U.S. Geological Survey

U.S. Department of the Interior
SALLY JEWELL, Secretary

U.S. Geological Survey
Suzette M. Kimball, Director

U.S. Geological Survey, Reston, Virginia: 2017

For more information on the USGS—the Federal source for science about the Earth, its natural and living resources, natural hazards, and the environment—visit http://www.usgs.gov or call 1–888–ASK–USGS.

For an overview of USGS information products, including maps, imagery, and publications, visit http://store.usgs.gov/.

Suggested citation:
Garcia, C.A., Jackson, T.R., Halford, K.J., Sweetkind, D.S., Damar, N.A., Fenelon, J.M., and Reiner, S.R., 2017, Hydraulic characterization of volcanic rocks in Pahute Mesa using an Integrated Analysis of 16 multiple-well aquifer tests, Nevada National Security Site, 2009–14: U.S. Geological Survey Scientific Investigations Report 2016-5151, 62 p., *https://doi.org/10.3133/sir20165151*.

ISSN 2328-0328 (online)

Acknowledgments

This report was made possible by funding from the U.S. Department of Energy under Interagency Agreement DE-NA0001654 with the Department of Energy, National Nuclear Security Administration.

The authors gratefully acknowledge the U.S. Department of Energy (DOE), Navarro Nevada Environmental Services, LLC., Navarro-Intera, LLC, and Navarro for providing aquifer test data at pumping wells, long-term water-level monitoring data at observation and background wells, and the draft Phase II hydrostratigraphic framework model; Jeffery Wurtz and Daniel Neubauer of Navarro and Jeffery Sanchez of Navarro-Intera, LLC, for data collection and data processing; and Peter Martian of Navarro and Rishi Parashar of the Desert Research Institute for helpful review comments.

The authors also gratefully acknowledge Terry L. Miller, Glenn L. Locke, and Gary L. Otto, retired, for data collection and data processing and Shana L. Mashburn and Marshall W. Gannett, all of the U.S. Geological Survey, for helpful review comments.

Contents

Figures

Tables

Conversion Factors

U.S. customary units to International System of Units

Multiply	By	To obtain
	Length	
inch (in.)	2.54	centimeter (cm)
foot (ft)	0.3048	meter (m)
mile (mi)	1.6093	kilometer (km)
	Area	
square foot (ft^2)	0.0929	square meter (m^2)
square mile (mi^2)	2.59	square kilometer (km^2)
	Volume	
gallon (gal)	3.7854	liter (L)
million gallons (Mgal)	3.7854	million liters (ML)
cubic mile (mi^3)	4.168	cubic kilometer (km^3)
	Flow rate	
gallon per minute (gal/min)	0.2642	liter per minute (L/min)
	Hydraulic conductivity or transmissivity	
foot per day (ft/d)	0.0000035	meter per second (m/s)
foot per day (ft/d)	0.3048	meter per day (m/d)
foot squared per day (ft^2/d)	0.00000011	meter squared per second (m^2/s)

Temperature in degrees Celsius (°C) may be converted to degrees Fahrenheit (°F) as follows:

$$°F = (1.8 \times °C) + 32$$

Temperature in degrees Fahrenheit (°F) may be converted to degrees Celsius (°C) as follows:

$$°C = (°F - 32) / 1.8$$

Datums

Vertical coordinate information is referenced to the National Geodetic Vertical Datum of 1929 (NGVD 29).

Horizontal coordinate information is referenced to the North American Datum of 1983 (NAD 83).

Elevation, as used in this report, refers to distance above the vertical datum.

Supplemental Information

*Transmissivity: The standard unit for transmissivity is cubic foot per day per square foot times foot of aquifer thickness [(ft^3/d)/ft^2)*ft]. In this report, the mathematically reduced form, foot squared per day (ft^2/d), is used for convenience.

Abbreviations

3D HFM	three-dimensional hydrostratigraphic framework model
ATWTA	Ammonia Tanks welded-tuff aquifer
BA	Benham aquifer
CHLFA	Calico Hills lava-flow aquifer
CHZCM	Calico Hills zeolitic composite unit
DOE	U.S. Department of Energy
FCCM	Fortymile Canyon composite unit
FCCU	Fluorspar Canyon confining unit
FCULFA	Fortymile Canyon upper lava-flow aquifer
HFM	hydrostratigraphic framework model
HSU	hydrostratigraphic unit
LPCU	Lower Paintbrush confining unit
mCCU	modified clastic confining unit
mCFCM	modified Crater Flat composite unit
mCHLFA5	modified Calico Hills lava-flow aquifer 5
mCPA	modified Comb Peak aquifer
mFCCM1	modified Fortymile Canyon composite unit 1
mFCCM2	modified Fortymile Canyon composite unit 2
mFCCM3	modified Fortymile Canyon composite unit 3
mFCCU3	modified Fortymile Canyon confining unit 3
mHSU	modified hydrostratigraphic unit
mICU	modified intrusive confining unit
MNW	multi-node well
mRMCM	modified Rainier Mesa composite unit
mRMWTA1	modified Rainier Mesa welded-tuff aquifer 1
mRMWTA2	modified Rainier Mesa welded-tuff aquifer 2
mTCA	modified Tiva Canyon aquifer
mUPCU	modified Upper Paintbrush confining unit
NNSS	Nevada National Security Site
NTMMSZ	Northern Timber Mountain moat structural zone
PEST	Parameter ESTimation
RMS	root-mean square
RMWTA	Rainier Mesa welded-tuff aquifer
SCCC	Silent Canyon caldera complex
SPA	Scrugham Peak aquifer
SWNVF	southwestern Nevada volcanic field
TCA	Tiva Canyon aquifer
TCVA	Thirsty Canyon volcanic aquifer
THCM	Tannenbaum Hill composite unit
TMCC	Timber Mountain caldera complex
TMCCSM	Timber Mountain caldera complex structural margin
TMWTA	Timber Mountain welded-tuff aquifer
TSA	Topopah Spring aquifer
USGS	U.S. Geological Survey

Hydraulic Characterization of Volcanic Rocks in Pahute Mesa Using an Integrated Analysis of 16 Multiple-Well Aquifer Tests, Nevada National Security Site, 2009–14

By C. Amanda Garcia, Tracie R. Jackson, Keith J. Halford, Donald S. Sweetkind, Nancy A. Damar, Joseph M. Fenelon, and Steven R. Reiner

Abstract

An improved understanding of groundwater flow and radionuclide migration downgradient from underground nuclear-testing areas at Pahute Mesa, Nevada National Security Site, requires accurate subsurface hydraulic characterization. To improve conceptual models of flow and transport in the complex hydrogeologic system beneath Pahute Mesa, the U.S. Geological Survey characterized bulk hydraulic properties of volcanic rocks using an integrated analysis of 16 multiple-well aquifer tests. Single-well aquifer-test analyses provided transmissivity estimates at pumped wells. Transmissivity estimates ranged from less than 1 to about 100,000 square feet per day in Pahute Mesa and the vicinity. Drawdown from multiple-well aquifer testing was estimated and distinguished from natural fluctuations in more than 200 pumping and observation wells using analytical water-level models. Drawdown was detected at distances greater than 3 miles from pumping wells and propagated across hydrostratigraphic units and major structures, indicating that neither faults nor structural blocks noticeably impede or divert groundwater flow in the study area.

Consistent hydraulic properties were estimated by simultaneously interpreting drawdown from the 16 multiple-well aquifer tests with an integrated groundwater-flow model composed of 11 well-site models—1 for each aquifer test site. Hydraulic properties were distributed across volcanic rocks with the Phase II Pahute Mesa-Oasis Valley Hydrostratigraphic Framework Model. Estimated hydraulic-conductivity distributions spanned more than two orders of magnitude in hydrostratigraphic units. Overlapping hydraulic conductivity ranges among units indicated that most Phase II Hydrostratigraphic Framework Model units were not hydraulically distinct. Simulated total transmissivity ranged from 1,600 to 68,000 square feet per day for all pumping wells analyzed. High-transmissivity zones exceeding 10,000 square feet per day exist near caldera margins and extend along the northern and eastern Pahute Mesa study area and near the southwestern edge of the study area. The estimated hydraulic-property distributions and observed hydraulic connections among geologic structures improved the characterization and representation of groundwater flow at Pahute Mesa.

Introduction

Accurate characterization of groundwater flow is critical to predicting radionuclide transport. Of the high-yield nuclear devices tested at the Nevada National Security Site, 85 were detonated on the eastern side of Pahute Mesa, and most were detonated near or in volcanic rock aquifers (Laczniak and others, 1996; U.S. Department of Energy, 1997; Pawloski and others, 2001; Wolfsberg and others, 2002; Fenelon and others, 2010). The rate and direction of contaminant transport beyond the immediate zone affected by nuclear tests is controlled by the hydraulic properties of hydrostratigraphic units and the hydraulic connections across hydrostratigraphic units and structural features. At Pahute Mesa (fig. 1), faults divide complexly layered volcanic aquifers and confining units into distinct structural blocks (Warren and others, 2000), but the degree of hydraulic connection in aquifers and across these features is poorly understood because limited subsurface geologic and hydraulic data exist.

Hydraulic testing and characterization of hydrostratigraphic units and structures to evaluate groundwater flow and radionuclide transport at Pahute Mesa have been ongoing since the early 1960s (Blankennagel and Weir, 1973). Preliminary (Phase I) hydraulic characterization of Pahute Mesa focused on accurately simulating groundwater movement and radionuclide transport from underground-test cavities (Stoller-Navarro Joint Venture, 2009). Although several studies provided hydraulic-property estimates of volcanic rocks (Winograd and others, 1971; Blankennagel and Weir, 1973), the dataset used in Phase I simulations was spatially limited compared to the areal extent of Pahute Mesa.

Uncertainty from limited hydraulic- and transport-property estimates severely limited the utility of Phase I groundwater-flow and radionuclide-transport simulations in Pahute Mesa (Stoller-Navarro Joint Venture, 2009). Preliminary simulations indicated hydraulic properties, such as transmissivity and hydraulic conductivity, and contaminant-transport boundary forecasts were uncertain because predicted radionuclide migration extended far beyond documented contaminated areas (Stoller-Navarro Joint Venture, 2009; U.S. Department of Energy, 2009). Inaccurate simulation of preferential

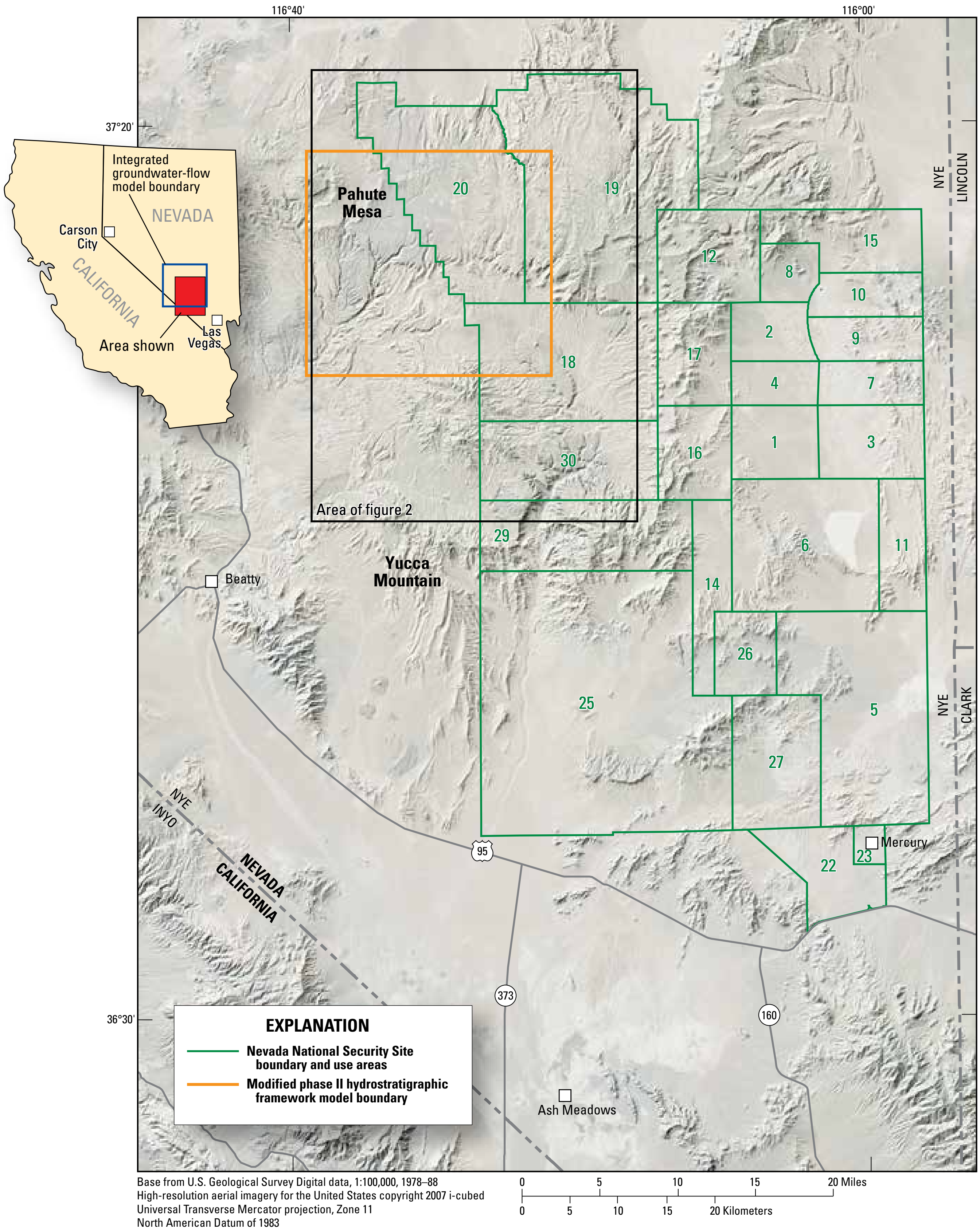

Figure 1. Pahute Mesa and model boundaries in the area of the Nevada National Security Site.

migration pathways highlighted the need for additional data collection and led to the initiation of subsequent, Phase II studies. One objective of Phase II studies is to improve conceptualization of transmissive flow paths in the complex hydrogeologic system by performing and analyzing aquifer tests (U.S. Department of Energy, 2009). During 2009–2014, Navarro-Intera, LLC, did 16 aquifer tests at Pahute Mesa, most of which induced pumping responses at multiple observation wells, more than a mile (mi) from pumping wells.

Aquifer testing provides the most integrated assessment of hydraulic connectivity in complex geologic systems (Yobbi and Halford, 2008). The aquifer volume investigated increases with the distance between the pumping well and observation wells where drawdown is detected. Drawdown detection across structural blocks provides direct evidence of hydraulic connections between structural features and aquifers. At Pahute Mesa, drawdown detection was limited by environmental water-level fluctuations that frequently exceeded the pumping signal (Risser and Bird, 2003; Halford, 2006).

Aquifer-test data from complexly layered aquifers and confining units frequently are interpreted using numerical models to evaluate hydraulic properties of the groundwater-flow system. Numerical simulations that combine observed drawdowns from aquifer testing with knowledge of the hydrogeologic framework provide a more accurate characterization of complex groundwater systems than analytical models alone (Walton, 2008; Yobbi and Halford, 2008). The flexibility of numerical models allows for hydraulic characterization of hydrostratigraphic units and structural features and for evaluation of structural effects on drawdown behavior (Renard, 2005).

Simultaneous interpretation of multiple aquifer tests provides a consistent set of hydraulic-property estimates for areas that overlap. Drawdowns from multiple aquifer tests at Pahute Mesa propagated through the same hydrostratigraphic units and structures. Hydraulic-property estimates of hydrostratigraphic units and structures are inconsistent when each aquifer test is analyzed independently. A comprehensive, integrated numerical analysis was warranted because hydraulic properties of these units and structures affect groundwater-flow conceptualization at Pahute Mesa.

Purpose and Scope

The purpose of this report is to document the integrated analysis of 16 multiple-well aquifer tests to estimate hydraulic properties of volcanic rocks in Pahute Mesa. The primary purpose of this analysis was to estimate the total transmissivity around each pumping well for the U.S. Department of Energy. Transmissivity and storage-property estimates for the volcanic rocks at Pahute Mesa are needed to constrain hydraulic properties used in groundwater-flow and contaminant transport models for the U.S. Department of Energy, Nevada National Security Site.

A cumulative volume of 63 million gallons was pumped and water-level changes were observed in 34 wells during these aquifer tests. Drawdowns were distinguished from environmental water-level fluctuations by interpreting water-level responses in pumping and observation wells using analytical models, so that hydraulic properties could be estimated. Drawdown estimates from measured water levels, referred to as “drawdown observations,” and the methods used to analyze single- and multiple-well aquifer tests and pumping-related discharge data are provided in this report. Drawdown observation and pumping datasets are available as an online data release at *https://doi.org/10.5066/F7Z60M6H*. Well construction data also are provided in this report.

Hydraulic properties, including hydraulic conductivity, specific yield, and specific storage, were estimated by fitting simulated drawdowns to observed drawdowns using numerical groundwater-flow models. To simulate drawdown responses to pumping during the 16 multiple-well aquifer tests, 11 groundwater-flow models were developed, where aquifer testing at each well site was simulated by at least one model. The groundwater-flow models used a single hydrostratigraphic framework model to estimate hydraulic properties in the hydrostratigraphic units. Groundwater-flow models were integrated to simultaneously interpret multiple aquifer tests that affect overlapping volumes of aquifer. Groundwater-flow model integration comprised simultaneous calibration of all models to a single set of parameters using Parameter ESTimation (PEST; Doherty, 2016). The integrated groundwater-flow model, hydrostratigraphic framework model, and supporting documentation are available as an online data release at *https://doi.org/10.5066/F76H4FJQ*.

Description of Study Area

Pahute Mesa is a 200-square-mile (mi^2) elevated plateau in the northwestern part of the Nevada National Security Site (NNSS), about 130 mi northwest of Las Vegas, Nevada (fig. 1). The plateau elevation slopes from about 5,500 to 7,000 feet (ft) from the western to the eastern margin, respectively (Laczniak and others, 1996). Pahute Mesa has an average annual precipitation rate of 8 inches (1964–2011, National Oceanic and Atmospheric Administration, 2015). Depth to water in the Pahute Mesa study area (fig. 2) increased from the southwest to the northeast and ranged from about 300 to more than 2,000 ft below land surface (Fenelon and others, 2010). The elevation of groundwater levels ranged from 4,100 ft in the central and southern parts of the Pahute Mesa study area to 4,700 ft in the northern and eastern parts; therefore, groundwater generally flows south-southwestward. Groundwater from Pahute Mesa discharges to Oasis Valley, near Beatty, Nevada (Fenelon and others, 2010).

Hydrogeology

The multiple-well aquifer-test study area lies in the southwestern Nevada volcanic field (SWNVF; Byers and others, 1989), which is dominated by a series of nested calderas that erupted episodically from about 15.1 to 7.5 million years ago (Byers and others, 1976b; Carr and others, 1986; Sawyer and others, 1994). The volcanic rocks of the SWNVF include voluminous, regionally extensive, silicic, ash-flow tuffs formed during caldera-forming eruptions; thick sequences of welded tuff that ponded in the calderas; small-volume pyroclastic deposits and silicic to mafic lava flows erupted from many small volcanic vents; fallout tephra deposits; and minor redeposited tuffaceous and epiclastic rocks (Byers and others, 1976b; Carr and others, 1986; Byers and others, 1989; Ferguson and others, 1994; Sawyer and others, 1994).

The Pahute Mesa volcanic plateau is capped by some of the youngest ash-flow tuffs in the SWNVF, which bury much of the older volcanic stratigraphy and structure (Sawyer and Sargent, 1989; Ferguson and others, 1994). Knowledge of older volcanic stratigraphic units was derived from numerous boreholes constructed during nuclear testing and post testing (Wood, 2009; Pawloski and others, 2010). The deepest borehole on Pahute Mesa (*UE-20f*; fig. 2) penetrates 13,686 ft of caldera-filling volcanic rock without encountering subvolcanic bedrock (Wood, 2009). Other deep boreholes at Pahute Mesa that bottom in volcanic rocks were inferred to penetrate about half of the total thickness of volcanic rocks that fill the depression, as defined by gravity studies (Mankinen and others, 1999; McKee and others, 2001).

The wells monitored during multiple-well aquifer testing were completed in Tertiary volcanic rocks that underlie Pahute Mesa, including, from old to young, the Belted Range Group, the Crater Flat Group, the Calico Hills Formation, the Paintbrush Group, the Timber Mountain Group, the volcanics of Fortymile Wash, and the Thirsty Canyon Group (nomenclature and ages from Sawyer and others, 1994; fig. 3). These units compose most of the surface and subsurface volcanic deposits of the SWNVF in the area of Pahute Mesa and include all of the major volcanic aquifers.

Calderas and Structural Setting

Pahute Mesa overlies the Silent Canyon caldera complex (SCCC), which consists of two overlapping buried calderas (fig. 2): the Grouse Canyon caldera, associated with the eruption of the Belted Range Group, and the Area 20 caldera, associated with the eruption of the Crater Flat Group (Sawyer and Sargent, 1989; Ferguson and others, 1994; Sawyer and others, 1994). Both calderas are partly filled by syn-caldera tuff and lava of the Belted Range and Crater Flat Groups and post-caldera tuff and lava of the Calico Hills Formation (figs. 4, 5; Ferguson and others, 1994). The upper one-third of the volcanic rocks in the SCCC are ash-flow sheets and lavas that have sources to the south or west of Pahute Mesa, including rocks of the Paintbrush Group, which erupted from the Claim Canyon caldera (fig. 3; Ferguson and others, 1994; Sawyer and others, 1994) and from localized vents north of Yucca Mountain (Day and others, 1998; Dickerson and Drake, 1998) and Pahute Mesa (Prothro and Drellack, 1997). Successively younger volcanic units in this upper volcanic section become progressively thinner and more constant in thickness as they filled, and ultimately buried, the early caldera-related volcanic depressions (figs. 4, 5; McKee and others, 2001; Bechtel Nevada, 2002).

The Timber Mountain caldera complex (TMCC), south of Pahute Mesa, consists of two nested calderas; the Rainier Mesa caldera, associated with the eruption of the Rainier Mesa Tuff, and the Ammonia Tanks caldera, associated with the eruption of the Ammonia Tanks Tuff (figs. 2, 3; Byers and others, 1976a, b; Sawyer and others, 1994). Unlike the SCCC, the TMCC is not buried by younger volcanic units. Instead, primary caldera-related features are topographically expressed, including more than half the circumference of the caldera topographic margin and a central resurgent dome (Byers and others, 1976a; Slate and others, 1999). The two nested calderas of the TMCC have largely coincident structural margins on their north and south sides (Slate and others, 1999; Bechtel Nevada, 2002). Wells drilled in the TMCC penetrate either partly to densely welded Rainier Mesa or Ammonia Tanks Tuff, several times thicker than equivalent rocks outside the caldera (U.S. Department of Energy, 2002a–d, f–g; 2013), or thick sections of highly heterogeneous caldera megabreccia and variably welded ash-flow tuff (Wood, 2009). The youngest volcanic units at Pahute Mesa are ash-flow tuffs of the Thirsty Canyon Group erupted from the Black Mountain caldera (fig. 3; Vogel and others, 1989; Sawyer and others, 1994; Slate and others, 1999).

Warren and others (2000) subdivided Pahute Mesa and the surrounding region into numerous structural blocks defined by north-striking normal faults and buried, west-northwest trending structural zones (fig. 2). The structural blocks have distinct stratigraphic and structural character, based on changes in elevation, dip, or thickness of volcanic units, as defined by borehole data (Warren and others, 2000).

The study area comprises buried caldera margins of the SCCC and the TMCC (fig. 2). Geophysical evidence indicates that a deeply buried, structural ridge of nonvolcanic bedrock, designated the northwestern Timber Mountain Bench (Warren and others, 2000), separates the two caldera complexes (Grauch and others, 1999; Mankinen and others, 1999). The northwestern Timber Mountain Bench, referred to as the “bench,” appears to have been a structural high during eruption of Rainier Mesa Tuff, but was subsequently downdropped by more than 1,000 ft to the southwest by offset on the northern Timber Mountain moat structural zone (NTMMSZ), creating a structural trough that controlled the deposition of the thick, post-Rainier Mesa Tuff rhyolite of Tannenbaum Hill (fig. 5; U.S. Department of Energy, 2000).

Major northwest- to northeast-striking, steeply west-dipping, normal faults disrupt the volcanic-rock section in the multiple-well aquifer-test study area (figs. 2, 4). Many of these faults are identified on surface geologic maps (Orkild and others, 1969; Slate and others, 1999), but some, such as the *ER-20-7* fault (fig. 2), are known only through drilling (U.S. Department of Energy, 2010a). Stratigraphic data from boreholes on Pahute Mesa provided some checks on structural extents and displacements along the faults. In general, the volcanic section dips eastward into the westward-dipping normal

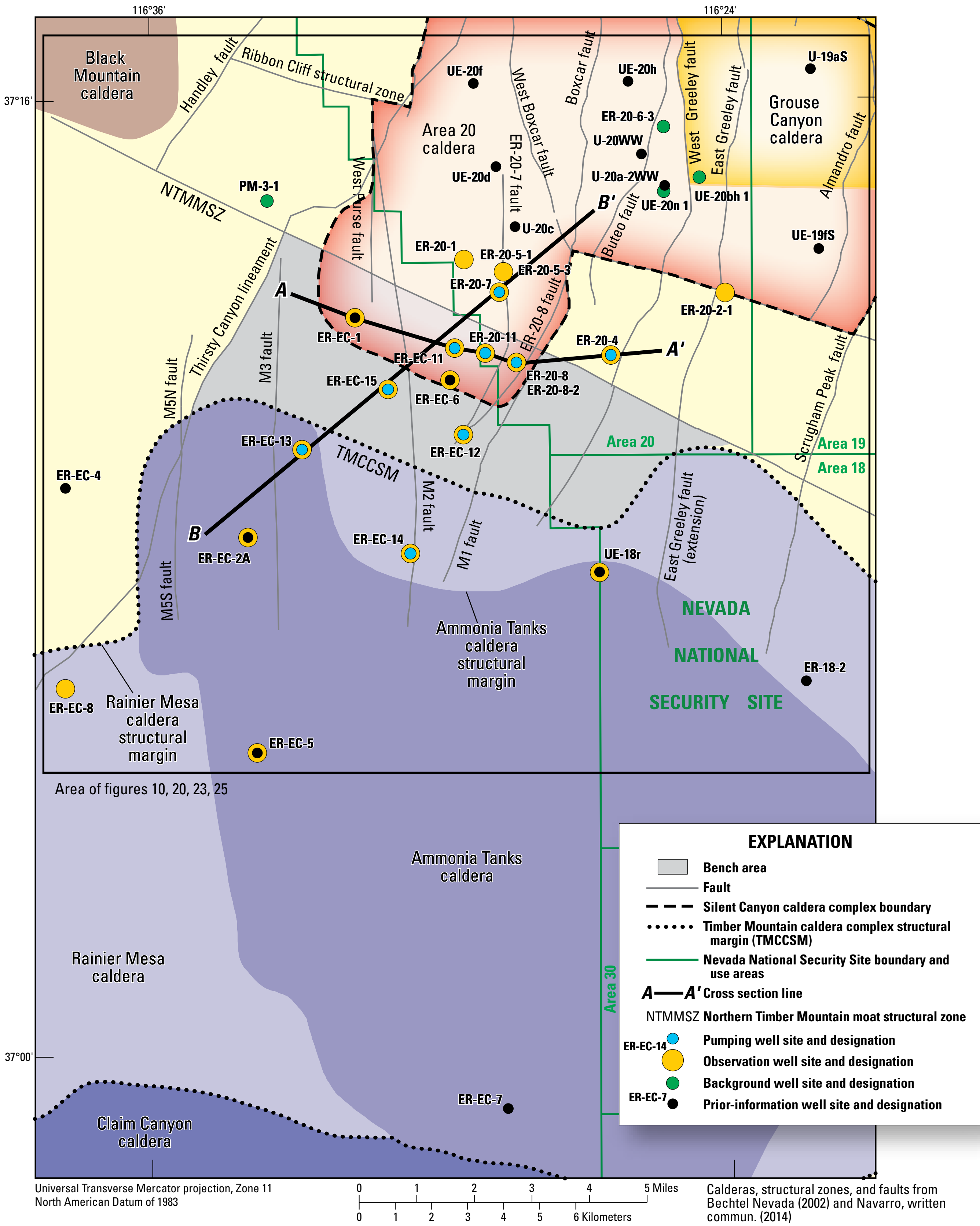

Figure 2. Pahute Mesa study area, including geologic structures, calderas, cross-section traces, and well sites associated with multiple-well aquifer tests, 2009–14.

Group[1]	Age[1] (millions of years)	Volcanic center[1]	HSU[2]	HSU thickness[3] (feet)	Hydrostratigraphic unit (HSU) name[2]
			AA	328	Alluvial aquifer
			YVCU	984	Younger volcanic confining unit
Thirsty Canyon Group	9.4–9.15	Black Mountain caldera	TCVA	6,890	Thirsty Canyon volcanic aquifer
Volcanics of Fortymile Wash	11.45–10.3	Diverse vent areas	FCCM	4,757	Fortymile Canyon composite unit
			FCULFA 1–7	820–1,640	Fortymile Canyon upper lava-flow aquifers 1–7
			FCWTA	1,148	Fortymile Canyon welded-tuff aquifer
			FCLLFA	164	Fortymile Canyon lower lava-flow aquifer
			BWWTA	492	Beatty Wash welded-tuff aquifer
			BWCU	984	Beatty Wash confining unit
Timber Mountain Group	11.6–11.45	Timber Mountain caldera complex	ATWTA	820	Ammonia Tanks welded-tuff aquifer
			ATCCU	1,312	Ammonia Tanks caldera confining unit
			TMUWTA	4,757	Timber Mountain upper welded-tuff aquifer
			THLFA	1,476	Tannenbaum Hill lava-flow aquifer
			THCM	1,312	Tannenbaum Hill composite unit
			THCU	1,312	Tannenbaum Hill confining unit
			TMWTA	1,312	Timber Mountain welded-tuff aquifer
			TMLVTA	1,148	Timber Mountain lower vitric-tuff aquifer
			RMWTA	5,249	Rainier Mesa welded-tuff aquifer
			FCCU	984	Fluorspar Canyon confining unit
			WWA	820	Windy Wash aquifer
Paintbrush Group		Claim Canyon caldera and local vents	CPA	656	Comb Peak aquifer
			PBPCU	656	Post-Benham Paintbrush confining unit
			BA	1,312	Benham aquifer
			UPCU	820	Upper Paintbrush confining unit
			SPA	492	Scrugham Peak aquifer
			MPCU	328	Middle Paintbrush confining unit
	12.7		TCA	820	Tiva Canyon aquifer
			PVTA	492	Paintbrush vitric-tuff aquifer
			LPCU	984	Lower Paintbrush confining unit
			PLFA	1,640	Paintbrush lava-flow aquifer
	12.8		TSA	656	Topopah Spring aquifer
Calico Hills Formation	12.9	Local vents	CHVTA	1,969	Calico Hills vitric-tuff aquifer
			CHZCM	3,937	Calico Hills zeolitic composite unit
			CHLFA 1–5	164–2,297	Calico Hills lava-flow aquifers 1–5
Crater Flat Group	13.5–13.1	Area 20 caldera	IA	1,640	Inlet aquifer
			CFCM	1,476	Crater Flat composite unit
			CFCU	1,312	Crater Flat confining unit
			BFCU	2,789	Bullfrog confining unit
Belted Range Group	13.85–13.5	Grouse Canyon caldera	BRA	3,445	Belted Range aquifer
Pre-Belted Range Group volcanic rocks			PBRCM	5,906	Pre-Belted Range composite unit
			SCVCU	2,625	Silent Canyon volcanic confining unit
Pre-volcanic rocks			LCCU1	656	Lower clastic confining unit, thrusted
			UCCU	2,461	Upper clastic confining unit
			LCA	4,265	Lower carbonate aquifer
Caldera-related intrusive rocks			BMICU	164	Black Mountain intrusive confining unit
			RMICU	2,297	Rainier Mesa intrusive confining unit
			ATICU	2,953	Ammonia Tanks intrusive confining unit

[1] Stratigraphic assignment, age, and inferred volcanic source area after Sawyer and others (1994).
[2] Hydrostratigraphic unit names and abbreviations after Prothro and others (2009).
[3] Thickness based on HSUs vertically sampled at a 164-feet (50-meter) interval.

Figure 3. Section showing ages of major volcanic groups, associated caldera or volcanic center, and hydrostratigraphic unit names and abbreviations, Pahute Mesa, Nevada National Security Site and vicinity.

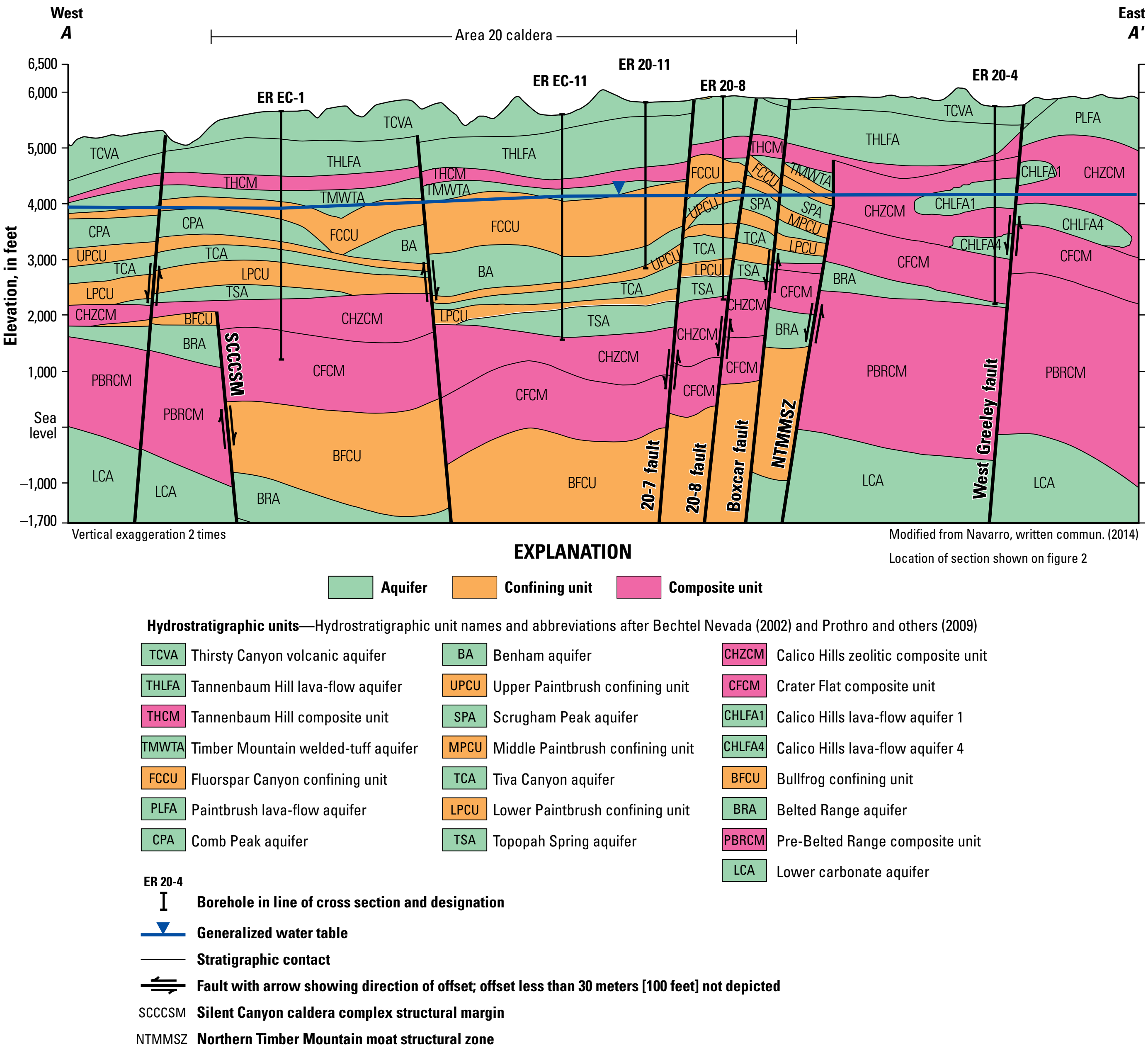

Figure 4. West-east geologic cross section across the Silent Canyon caldera complex, showing calderas, faults, hydrostratigraphic units, and key boreholes, Pahute Mesa, Nevada National Security Site and vicinity.

faults; in places, the volcanic-rock section also has a strong northward component of dip (fig. 5).

Hydrostratigraphy

Stratigraphic units at the NNSS and Pahute Mesa have been subdivided into hydrostratigraphic units using a geology-based approach based on physical differences in rock type and the inferred potential of the rock unit to transmit groundwater (Bechtel Nevada, 2002; Prothro and others, 2009). Hydraulic properties of volcanic deposits depend mostly on the mode of eruption and cooling, on the extent of primary and secondary fracturing, and on the degree to which secondary alteration (crystallization of volcanic glass and zeolitic alteration) has affected primary permeability (Blankennagel and Weir, 1973; Laczniak and others, 1996; Prothro and others, 2009).

On the basis of physical properties, volcanic rock units are designated as aquifers, confining units, or composite units, which may contain a mixture of aquifers and confining units (fig. 3; Bechtel Nevada, 2002; Prothro and others, 2009; Fenelon and others, 2010). Densely welded parts of outflow-tuff sheets typically have well-connected fracture networks and minimal secondary alteration and compose many of the volcanic aquifers at the NNSS (Blankennagel and Weir, 1973; Laczniak and others, 1996; Prothro and others, 2009).

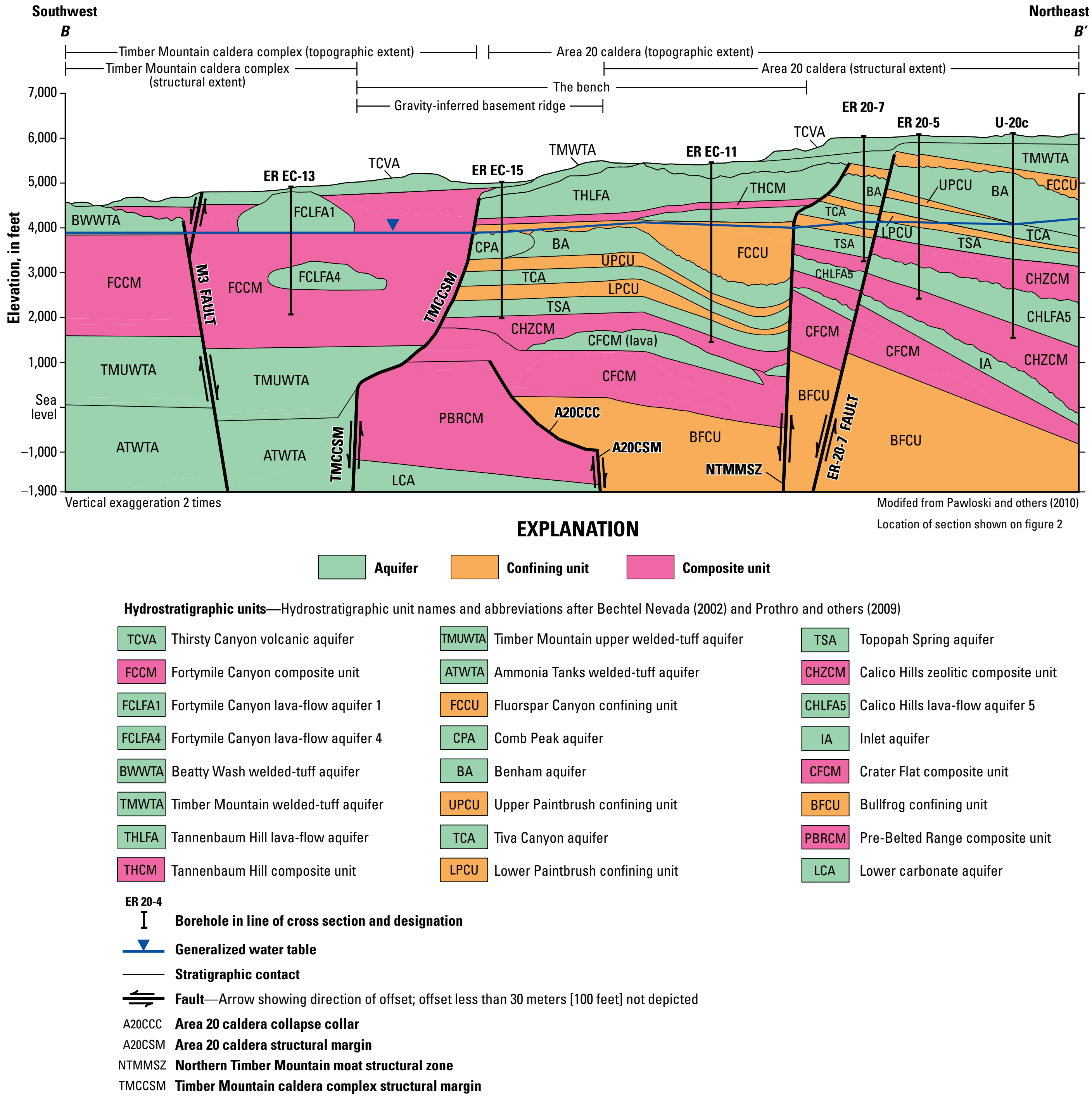

Figure 5. Southwest-northeast cross section across the bench area showing caldera complexes, the bench area, hydrostratigraphic units, and key boreholes.

Rhyolite lava flows with fracture-related secondary permeability and vitric ash-fall tuffs with considerable primary porosity and permeability also are designated as volcanic aquifers (Prothro and Drellack, 1997; Bechtel Nevada, 2002). These units are relatively restricted spatially, but rhyolitic lava flows in the Paintbrush Group form the major volcanic-rock aquifers at Pahute Mesa (fig. 3; Blankennagel and Weir, 1973; Prothro and others, 2009). Air-fall tuff and non-welded or partly welded tuff are designated as confining units where porosity is occluded as a result of zeolitic alteration of rock-forming minerals and glass to zeolite, clay, carbonate, silica, and other minerals in the older, deeper parts of the volcanic section (Laczniak and others, 1996; Prothro and others, 2009). Thick sequences of intracaldera volcanic rocks possess more complex welding zonation, greater lithologic diversity, and a greater degree of secondary alteration than equivalent outflow tuff (Blankennagel and Weir, 1973) and are classified hydrogeologically as volcanic composite units (fig. 3; Bechtel Nevada, 2002; Prothro and others, 2009; Fenelon and others, 2010). At Pahute Mesa, rocks of the volcanics of Fortymile Wash and the Calico Hills Formation (fig. 3) feature multiple rhyolite lava flows interbedded with non-welded tuff, forming a complex package of alternating volcanic aquifers and confining units; where hydraulic data were insufficient or the geology is highly variable, these complex packages were defined as a volcanic composite unit (Prothro and others, 2009; Fenelon and others, 2010).

Hydrostratigraphic Framework Models at Pahute Mesa

Geologic variations in the Pahute Mesa area create a complex hydrostratigraphic framework consisting of interbedded aquifers and confining units with offsets caused by normal faults, buried structural zones, and caldera margins (Laczniak and others, 1996; Warren and others, 2000). The distribution and thickness of the hydrostratigraphic units and their relation to the geologic structure were defined with a digital, three-dimensional hydrostratigraphic framework model (3D HFM) of the Pahute Mesa-Oasis Valley area, as part of the U.S. Department of Energy's Underground Test Area Project (Bechtel Nevada, 2002). The digital 3D HFM of the Pahute Mesa-Oasis Valley area, which is more than 2,700 square kilometers (km^2), depicts the thickness, extent, and geometric relationships of subsurface hydrostratigraphic units and the major structural features. The structural block model conceptualization of Warren and others (2000) was incorporated into the 3D HFM of the Pahute Mesa area (Bechtel Nevada, 2002) where abrupt changes in unit thickness and elevation were modeled across structural block boundaries. The 3D HFM (Bechtel Nevada, 2002), referred to in subsequent U.S. Department of Energy (DOE) reports as the "Phase 1 HFM," includes 48 hydrostratigraphic units (HSUs) variably intersected by 37 faults.

A revised "Phase II HFM" of the Pahute Mesa-Oasis Valley area was constructed to incorporate data from the 10 boreholes constructed since 2002 (for example, U.S. Department of Energy, 2000; 2010a, b) and to include the revision of subsurface geologic interpretations and modification of the digital framework modeling process. Revisions to the 3D HFM in the Phase II HFM included (1) addition of new and revised borehole data and modification of the geometry of faults and HSU boundaries; (2) addition of newly interpreted faults (*ER-20-7*, *ER-20-8*, and Purse faults; fig. 2) in the SCCC; and (3) subdivision of stratigraphically complex units, such as the volcanics of Fortymile Wash and the Calico Hills Formation (fig. 3), previously defined as composite units (Navarro, written commun., 2014). The Phase II HFM (Navarro, written commun., 2014) included 74 HSUs variably intersected by 82 faults. Of the 74 HSUs, 55 intersected the aquifer-test study area evaluated in this study.

Well Network and Data Collection

A network of 38 wells at 26 well sites was monitored by Navarro-Intera, LLC, and the U.S. Geological Survey (USGS) during the 16 multiple-well aquifer tests on Pahute Mesa. Wells monitored at these well sites are identified as pumping, observation, or background wells (table 1). Observation wells were within a few miles of the pumping well and were instrumented to monitor pumping-induced, water-level changes during well development and aquifer testing on Pahute Mesa. Background wells were distant from the pumping well and assumed to be unaffected by well development and aquifer testing on Pahute Mesa. These wells were instrumented to monitor environmental water-level changes for multiple-well aquifer-test analyses. Hydraulic-property estimates from analytical and numerical analyses of 35 single- and multiple-well aquifer tests, from mostly outside the area investigated by the 16 multiple-well aquifer tests evaluated in this study, served as "prior information" that constrained hydraulic properties estimated in this study (table 1).

As used in this report, a well is defined as a single, temporary or permanent completion in a borehole, where each completion defines a unique set of open intervals. By this definition, many boreholes in the study area contain multiple well completions. Multiple-well boreholes might consist of temporary completions, where measurements are collected in packed-off intervals, or permanent completions, such as multiple monitoring tubes installed in the annulus of a main well completion. Naming conventions for the wells and boreholes in this report follow. A well that is the sole completion interval in a borehole is assigned the name of the borehole. In most cases, a well name consists of the borehole name, followed by one of the expressions: *main*, *main upper zone*, *main intermediate zone*, *main lower zone*, *shallow*, *intermediate*, or *deep*. Well names with the "main" designation generally represent the larger, "main" borehole, whereas designations such as shallow, intermediate, and deep typically denote observation-well piezometers installed in or next to the "main" borehole. In this study, well names that include the borehole name only or the borehole name followed by the "main" designation generally denote pumping wells. All well names in this report are consistent with those used in the U.S. Geological Survey National Water Information System database and are italicized in the text for clarity. References to well sites and boreholes are not italicized.

Well-construction information for pumping and observation wells monitored during the multiple-well aquifer tests are provided in table 2 and appendix 1. Construction information was obtained primarily from completion reports and written communications from the U.S. Department of Energy (DOE), Navarro, Navarro-Intera, LLC, Stoller-Navarro Joint Venture, and the USGS. Most observation and pumped wells were completed during 2009–14. The exceptions were *ER-20-1*, *ER-20-2-1*, *ER-20-5-1*, *ER-20-5-3*, and *UE-18r*, which were completed during the 1990s or earlier.

Table 1. Site location information for pumping, observation, background, and prior-information wells evaluated during multiple-well aquifer testing at Pahute Mesa, Nevada National Security Site, 2009–14.

[Names are listed in alphabetical order. Bold part of name is well site as shown on figure 2. U.S. Geological Survey site identification number is a unique 15-digit number identifying well. Latitude and longitude referenced to North American Datum of 1983. Elevation referenced to National Geodetic Vertical Datum of 1988]

Well name	U.S. Geological Survey site identification number	Latitude (decimal degrees)	Longitude (decimal degrees)	Land-surface elevation (feet)
Pumping wells				
ER-20-4 *main*	371143116262503	37.195	−116.442	5,736
ER-20-7	371247116284502	37.213	−116.481	6,209
ER-20-8 *main upper zone*	371135116282601	37.193	−116.476	5,848
ER-20-8 *main lower zone*	371135116282601	37.193	−116.476	5,848
ER-20-8-2 *main*	371135116282701	37.193	−116.476	5,849
ER-20-11 *main*	371146116290301	37.196	−116.486	5,834
ER-EC-11 *main*	371151116294101	37.197	−116.497	5,656
ER-EC-12 *main upper zone*	371024116293101	37.173	−116.494	5,532
ER-EC-12 *main lower zone*	371024116293101	37.173	−116.494	5,532
ER-EC-13 *main upper zone*	371010116325401	37.169	−116.550	5,175
ER-EC-13 *main lower zone*	371010116325401	37.169	−116.550	5,175
ER-EC-14 *main upper zone*	370825116302401	37.140	−116.512	5,186
ER-EC-14 *main lower zone*	370825116302401	37.140	−116.512	5,186
ER-EC-15 *main upper zone*	371110116310501	37.186	−116.520	5,365
ER-EC-15 *main intermediate zone*	371110116310501	37.186	−116.520	5,365
ER-EC-15 *main lower zone*	371110116310501	37.186	−116.520	5,365
Observation wells				
ER-20-1	371321116292301	37.222	−116.493	6,181
ER-20-2-1	371246116240101	37.213	−116.402	6,705
ER-20-4 deep *(main)*	371143116262503	37.195	−116.442	5,736
ER-20-4 *shallow*	371143116262504	37.195	−116.442	5,736
ER-20-5-1	371312116283801	37.220	−116.479	6,242
ER-20-5-3	371311116283801	37.220	−116.479	6,242
ER-20-7	371247116284502	37.213	−116.481	6,209
ER-20-8 *deep*	371135116282602	37.193	−116.476	5,848
ER-20-8 *intermediate*	371135116282603	37.193	−116.476	5,848
ER-20-8 *shallow*	371135116282604	37.193	−116.476	5,848
ER-20-8-2	371135116282701	37.193	−116.476	5,849
ER-20-11	371146116290301	37.196	−116.486	5,834
ER-EC-1	371223116314701	37.206	−116.532	6,026
ER-EC-2A	370852116340502	37.145	−116.569	4,902
ER-EC-5	370504116335201	37.084	−116.566	5,077
ER-EC-6 *deep*	371120116294803	37.189	−116.499	5,604
ER-EC-6 *intermediate*	371120116294804	37.189	−116.499	5,604
ER-EC-6 *shallow*	371120116294805	37.189	−116.499	5,604
ER-EC-8	370610116375301	37.103	−116.633	4,334
ER-EC-11 *deep*	371151116294102	37.197	−116.497	5,656
ER-EC-11 *intermediate*	371151116294103	37.197	−116.497	5,656
ER-EC-11 *shallow*	371151116294104	37.197	−116.497	5,656
ER-EC-12 *deep*	371024116293102	37.173	−116.494	5,532
ER-EC-12 *intermediate*	371024116293103	37.173	−116.494	5,532
ER-EC-12 *shallow*	371024116293104	37.173	−116.494	5,532

Table 1. Site location information for pumping, observation, background, and prior-information wells evaluated during multiple-well aquifer testing at Pahute Mesa, Nevada National Security Site, 2009–14.—Continued

[Names are listed in alphabetical order. Bold part of name is well site as shown on figure 2. U.S. Geological Survey site identification number is a unique 15-digit number identifying well. Latitude and longitude referenced to North American Datum of 1983. Elevation referenced to National Geodetic Vertical Datum of 1988]

Well name	U.S. Geological Survey site identification number	Latitude (decimal degrees)	Longitude (decimal degrees)	Land-surface elevation (feet)
ER-EC-13 deep	371010116325402	37.169	−116.550	5,175
ER-EC-13 intermediate	371010116325403	37.169	−116.550	5,175
ER-EC-13 shallow	371010116325404	37.169	−116.550	5,175
ER-EC-14 deep	370825116302402	37.140	−116.512	5,186
ER-EC-14 shallow	370825116302403	37.140	−116.512	5,186
ER-EC-15 deep	371110116310502	37.186	−116.520	5,365
ER-EC-15 intermediate	371110116310503	37.186	−116.520	5,365
ER-EC-15 shallow	371110116310504	37.186	−116.520	5,365
UE-18r	370806116264001	37.135	−116.447	5,538
Background wells				
ER-20-6-3	371533116251801	37.259	−116.423	6,466
PM-3-1	371421116333703	37.239	−116.562	5,823
UE-20n 1	371425116251902	37.240	−116.424	6,461
UE-20bh 1	371442116243301	37.245	−116.411	6,637
Prior-information wells				
ER-18-2	370615116222401	37.104	−116.375	5,437
ER-20-6-3	371533116251801	37.259	−116.423	6,466
ER-EC-1	371223116314701	37.206	−116.532	6,026
ER-EC-2A	370852116340502	37.145	−116.569	4,902
ER-EC-4	370935116375301	37.159	−116.633	4,760
ER-EC-5	370504116335201	37.084	−116.566	5,077
ER-EC-6	371120116294801	37.189	−116.499	5,604
ER-EC-7	365910116284401	36.985	−116.480	4,805
ER-EC-8	370610116375301	37.103	−116.633	4,334
PM-3-1	371421116333703	37.239	−116.562	5,823
U-19aS	371630116221201	37.275	−116.372	6,761
U-20WW	371505116254501	37.251	−116.431	6,468
U-20a-2WW	371434116251601	37.243	−116.423	6,472
U-20c	371353116282507	37.231	−116.475	6,281
UE-18r	370806116264001	37.135	−116.447	5,538
UE-19fS	371329116220302	37.225	−116.369	6,735
UE-20bh 1	371442116243301	37.245	−116.411	6,637
UE-20d	371452116284901	37.248	−116.482	6,253
UE-20f	371617116291701	37.271	−116.490	6,116
UE-20h	371618116260201	37.272	−116.436	6,557

Table 2. Well construction and hydrostratigraphic units open to pumping, observation, background, and prior-information wells evaluated during multiple-well aquifer testing at Pahute Mesa, Nevada National Security Site, 2009–14.

[**Well names** are listed in alphabetical order. Bold part of name is well site as shown on figure 2. Total borehole **drilled depth**, in feet below land surface (bls). **Diameter of casing** in well. **Depth to top and bottom of open casing** in well. The openings may be perforated or screened intervals. **Depth to top and bottom open annulus** in well. Open annulus includes (1) the space between the well casing and borehole that is either empty or filled with sand and/or gravel, or (2) uncased open hole deeper than the well casing and shallower or equal to well depth. **Depth to static water level:** Depth to the static water level in the well. Hydrostratigraphic units: Saturated hydrostratigraphic units in contact with open casing or open annulus. Units less than 10 feet thick are not included. **Hydrostratigraphic units** in bold type are the primary water-producing unit(s) for the well. **Abbreviations:** ATCCU, Ammonia Tanks caldera confining unit; ATWTA, Ammonia Tanks welded-tuff aquifer; BA, Benham aquifer; BFCU, Bullfrog confining unit; BRA, Belted Range aquifer; BWCU, Beatty Wash confining unit; BWWTA, Beatty Wash welded-tuff aquifer; CFCM, Crater Flat composite unit; CFCU, Crater Flat confining unit; CHLFA, Calico Hills lava-flow aquifer; CHZCM, Calico Hills zeolitic composite unit; CPA, Comb Peak aquifer; FCCM, Fortymile Canyon composite unit; FCCU, Fluorspar Canyon confining unit; FCULFA, Fortymile Canyon lava-flow aquifer; IA, Inlet aquifer; LPCU, Lower Paintbrush confining unit; MPCU, Middle Paintbrush confining unit; PBPCU, Post-Benham Paintbrush confining unit; PBRCM, Pre-Belted Range composite unit; RMWTA, Rainier Mesa welded-tuff aquifer; SPA, Scrugham Peak aquifer; TCA, Tiva Canyon aquifer; TCVA, Thirsty Canyon volcanic aquifer; THCM, Tannenbaum Hill composite unit; THCU, Tannenbaum Hill confining unit; THLFA, Tannenbaum Hill lava-flow aquifer; TMUWTA, Timber Mountain upper welded-tuff aquifer; TMWTA, Timber Mountain welded-tuff aquifer; TSA, Topopah Spring aquifer; UPCU, Upper Paintbrush confining unit; N/A, no open casing—open interval is uncased open hole]

Well name	Drilled depth (feet bls)	Diameter of casing (inches)	Depth to top and bottom of open casing (feet bls)	Depth to top and bottom of open annulus (feet bls)	Depth to static water level (feet bls)	Hydrostratigraphic units
Pumping wells						
ER-20-4 *main*	3,499	2.36	2,485–3,002	2,415–3,053	1,521	**CHLFA4**, CFCU
ER-20-7	2,936	5.50	2,360–2,875	2,292–2,936	2,023	LPCU, **TSA**, CHZCM
ER-20-8 *main upper zone*	3,442	5.50	2,486–2,912	2,440–2,940	1,667	MPCU, **TCA**, LPCU
ER-20-8 *main lower zone*	3,442	5.50	3,141–3,302	3,070–3,442	1,667	LPCU, **TSA**, CHZCM
ER-20-8-2 *main*	2,338	7.62	1,680–2,263	1,626–2,338	1,668	UPCU, **SPA**, MPCU
ER-20-11 *main*	3,004	6.62	2,612–2,967	2,562–3,004	1,655	FCCU, **BA**, UPCU
ER-EC-11 *main*	4,149	7.62	3,644–4,101 3,184–3,374	3,590–4,148 3,213–3,385	1,476	**TCA**, **TSA**, CHZCM
ER-EC-12 *main upper zone*	4,069	6.10	1,931–2,681	1,854–2,744	1,361	TMWTA, **TCA**, LPCU
ER-EC-12 *main lower zone*	4,069	6.10	3,259–3,719	3,188–3,770	1,361	**TSA**, CHZCM
ER-EC-13 *main upper zone*	3,000	6.62	1,888–2,097	1,835–2,136	1,010	**FCULFA4**
ER-EC-13 *main lower zone*	3,000	5.50	2,286–2,601	2,240–2,680	1,010	**FCULFA4**, FCCM
ER-EC-14 *main upper zone*	2,378	6.62	1,359–1,666	1,295–1,704	1,023	**RMWTA**
ER-EC-14 *main lower zone*	2,378	6.62	1,953–2,264	1,889–2,372	1,023	**RMWTA**
ER-EC-15 *main upper zone*	3,254	7.62	1,393–1,739	1,191–1,768	1,191	**CPA**, PBPCU
ER-EC-15 *main intermediate zone*	3,254	5.50	2,157–2,408	2,108–2,422	1,191	UPCU, **TCA**, LPCU
ER-EC-15 *main lower zone*	3,254	5.50	2,807–3,122	2,752–3,189	1,191	**TSA**, CHZCM
Observation wells						
ER-20-1	2,065	24	N/A	1,940–2,065	1,989	**TCA**
ER-20-2-1	2,524	2.88	2,368–2,494	2,293–2,524	2,274	**CHZCM**
ER-20-4 *deep (main)*	3,499	2.36	2,485–3,002	2,415–3,053	1,521	**CHLFA4**, CFCU
ER-20-4 *shallow*	3,499	2.44	1,521–1,602	1,524–2,336	1,521	**CHLFA1**, CHZCM
ER-20-5-1	2,823	2.88	2,315–2,374	2,249–2,655	2,053	**TSA**, CHZCM
ER-20-5-3	4,294	5.50	3,430–3,882	3,348–3,954	2,057	**CHLFA5**, CHZCM
ER-20-7	2,936	5.50	2,360–2,875	2,292–2,924	2,023	LPCU, **TSA**, CHZCM
ER-20-8 *deep*	3,442	2.88	3,141–3,302	3,070–3,442	1,667	LPCU, **TSA**, **CHZCM**
ER-20-8 *intermediate*	3,442	2.88	2,498–2,909	2,440–2,940	1,667	MPCU, **TCA**, LPCU
ER-20-8 *shallow*	3,442	1.6	2,088–2,119	1,614–2,150	1,667	UPCU, **SPA**
ER-20-8-2	2,338	2.88	1,663–2,234	1,626–2,338	1,668	UPCU, **SPA**, MPCU
ER-20-11	3,004	2.88	2,609–2,965	2,562–3,004	1,655	FCCU, **BA**, UPCU
ER-EC-1	5,000	5.50	2,298–2,821 3,348–3,760 4,448–4,750	2,258–2,863 3,286–3,776 4,399–4,895	1,856	**CPA**, UPCU, **TCA**, LPCU, **TSA**, **CHZCM**, **CFCM**
ER-EC-2A	4,902	5.50	1,707–2,179 3,077–3,549 4,487–4,916	1,635–2,236 3,025–3,450 4,410–4,974	755	**FCCM**, BWCU, **ATWTA**
ER-EC-5	2,500	5.50	1,197–1,398 1,892–2,094 2,246–2,417	1,187–1,444 1,855–2,146 2,223–2,480	1,016	**ATWTA**

Table 2. Well construction and hydrostratigraphic units open to pumping, observation, background, and prior-information wells evaluated during multiple-well aquifer testing at Pahute Mesa, Nevada National Security Site, 2009–14.—Continued

[**Well names** are listed in alphabetical order. Bold part of name is well site as shown on figure 2. Total borehole **drilled depth**, in feet below land surface (bls). **Diameter of casing** in well. **Depth to top and bottom of open casing** in well. The openings may be perforated or screened intervals. **Depth to top and bottom open annulus** in well. Open annulus includes (1) the space between the well casing and borehole that is either empty or filled with sand and/or gravel, or (2) uncased open hole deeper than the well casing and shallower or equal to well depth. **Depth to static water level:** Depth to the static water level in the well. Hydrostratigraphic units: Saturated hydrostratigraphic units in contact with open casing or open annulus. Units less than 10 feet thick are not included. **Hydrostratigraphic units** in bold type are the primary water-producing unit(s) for the well. **Abbreviations:** ATCCU, Ammonia Tanks caldera confining unit; ATWTA, Ammonia Tanks welded-tuff aquifer; BA, Benham aquifer; BFCU, Bullfrog confining unit; BRA, Belted Range aquifer; BWCU, Beatty Wash confining unit; BWWTA, Beatty Wash welded-tuff aquifer; CFCM, Crater Flat composite unit; CFCU, Crater Flat confining unit; CHLFA, Calico Hills lava-flow aquifer; CHZCM, Calico Hills zeolitic composite unit; CPA, Comb Peak aquifer; FCCM, Fortymile Canyon composite unit; FCCU, Fluorspar Canyon confining unit; FCULFA, Fortymile Canyon lava-flow aquifer; IA, Inlet aquifer; LPCU, Lower Paintbrush confining unit; MPCU, Middle Paintbrush confining unit; PBPCU, Post-Benham Paintbrush confining unit; PBRCM, Pre-Belted Range composite unit; RMWTA, Rainier Mesa welded-tuff aquifer; SPA, Scrugham Peak aquifer; TCA, Tiva Canyon aquifer; TCVA, Thirsty Canyon volcanic aquifer; THCM, Tannenbaum Hill composite unit; THCU, Tannenbaum Hill confining unit; THLFA, Tannenbaum Hill lava-flow aquifer; TMUWTA, Timber Mountain upper welded-tuff aquifer; TMWTA, Timber Mountain welded-tuff aquifer; TSA, Topopah Spring aquifer; UPCU, Upper Paintbrush confining unit; N/A, no open casing—open interval is uncased open hole]

Well name	Drilled depth (feet bls)	Diameter of casing (inches)	Depth to top and bottom of open casing (feet bls)	Depth to top and bottom of open annulus (feet bls)	Depth to static water level (feet bls)	Hydrostratigraphic units
ER-EC-6 *deep*	5,000	5.50	3,437–3,811	3,392–3,820	1,426	**TSA**, **CHZCM**
ER-EC-6 *intermediate*	5,000	5.50	2,194–2,507	2,138–2,510	1,425	UPCU, **TCA**
ER-EC-6 *shallow*	5,000	5.50	1,628–1,870	1,581–1,948	1,425	FCCU, **BA**
ER-EC-8	2,000	5.50	683–984 1,447–1,507 1,676–1,948	632–1050 1,388–1,558 1,626–1,990	322	**FCCM**, **BWWTA**, BWCU, **ATWTA**
ER-EC-11 *deep*	4,149	2.88	3,641–4,094	3,590–4,148	1,476	**TSA**, CHZCM
ER-EC-11 *intermediate*	4,149	2.88	3,159–3,378	3,196–3,385	1,477	**TCA**
ER-EC-11 *shallow*	4,149	2.38	2,678–2,991	1,662–3,024	1,477	FCCU, **BA**
ER-EC-12 *deep*	4,069	2.36	3,877–3,919	3,820–3,919	1,359	**CHZCM**, CFCU
ER-EC-12 *intermediate*	4,069	2.36	3,240–3,722	3,188–3,770	1,361	**TSA**, CHZCM
ER-EC-12 *shallow*	4,069	2.36	1,919–2,681	1,854–2,744	1,362	TMWTA, **TCA**, LPCU
ER-EC-13 *deep*	3,000	2.88	2,292–2,611	2,240–2,680	1,010	**FCULFA4**, FCCM
ER-EC-13 *intermediate*	3,000	2.88	1,900–2,100	1,835–2,136	1,010	**FCULFA4**
ER-EC-13 *shallow*	3,000	2.88	1,014–1,094	1,089–1,541	1,010	**FCCM**
ER-EC-14 *deep*	2,378	2.88	1,945–2,257	1,889–2,372	1,023	**RMWTA**
ER-EC-14 *shallow*	2,378	2.88	1,352–1,664	1,295–1,704	1,023	**RMWTA**
ER-EC-15 *deep*	3,254	2.88	2,800–3,120	2,752–3,189	1,187	**TSA**, CHZCM
ER-EC-15 *intermediate*	3,254	2.88	2,156–2,395	2,108–2,422	1,189	UPCU, **TCA**, LPCU
ER-EC-15 *shallow*	3,254	2.88	1,381–1,741	1,191–1,768	1,191	FCCU, **CPA**
UE-18r	5,004	10.05	N/A	1,629–5,004	1,363	**ATWTA**, ATCCU, **THLFA**, THCU, **RMWTA**
Background wells						
ER-20-6-3	3,200	2.88	2,510–2,802	2,453–2,807	2,015	**CHLFA3**
PM-3-1	3,019	2.88	1,920–2,145	1,872–2,192	1,457	UPCU, **TCA**, LPCU
UE-20n 1	3,300	8.75	N/A	2,308–2,834	2,041	**CHLFA4**
UE-20bh 1	2,810	12.25	N/A	1,941–2,810	2,213	**CHLFA4**, **CHLFA5**, **CHZCM**
Prior-information wells[1]						
ER-18-2	2,500	5.50	1,890–2,101	1,351–2,488	1,210	**RMWTA**
ER-EC-4	3,487	5.50	989–1,221 1,910–2,253 3,103–3,405	965–1,240 1,874–2,296 3,074–3,468	748	**TCVA**, FCCM, **TMUWTA**, THCM, **TMWTA**, PBRCM
ER-EC-7	1,386	5.50	920–979 1,215–1,304	912–1,024 1,184–1,310	746	**FCULFA6**, **FCULFA7**
U-19aS	3,584	108	N/A	3,145–3,343	2,046	CFCU, BFCU
U-20WW	3,268	13.38	2,271–3,035	2,053–3,268	2,053	**CHLFA1**, **CHZCM**, **CHLFA4**
U-20a-2WW	4,500	7.82	N/A	2,065–4,500	2,065	**CHLFA1**, **CHZCM**, **CHLFA4**
U-20c	4,800	108	N/A	4,541–4,800	2,103	**CHZCM**, IA
UE-19fs	4,779	9.88	N/A	2,565–4,779	2,305	**CHZCM**, **IA**, **CFCU**

Table 2. Well construction and hydrostratigraphic units open to pumping, observation, background, and prior-information wells evaluated during multiple-well aquifer testing at Pahute Mesa, Nevada National Security Site, 2009–14.—Continued

[**Well names** are listed in alphabetical order. Bold part of name is well site as shown on figure 2. Total borehole **drilled depth**, in feet below land surface (bls). **Diameter of casing** in well. **Depth to top and bottom of open casing** in well. The openings may be perforated or screened intervals. **Depth to top and bottom open annulus** in well. Open annulus includes (1) the space between the well casing and borehole that is either empty or filled with sand and/or gravel, or (2) uncased open hole deeper than the well casing and shallower or equal to well depth. **Depth to static water level:** Depth to the static water level in the well. Hydrostratigraphic units: Saturated hydrostratigraphic units in contact with open casing or open annulus. Units less than 10 feet thick are not included. **Hydrostratigraphic units** in bold type are the primary water-producing unit(s) for the well. **Abbreviations:** ATCCU, Ammonia Tanks caldera confining unit; ATWTA, Ammonia Tanks welded-tuff aquifer; BA, Benham aquifer; BFCU, Bullfrog confining unit; BRA, Belted Range aquifer; BWCU, Beatty Wash confining unit; BWWTA, Beatty Wash welded-tuff aquifer; CFCM, Crater Flat composite unit; CFCU, Crater Flat confining unit; CHLFA, Calico Hills lava-flow aquifer; CHZCM, Calico Hills zeolitic composite unit; CPA, Comb Peak aquifer; FCCM, Fortymile Canyon composite unit; FCCU, Fluorspar Canyon confining unit; FCULFA, Fortymile Canyon lava-flow aquifer; IA, Inlet aquifer; LPCU, Lower Paintbrush confining unit; MPCU, Middle Paintbrush confining unit; PBPCU, Post-Benham Paintbrush confining unit; PBRCM, Pre-Belted Range composite unit; RMWTA, Rainier Mesa welded-tuff aquifer; SPA, Scrugham Peak aquifer; TCA, Tiva Canyon aquifer; TCVA, Thirsty Canyon volcanic aquifer; THCM, Tannenbaum Hill composite unit; THCU, Tannenbaum Hill confining unit; THLFA, Tannenbaum Hill lava-flow aquifer; TMUWTA, Timber Mountain upper welded-tuff aquifer; TMWTA, Timber Mountain welded-tuff aquifer; TSA, Topopah Spring aquifer; UPCU, Upper Paintbrush confining unit; N/A, no open casing—open interval is uncased open hole]

Well name	Drilled depth (feet bls)	Diameter of casing (inches)	Depth to top and bottom of open casing (feet bls)	Depth to top and bottom of open annulus (feet bls)	Depth to static water level (feet bls)	Hydrostratigraphic units
UE-20d	4,492	9.62	N/A	2,447–4,492	2,074	UPCU, **TCA**, LPCU, **TSA**, **CHZCM**, **CHLFA5**
UE-20f	13,686	8.75	N/A	4,456–13,686	1,776	**IA**, **CFCM**, BFCU, BRA, PBRCM
UE-20h	7,207	9.88	N/A	2,538–7,207	2,111	**CHLFA4**, CFCU, BFCU

[1] Prior-information wells other than observation and background wells.

Wells pumped during the 16 multiple-well aquifer tests (table 3) contained a main casing with one, two, or three completions. Packers or bridge plugs in the main casing often isolated completions, so that individual completions could be pumped (table 4). Aquifer tests in multiple-completion wells were designated as *main upper zone*, *main intermediate zone*, or *main lower zone*. Many pumping wells also contained piezometers completed in the annulus alongside the main completion zone or in shallower or deeper zones in the borehole. Piezometers in multiple-completion wells represented observation wells with the designation of *shallow*, *intermediate*, or *deep* (tables 1, 2). Distances between pumping and observation wells ranged from less than a foot to a few miles.

Observation-well sites north of the bench and west of the Boxcar fault (ER-20-1, ER-20-5 and ER-20-7; fig. 2) penetrated about 2,000 ft of unsaturated rock. In these wells, the water table is in the Tiva Canyon aquifer (TCA) or Lower Paintbrush confining unit (LPCU). Major water-producing hydrostratigraphic units are the TCA and Topopah Spring aquifer (TSA), with some production from Calico Hills lava-flow aquifers (CHLFA1-5) in the Calico Hills zeolitic composite unit (CHZCM; fig. 5).

The major water-producing units in observation wells north of the bench and east of the Boxcar fault (*ER-20-4* and *ER-20-2-1*; fig. 4) are CHLFA1-5 and CHZCM. The water table in *ER-20-2-1* well is in the CHZCM (appendix 1).

Observation-well sites in the bench area included ER-20-8, ER-20-11, ER-EC-1, ER-EC-6, ER-EC-11, ER-EC-12, and ER-EC-15 (fig. 2). These wells penetrated about 1,200 to 1,800 ft of unsaturated rock before intersecting the water table in the Timber Mountain welded-tuff aquifer (TMWTA), Benham aquifer (BA), Fluorspar Canyon confining unit (FCCU), or Tannenbaum Hill composite unit (THCM; figs. 4, 5). Wells in the bench area were constructed to monitor five water-producing hydrostratigraphic units: BA, Scrugham Peak aquifer (SPA), TCA, TSA, and Comb Peak aquifer. The CHZCM and Crater Flat composite unit also supply water to observation wells in the bench area (table 2).

South of the bench, well sites ER-EC-2A, ER-EC-4, ER-EC-5, ER-EC-8, ER-EC-13, ER-EC-14, and UE-18r (fig. 2) penetrated about 300 to 1,400 ft of unsaturated rock and intersect the water table in the Fortymile Canyon lava-flow aquifer 2 (FCULFA2), Fortymile Canyon composite unit (FCCM), THCM, Beatty Wash confining unit, and Thirsty Canyon volcanic aquifer (TCVA; table 2; fig. 5; appendix 1). Variations in unsaturated-zone thickness primarily result from land-surface elevation differences between wells. The water-producing hydrostratigraphic units in these wells are lava-flow aquifers in the FCULFA4, FCCM, and TCVA and welded-tuff aquifers in the Timber Mountain welded-tuff aquifer (TMWTA), Timber Mountain Upper welded-tuff aquifer, Ammonia Tanks welded-tuff aquifer (ATWTA), Beatty Wash welded-tuff aquifer, and Rainier Mesa welded-tuff aquifer (RMWTA; table 2; fig. 5; appendix 1).

Data collected during the 16 multiple-well aquifer tests included pumping schedules and continuous water-level, temperature, and barometric-pressure measurements. Water levels and temperatures were measured intermittently in 34 observation wells, 4 background wells, and 16 pumping wells from November 2009 to October 2014 (fig. 6). Each aquifer test typically consisted of three phases during a 30-day pumping schedule. Well development and step-drawdown tests were done during the first 10-day period. There was no pumping, and water levels recovered during the second 10-day period.

Table 3. Pumping wells, pumping periods, and volume discharged during each aquifer test, Pahute Mesa, Nevada National Security Site, 2009–14.

[**Well names** are listed in alphabetical order. Bold part of name is well site as shown on figure 2. Discharge data is from Navarro-Intera, LLC, daily drilling reports (Navarro-Intera, LLC, written commun., 2014). Drilling reports for wells ER-20-8-2 main and ER-EC-11 main are from Navarro (written commun., 2014). **Aquifer test description:** well development (WD) includes development and step drawdown tests, whereas the constant-rate test (CRT) is a period where the pumping rate remained mostly unchanged. **Period of analysis:** Start and end of well development and constant-rate testing periods determined from Navarro-Intera, LLC, and Navarro daily drilling reports. **Approximate discharge rate:** represents the pumping rate when the pump was on during the period of analysis. **Abbreviations:** mm/dd/yyyy, month/day/year; gal/min, gallons per minute; Mgal, millions of gallons; WD, well development; CRT, constant-rate pumping test; —, no data; <, less than]

Pumping-well name	Aquifer-test description	Period of Analysis (mm/dd/yyyy)		Approximate discharge rate (gal/min)	Approximate volume discharged (Mgal)
		Start	End		
ER-20-4 *main*	WD	08/30/2011	09/08/2011	250	1.9
	CRT	09/13/2011	09/21/2011	280	3.3
ER-20-7	WD	09/14/2010	09/17/2010	290	1.3
	CRT	09/21/2010	09/24/2010	280	1.1
ER-20-8 *main upper zone*[1]	WD	05/18/2011	05/26/2011	110	1.2
	CRT	06/18/2011	06/27/2011	140	1.9
ER-20-8 *main lower zone*[2]	WD	07/15/2011	07/27/2011	105	1.2
	CRT	07/29/2011	08/08/2011	130	1.9
ER-20-8-2 *main*	WD	11/28/2009	12/10/2009	130	0.9
	CRT	12/11/2009	12/18/2009	130	1
ER-20-11 *main*	WD	06/11/2013	07/11/2013	245	2.8
	CRT	07/16/2013	08/05/2013	285	8
ER-EC-11 *main*	WD	04/30/2010	05/04/2010	270	1.7
	CRT	05/10/2010	05/19/2010	300	3.8
ER-EC-12 *main upper zone*[1]	WD	10/11/2011	11/10/2011	100	1.2
	CRT	11/20/2011	11/28/2011	83	1.1
ER-EC-12 *main lower zone*[2]	WD	02/29/2012	03/13/2012	40	<0.1
	CRT	03/19/2012	03/19/2012	10	0.0006
ER-EC-13 *main upper zone*[1]	WD	06/22/2012	06/29/2012	240	2.4
	CRT	07/03/2012	07/08/2012	300	2.2
	WD	07/12/2012	07/13/2012	300	0.5
ER-EC-13 *main lower zone*[2]	WD[3]	07/21/2012	07/27/2012	240	2
	CRT[3]	07/30/2012	08/02/2012	200	0.8
	WD	03/07/2013	03/15/2013	200	1.8
	CRT	03/20/2013	03/29/2013	300	3.9
ER-EC-14 *main upper zone*[1]	WD	03/14/2014	03/22/2014	150	1.6
	CRT	03/27/2014	04/07/2014	150	2.4
ER-EC-14 *main lower zone*[1]	WD	04/18/2014	04/28/2014	220	3.2
	CRT	05/02/2014	05/12/2014	270	3.8
ER-EC-15 *main upper zone*[1]	WD	09/17/2013	10/03/2013	119	1.6
	CRT	10/21/2013	10/29/2013	124	1.4
ER-EC-15 *main intermediate zone*[1,2]	WD	12/18/2013	01/09/2014	13	<0.1
	CRT	01/10/2014	01/10/2014	9	—
ER-EC-15 *main lower zone*[2]	WD	01/22/2014	02/01/2014	21	0.3
	CRT	02/12/2014	02/18/2014	20	0.2

[1] Bridge plug used to isolate the pumping interval from other open intervals in the pumping well.

[2] Straddle packer used to isolate the pumping interval from other open intervals in the pumping well.

[3] Leaking packer led to inadvertent pumping of upper and lower zones.

Table 4. Packer and bridge-plug history in pumping wells during multiple-well aquifer testing at Pahute Mesa, Nevada National Security Site, 2009–14.

[**Well names** are listed in alphabetical order. Bold part of name is well site as shown on figure 2. **Start/End date:** Effective dates when flow isolation devices were installed. Flow isolation devices were not installed beyond the date ranges specified below. **Flow-isolation device:** Equipment used to control the well open interval. **Flow isolation device interval:** For bridge plugs: Depth to the top of the bridge plug. For straddle packers: Depth to the top of the upper and lower packers. **Pumping well zone (HSU):** Describes the pumping zone during the period when the flow isolation device was installed and the major water-producing hydrostratigraphic units (HSUs) affected by the aquifer test listed. **Pumping well open interval:** Depth of the well interval open to surrounding rock units. **Abbreviations:** bls, below land surface; CPA, Comb Peak aquifer; FCULFA4, Fortymile Canyon lava-flow aquifer 4; RMWTA, Rainier Mesa welded-tuff aquifer; TCA, Tiva Canyon aquifer; TSA, Topopah Spring aquifer; mm/dd/yyyy, month/day/year; —, not applicable]

Well name	Start date (mm/dd/yyyy)	End date (mm/dd/yyyy)	Flow-isolation device	Flow-isolation device interval (feet bls)	Pumping well zone (HSU)	Pumping well open interval (feet bls)
***ER-20-8** main*	08/27/2009	07/12/2011	bridge plug	3,005	Upper zone (TCA)	2,440–2,940
	07/13/2011	08/22/2011	straddle packer	2,426 (upper), 3,011 (lower)	Lower zone (TSA)	3,070–3,442
	08/25/2011	09/30/2014	bridge plug	2,993		—
***ER-EC-11** main*	10/29/2009	04/15/2010	bridge plug	3,428		—
	06/27/2010	09/30/2014	bridge plug	3,433		—
***ER-EC-12** main*	08/04/2010	02/23/2012	bridge plug	2,825	Upper zone (TCA)	1,854–2,744
	02/23/2012	03/28/2012	straddle packer	1,884 (upper), 2,719 (lower)	Lower zone (TSA)	3,188–3,770
	03/29/2012	09/30/2014	bridge plug	2,813		—
***ER-EC-13** main*	11/04/2010	07/18/2012	bridge plug	2,228	Upper zone (FCULFA4)	1,836–2,136
	07/20/2012	01/30/2013	straddle packer	1,832 (upper), 2,123 (lower)	Lower zone (FCULFA4) [1]	2,240–2,680
	02/05/2013	04/10/2013	straddle packer	1,799 (upper), 2,197 (lower)	Lower zone (FCULFA4)	2,240–2,680
	04/11/2013	09/30/2014	bridge plug	2,224		—
***ER-EC-14** main*	10/24/2012	04/15/2014	bridge plug	1,776	Upper zone (RMWTA)	1,296–1,704
	04/16/2014	05/20/2014	straddle packer	1,326 (upper), 1,684 (lower)	Lower zone (RMWTA)	1,889–2,372
	05/21/2014	09/30/2014	bridge plug	1,770		—
***ER-EC-15** main*	12/10/2010	11/12/2013	bridge plugs	1,853 2,458	Upper zone (CPA)	1,191–1,768
	11/13/2013	01/14/2014	straddle packer, bridge plug	1,363 (upper straddle), 1,814 (lower straddle), 2,458 (bridge plug)	Intermediate zone (TCA)	2,108–2,422
	01/16/2014	02/26/2014	straddle packer	1,363 (upper), 2,466 (lower)	Lower zone (TSA)	2,752–3,189
	03/03/2014	09/30/2014	bridge plugs	1,853 2,458		—

[1] Upper packer measured at 1,904 feet bls on 11/8/2012 and removed.

The well was pumped at a constant rate during the last 10-day period. Pumping periods were briefer in low-productivity wells, where pumping could not be sustained (for example, *ER-EC-12 main lower zone* and *ER-EC-15 main intermediate and lower zones*) or in contaminated wells that had limited capacity for discharge-water storage (*ER-20-7*; table 3). Groundwater volumes discharged during aquifer testing ranged from less than 0.1 million gallons (Mgal; *ER-EC-12 main lower zone* and *ER-EC-15 main intermediate zone*) to 10.8 Mgal (*ER-20-11 main*). Table 3 summarizes the pumping periods and discharge volume for each of the aquifer tests. Raw and simplified pumping data also are available in a separate data release that can be accessed at: *https://doi.org/10.5066/F7Z60M6H*.

More than 200 pumping- and observation-well pairs were included in the integrated aquifer-test analysis. Horizontal distances between pumping and observation wells ranged from less than 0.5 to 23,000 feet. Observation wells monitored during aquifer testing were in two to four azimuthal quadrants around each pumping well and were screened across a range of HSUs. Submerged pressure transducers used to monitor water-levels in observation and background wells periodically failed, as characterized by erratic water-level measurements. Drawdown analyses for each aquifer test excluded observation and background wells where there were erratic measurements and incomplete records.

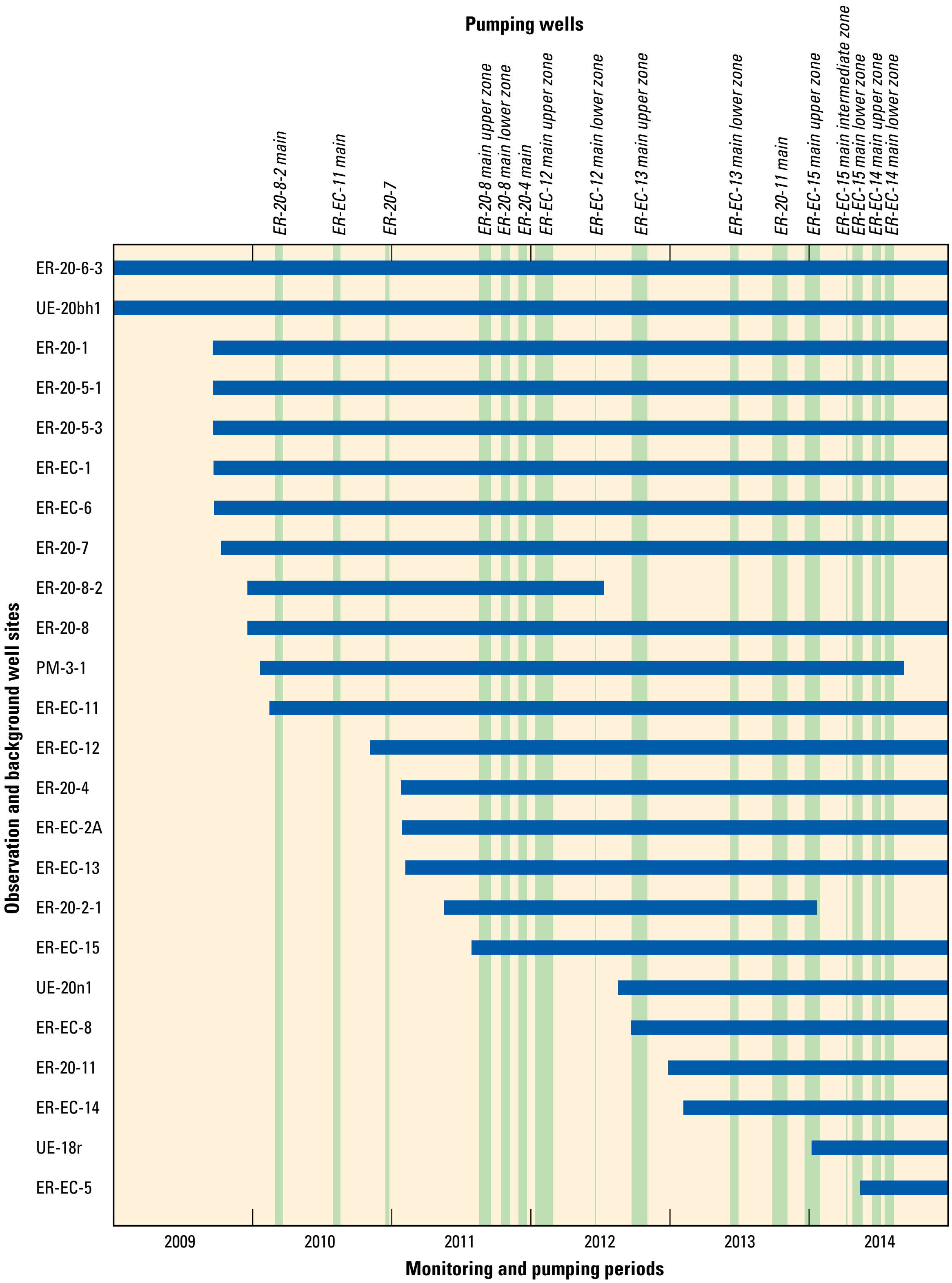

Figure 6. Water-level monitoring history for pumping wells and observation and background well sites, Pahute Mesa, Nevada National Security Site and vicinity, 2009–14.

Drawdown Observations

Drawdown observations between pumping and observation wells were used to estimate hydraulic properties around the pumping wells and for the HSUs (fig. 2; table 2). Drawdown observations were pumping-induced water-level changes in continuously measured water levels. Drawdowns at the pumped well primarily defined hydraulic-property estimates of HSUs near the pumping well. Drawdowns in distant observation wells defined the bulk hydraulic diffusivity (the ratio of transmissivity to storage coefficient) of HSUs and structures between pumping and observation wells.

Water-Level Models and Drawdown Estimation

Drawdowns from aquifer testing were differentiated from environmental fluctuations by analytical water-level models (Halford and others, 2012; Garcia and others, 2013). Environmental fluctuations caused by barometric and tidal forces acting on the deep, hard-rock aquifer system can trigger a foot or more of water-level change over only a few days (Fenelon, 2000). Similarly, recharge can cause long-term increases and decreases that are superimposed on the short-term fluctuations (Fenelon, 2000; Elliot and Fenelon, 2010). Water-level modeling provides a mechanism for distinguishing environmental fluctuations from pumping-induced drawdown in complex hydrogeologic systems and improving aquifer test interpretations (Halford and others, 2012; Garcia and others, 2013).

Water-level models analytically simulate all pumping and non-pumping stresses simultaneously during the period of aquifer-test data collection, which allows for differentiation between pumping and non-pumping stresses. Analysis periods typically comprised antecedent non-pumping, pumping, and recovery periods. Theis (1935) models approximated pumping signals by transforming time-varying pumping stresses into water-level drawdown responses. Environmental water-level fluctuations were approximated with modeled time series of barometric pressures, tide signals, and water levels from background wells unaffected by pumping stresses (fig. 7). Water levels from background wells were critical because they exhibited the sum of all interacting environmental fluctuations that presumably affected measured water levels in observation wells.

Theis models were generated from simplified pumping schedules because small pumping-rate fluctuations during well development and constant-rate testing minimally affect distant drawdowns. For example, the raw measured pumping schedule from *ER-EC-13 main lower zone* was simplified from more than 9,500 pumping records to 92 pumping steps while preserving intermittent non-pumping periods within the 30-day pumping schedule. The raw pumping schedule from *ER-20-11 main* was simplified from more than 13,000 pumping records to 129 pumping steps (fig. 8). Simplified pumping schedules were considered acceptable for observation wells beyond the pumping-well site because the aquifer responses to high-frequency changes in pumping (discharge) are attenuated by the aquifers (Garcia and others, 2013).

The analytically simulated water level representing the sum of all simulated stresses in the water-level model was calibrated to the measured water level by minimizing the root-mean-square (RMS) error of differences between the two time series (Halford and others, 2012). Amplitude and phase were adjusted in each time series during which environmental water-level fluctuations were simulated. Amplitudes were allowed to fluctuate in magnitude and direction to allow greater flexibility in fitting the frequencies of non-pumping signals. Transmissivity and storage coefficient were adjusted in the fit to the Theis models.

Multiple moving averages of barometric pressure and background water levels were included to account for the complex interactions among barometric pressure, background-well water levels, and earth tides. Barometric pressure has several frequencies of fluctuation, which affect water levels both in observation and background wells. While theoretical equations are used to model earth tides, these equations might not account for local conditions that could cause departures from theoretical earth tides. Adjustment of amplitude and phase for multiple moving averages provides a flexible mechanism for obtaining a good fit between measured and simulated water levels even if non-pumping stresses were not all accurately distinguished. Because the sum of all simulated stresses is calibrated to the measured water level, potential over- and underestimation of particular environmental frequencies is minimized.

Drawdown was computed as the summation of all Theis models and residual differences between measured and analytically simulated water levels. The summation of all Theis models inherently assumes that the principle of superposition applies to this application. The sum represents the direct estimate of the pumping signal, whereas residuals represent all unexplained water-level fluctuations (fig. 7). Residual water-level fluctuations primarily are random during non-pumping periods, but can contain unexplained components of the pumping signal during pumping periods, where residual fluctuations can follow a systematic pattern corresponding with pumping stresses (Halford and others, 2012). Raw and simplified pumping data, drawdown time-series data, and water-level models are available in a separate data release that can be accessed at: *https://doi.org/10.5066/F7Z60M6H*.

Single-Well Aquifer Tests

Transmissivity describes the rate of groundwater movement through a section of aquifer; it is expressed as the product of hydraulic conductivity and saturated aquifer thickness (Lohman, 1972); and it is the primary result from most aquifer tests (Halford and Yobbi, 2006). Single-well aquifer tests provide relatively certain estimates of transmissivity around pumping wells because flow rates through pumped wells are known. Multiple-well aquifer tests provide bulk transmissivity estimates between pumping and observation wells, but certainty in the transmissivity distribution across hydrostratigraphic units is limited by heterogeneities between pumping and observation wells.

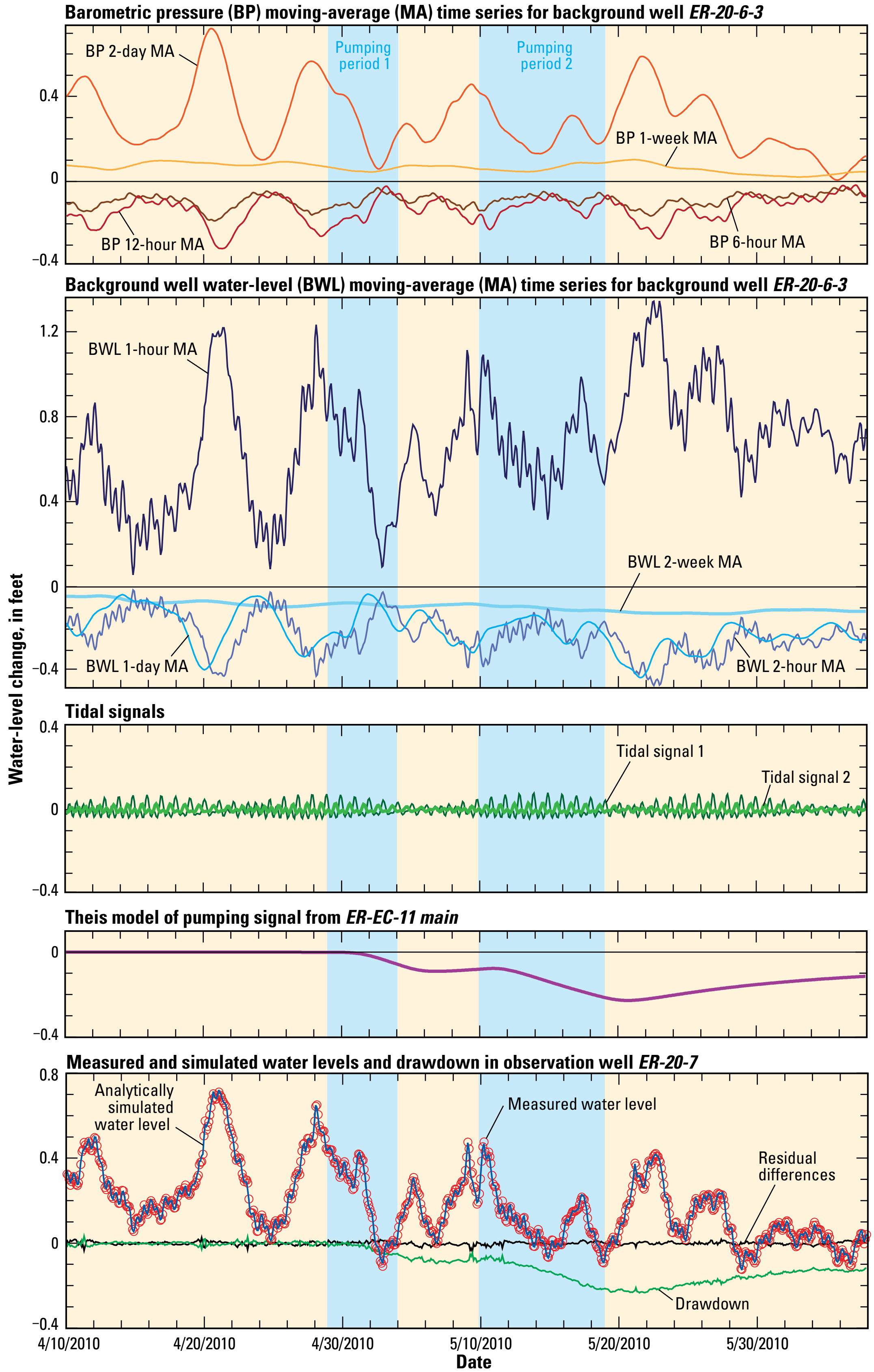

Figure 7. Component time series for well data, Pahute Mesa, Nevada National Security Site, April–June 2010, including barometric pressure; background-well water levels; tidal signals; Theis model of the pumping signal; and measured and analytically simulated water levels, observed drawdown, and fitting residuals determined from water-level modeling of water levels in observation well *ER-20-7* during pumping in *ER-EC-11 main*.

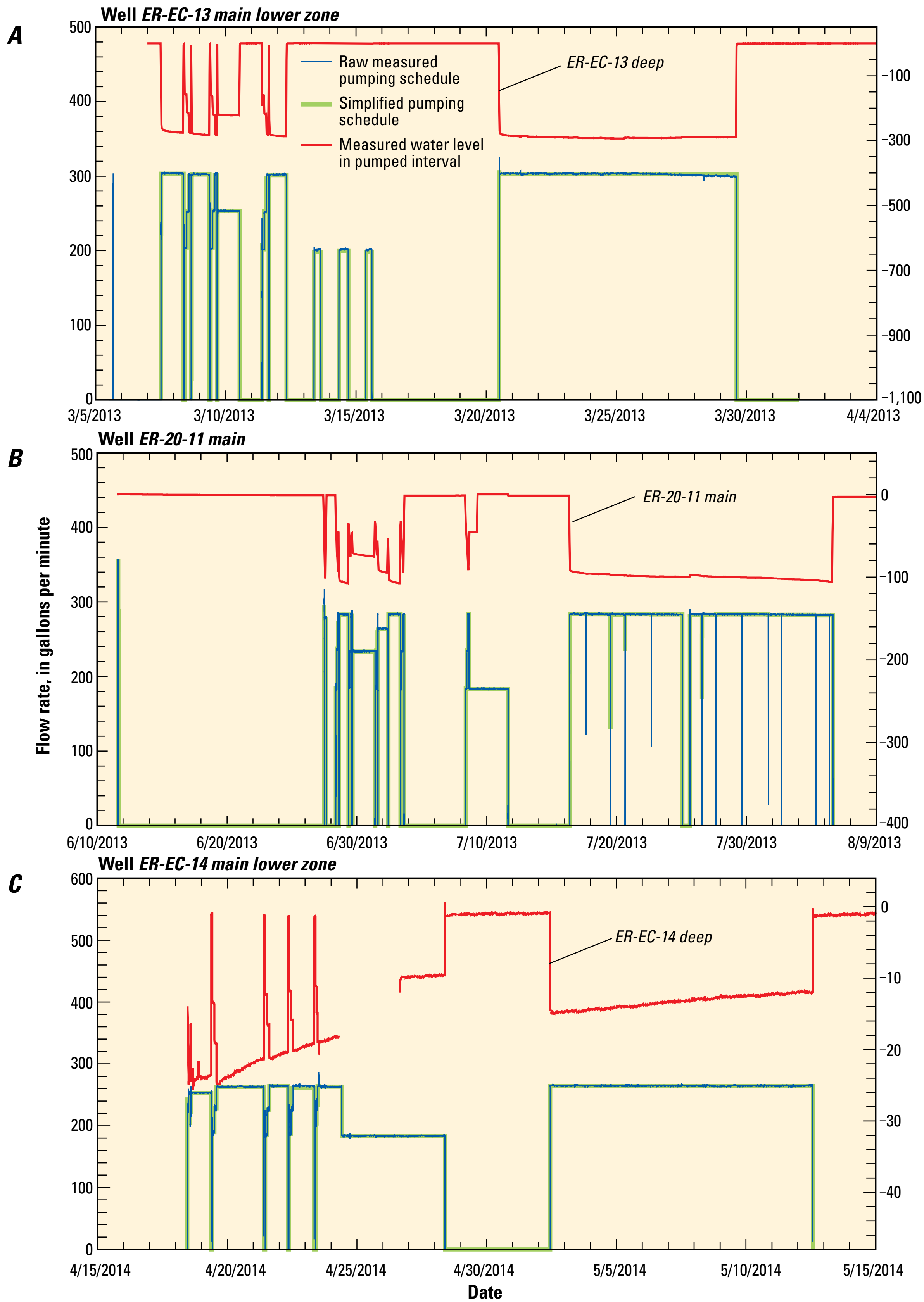

Figure 8. Simplified pumping schedules and water-level change in nearby observation wells for Pahute Mesa, Nevada National Security Site and vicinity, March 2013–May 2014: *A*, *ER-EC-13 main lower zone*; *B*, *ER-20-11 main*; and *C*, *ER-EC-14 main lower zone* aquifer tests.

Single-well aquifer tests were interpreted at all pumping wells by one or more of the following organizations: the USGS; Navarro-Intera, LLC; or Navarro. Most single-well aquifer tests were analyzed with the Cooper and Jacob (1946) approach, which requires that drawdown exhibits a definitive linear slope when graphed on a semi-log plot over time (table 5). Transmissivity is inversely proportional to this slope.

Single-well aquifer tests at the ER-EC-13 well site were analyzed with a two-dimensional radial MODFLOW model (Harbaugh and others, 2000) to investigate packer leakage between *upper* and *lower zones* (U.S. Geological Survey, 2015). Well *ER-EC-12 main lower zone* was analyzed as a slug test because the low transmissivity of 0.1 square foot per day (ft^2/d) precluded sustained pumping (U.S. Geological Survey, 2015). Aquifer tests were analyzed with water-level models in (1) *ER-EC-15 main intermediate* to estimate drawdown from an intermittent and unsustained discharge rate, (2) *ER-EC-11 main* to simultaneously interpret water-level change from pumping-induced drawdown and thermal expansion of the water column, and (3) *ER-20-8-2 main* to interpret drawdown from multiple pumping periods (table 5).

Specific-capacity estimates from single-well aquifer tests provide insight into the productivity of HSUs around pumping wells, despite uncertain drawdown interpretations. Specific-capacity estimates (table 5) were determined from constant-rate discharge (table 3) and maximum drawdowns in pumping wells (table 6). Specific capacities ranged from 0.02 gallons per minute per foot (gal/min/ft) at *ER-EC-12 main lower zone* to 32.5 gal/min/ft at *ER-20-8 main lower zone*. Sustained discharge rates greater than 250 gallons per minute (gal/min) during constant-rate testing were achieved at *ER-20-4 main*, *ER-20-7*, *ER-20-11 main*, *ER-EC-11 main*, *ER-EC-13 main upper and lower zones*, and *ER-EC-14 main lower zone*. The most productive wells, which had specific capacities above 20 gal/min/ft, included *ER-20-7*, *ER-20-8 main lower zone*, *ER-20-8-2 main*, and *ER-EC-14 main lower zone*. These wells are open to the TSA, BA, SPA, and RMWTA HSUs, respectively.

Empirical relations between specific capacity and transmissivity frequently are developed to estimate spatial distributions of transmissivity (Thomasson and others, 1960; Prudic, 1991; Yager and others, 2012). Specific capacity is a good estimator of transmissivity, and coefficients of determination typically range between 0.7 and 0.8. A local power-law relation was developed with results from 13 constant-rate aquifer tests (table 5), where transmissivity (ft^2/d) equaled 770 times specific capacity (gal/min/ft) raised by 1.2 (table 5). The coefficient of determination was 0.87.

Transmissivities of 10,000 ft^2/d or greater were estimated in five wells, and all estimates are uncertain (table 5). Water-level drawdown from aquifer testing is typically less in more transmissive aquifers and, therefore, is easily obscured by environmental fluctuations and factors confounding water level responses and measurements in the pumped well. Transmissivity uncertainty most often reflects transmissive aquifers where drawdowns are small relative to large water-level changes from thermal expansion of the water column, barometric pressure, and tidal signals. Thermal expansion of the water column was the primary source of transmissivity-estimate uncertainty in this study as environmental fluctuations were adequately modeled and removed from drawdown and recovery periods. Warmer water pumped from open intervals in deep-well completions gradually heats the water column between the screened interval and the pressure transducer, which is generally suspended higher in the water column. Gradual heating of the column causes the water column to expand and rise relative to the column under the initial ambient temperature. The rate of expansion or water-level rise is related to the pumped water temperature, water-column length, pumping rate, and temperature gradient along the water column. The effects of thermal expansion are greatest near the top of the water column where the transducer is generally deployed. Temperature changes in the water column were not measured; therefore, explicit calculation of thermal expansion was not possible. In the absence of temperature measurements, drawdown and thermal expansion cannot be differentiated because thermal and potential water-level changes are both responses to changes in pumping rates and are governed by the same diffusivity equations (Theis, 1935). Small drawdowns also can be obscured by water-level changes from frictional well loss, occasional leakage across packers and bridge plugs used to separate well completions, leaky confining units, electrical interference or pipe vibration during pumping, and declining pumping rates (table 5). Single well aquifer-tests were analyzed after frictional well losses stabilized, typically within 15–30 minutes after pumping commenced (Halford and Yobbi, 2006). Omitting early drawdown ensures that changes in measured water levels reflect aquifer hydraulics rather than well construction effects.

Thermal expansion was most evident when water levels in the pumped well and surrounding piezometers rose continually during pumping. Prior to March 2012, transducers were deployed within 50 ft of the static water level. This allowed water columns of more than 1,000 ft to expand between the transducer and well completion, and longer water columns typically contain larger water volumes for heating and

Table 5. Transmissivity and specific-capacity estimates from 16 single-well aquifer tests and confounding factors affecting transmissivity estimates in pumping wells.

[**Well names** are listed in alphabetical order. Bold part of name is well site as shown on figure 1. **Transmissivity estimation method:** B, Barker (1988); BR, Bouwer and Rice (1976) slug-test analysis; CJ, Cooper and Jacob (1946); DB (Dougherty and Babu, 1984); HJ, Hantush and Jacob (1955); MF, 2-dimensional radial MODFLOW model (Harbaugh and others, 2000); NS, nSIGHTS (Geofirma and INTERA, 2011); SC, specific capacity (local regression determined as the product of 770 and specific capacity to the power of 1.2); WLM, water-level model. **Transmissivity estimate:** Estimate assumes volume discharged was sampled from a circular volume surrounding the well. Typically Interpreted during the first 3 days of pumping. Values in paranthesis were determined by Navarro-Interra, LLC, or Navarro. **Transmissivity confounding factors:** drawdown was correlated with at least one of the following factors: W, well loss induced water-level change; T, temperature-induced water-level change; L, leakage across packer or bridge plug; P, a declining pumping rate; or U, an unknown factor. **Pumping signal clarity:** Characterizes the ability to clearly distinguish the pumping signal–clear indicates a distinct pumping signal and unclear indicates the pumping signal was obscured by confounding factors or environmental fluctuations. **Specific capacity:** Estimated as the ratio of the average pumping rate during the constant-rate test (table 3) to the maximum drawdown during the constant-rate test (table 6). **Hydrostratigraphic units:** Saturated hydrostratigraphic units in contact with open casing or open annulus. Units less than 10 feet thick are not included. Hydrostratigraphic units in bold type are the primary water-producing unit(s) for the well. **Abbreviations:** BA, Benham aquifer; CHLFA, Calico Hills lava-flow aquifer; CHZCM, Calico Hills zeolitic composite unit; CPA, Comb Peak aquifer; FCCM, Fortymile Canyon composite unit; FCCU, Fluorspar Canyon confining unit; FCULFA, Fortymile Canyon upper lava-flow aquifer; LPCU, Lower Paintbrush confining unit; MPCU, Middle Paintbrush confining unit; PBPCU, Post-Benham Paintbrush confining unit; RMWTA, Rainier Mesa welded-tuff aquifer; SPA, Scrugham Peak aquifer; TCA, Tiva Canyon aquifer; TMWTA, Timber Mountain welded-tuff aquifer; TSA, Topopah Spring aquifer; UPCU, Upper Paintbrush confining unit; ft^2/d, feet-squared per day; gal/min/ft, gallons per minute per foot; >, greater than; <, less than]

Pumping-well name	Observation-well name	Transmissivity: Estimation method	Transmissivity: Estimate (ft^2/d)	Transmissivity: Confounding factors	Pumping signal clarity	Specific capacity (gal/min/ft)	Hydrostratigraphic units
ER-20-4 *main*	***ER-20-4*** *deep*	CJ	[1] 1,700	W, T, P	clear	1.4	**CHLFA4**, CFCU
		CJ, B	[2] (3,000–4,400)				
ER-20-7	***ER-20-7***	CJ	[1]23,000	W, T	unclear	29.5	LPCU, **TSA**, CHZCM
		CJ	[3] (16,000)				
ER-20-8 *main upper zone*	***ER-20-8*** *intermediate*	CJ	[4]6,600	W, T	clear	8.8	MPCU, **TCA**, LPCU
		CJ	[2] (3,100)				
ER-20-8 *main lower zone*	***ER-20-8*** *deep*	CJ	[4]100,000	W, T	unclear	32.5	LPCU, **TSA**, CHZCM
ER-20-8-2 *main*	***ER-20-8-2*** *main*	WLM	[1]>10,000	W, T	unclear	21.7	UPCU, **SPA**, MPCU
ER-20-11 *main*	***ER-20-11***	CJ	[4]5,000	W	clear	2.5	FCCU, **BA**, UPCU
ER-EC-11 *main*	***ER-EC-11*** *main*	WLM	[1]>20,000	W, T, P	unclear	2.4	**TCA**, **TSA**, CHZCM
ER-EC-12 *main upper zone*	***ER-EC-12*** *shallow*	CJ	[4]300–400	W, T, L	clear	0.2	TMWTA, **TCA**, LPCU
ER-EC-12 *main lower zone*	***ER-EC-12*** *intermediate*	BR	[1] 0.1	W, T, L	clear	0.02	**TSA**, CHZCM
ER-EC-13 *main upper zone*	***ER-EC-13*** *intermediate*	MF	[1]3,600	W, L	clear	5.1	**FCULFA4**
ER-EC-13 *main lower zone*	***ER-EC-13*** *deep*	MF	[1]1,400	W, L	clear	1	**FCULFA4**, FCCM
ER-EC-14 *main upper zone*	***ER-EC-14*** *shallow*	CJ	700	W, L	clear	1.1	**RMWTA**
		CJ, DB	[5] (650–780)				
ER-EC-14 *main lower zone*	***ER-EC-14*** *deep*	SC[6]	[6] 30,000	W, L, U	unclear	23	**RMWTA**
		—	[5] (>20,000, 40,000)				
ER-EC-15 *main upper zone*	***ER-EC-15*** *shallow*	CJ	[1]3,200	W	clear	1	**CPA**, PBPCU
		HJ, CJ	[5] (610–2,700)				
ER-EC-15 *main intermediate zone*	***ER-EC-15*** *intermediate*	WLM	[1]<20	W	clear	0.1	UPCU, **TCA**, LPCU
		NS	[5] (130)				
ER-EC-15 *main lower zone*	***ER-EC-15*** *deep*	CJ	[1] 40	W	clear	0.2	**TSA**, CHZCM
		CJ, DB	[5] (40–45)				

[1] U.S. Geological Survey (2015).

[2] U.S. Department of Energy (2012).

[3] U.S. Department of Energy (2011).

[4] Determined in this study.

[5] U.S. Department of Energy (2015).

[6] Determined using 13 transmissivity estimates from U.S. Geological Survey (2015), and those determined in this study, excluding wells ER-EC-11 main and ER-EC-12 main lower zone.

Table 6. Summary of observed drawdown for pumping- and observation-well pairs during multiple-well aquifer testing at Pahute Mesa, Nevada National Security Site, 2009–14.

[**Well names** are listed in alphabetical order. Bold part of name is well site as shown on figure 1. Wells pumped during multiple-well aquifer testing. Values represent estimated maximum detected drawdown in feet, determined by matching measured water levels in the observation well to an analytically modeled curve of non-pumping and pumping responses. Values in parantheses represent ambiguous estimates. U, undetected; —, not estimated; <, less than]

Observation-well name	Pumping-well name and associated drawdown (feet)										
	ER-20-4 main	ER-20-7	ER-20-8 main upper and lower zones	ER-20-8-2 main	ER-20-11 main	ER-EC-11 main	ER-EC-12 main upper and lower zones	ER-EC-13 main upper zone	ER-EC-13 main lower zone	ER-EC-14 main upper and lower zones	ER-EC-15 main upper, intermediate, and lower zones
ER-20-1	—	0.16	—	(0.06)	—	0.07	—	—	—	—	—
ER-20-2-1	U	—	U	—	—	—	—	—	—	—	—
ER-20-4 *deep (main)*	[1,2]206	—	(<0.05)	—	(0.03)	—	—	—	—	—	[8]U
ER-20-4 shallow	[2]2.42	—	U	—	U	—	—	—	—	—	[8]U
ER-20-5-1	—	0.16	(0.03)	(0.05)	0.07	0.10	—	—	—	—	[8]U
ER-20-5-3	—	0.17	(0.02)	(0.06)	0.14	0.12	—	—	—	—	[8]U
ER-20-7	—	[1,2]9.5	0.10	(0.04)	0.24	0.23	—	U	U	—	[8]U
ER-20-8 *deep (main lower zone)*	(0.07)	0.12	[1,2]1.2–4.0	0.25	0.65	[4]0.17	—	—	—	(0.02)	[8]U
ER-20-8 *intermediate (main upper zone)*	U	(0.04)	[1,2]0.22–16	0.34	0.61	[4](0.05)	—	U	—	(0.03)	[8]U
ER-20-8 *shallow*	—	0.07	[2]0.26–0.8	0.46	0.60	[5](0.15)	—	(0.02)	U	U	[8]U
ER-20-8-2	U	—	0.38	[1,2]6.0	—	—	(0.03)	—	—	—	—
ER-20-11	—	—	—	—	[1]112	—	—	—	(0.02)	(0.03)	—
ER-EC-1	—	—	(0.04)	(0.05)	—	0.12	—	0.07	0.08	(0.07)	—
ER-EC-2A	—	—	U	—	U	—	—	(0.04)	0.05	(0.04)	[8]U
ER-EC-5	—	—	—	—	—	—	—	—	—	(0.04)	—
ER-EC-6 *deep*	—	(0.08)	0.13	(0.04)	0.45	0.55	[6](0.04)	U	—	(0.03)	[8](0.05)
ER-EC-6 *intermediate*	—	(0.07)	0.16	0.10	0.76	0.41	[6](0.05)	U	(0.03)	(0.03)	[8](0.04)
ER-EC-6 *shallow*	—	(0.09)	0.20	0.13	0.85	0.45	[6](0.04)	—	(0.02)	U	[8](0.04)
ER-EC-8	—	—	—	—	U	—	—	—	U	(0.02)	[8]U
ER-EC-11 *deep (main lower zone)*	—	0.09	0.18	—	0.71	[1,2]126	[6](0.03)	U	(0.02)	(0.04)	[8]U
ER-EC-11 *intermediate (main upper zone)*	—	0.10	0.16	0.13	0.71		(0.04)	U	(0.02)	(0.04)	[8]U
ER-EC-11 *shallow*	—	0.13	0.22	0.12	0.87	[2]1	(0.04)	U	(0.02)	—	[8]U
ER-EC-12 *deep*	—	—	0.10	—	0.21	—	[2]U	(0.03)	U	(0.04)	[8]U
ER-EC-12 *intermediate (main lower zone)*	—	—	[3]0.08	—	[3]0.06	—	[1,2,3]457	—	—	[3](0.08)	[8]U
ER-EC-12 *shallow (main upper zone)*	—	—	(0.03)	—	0.09	—	[1,2,3]371	0.06	0.05	0.19	[8]0.06
ER-EC-13 *deep (main lower zone)*	—	—	U	—	U	—	—	[3]1.7	[1]293	0.09	[8]U
ER-EC-13 *intermediate (main upper zone)*	—	—	U	—	U	—	—	[1,3]59	2	0.09	[8]U
ER-EC-13 *shallow*	—	—	U	—	U	—	—	[2]0.1	[2]0.02	0.08	[8]U

Table 6. Summary of observed drawdown for pumping- and observation-well pairs during multiple-well aquifer testing at Pahute Mesa, Nevada National Security Site, 2009–14.—Continued

[**Well names** are listed in alphabetical order. Bold part of name is well site as shown on figure 1. Wells pumped during multiple-well aquifer testing. Values represent estimated maximum detected drawdown in feet, determined by matching measured water levels in the observation well to an analytically modeled curve of non-pumping and pumping responses. Values in parantheses represent ambiguous estimates. U, undetected; —, not estimated; <, less than]

Observation-well name	Pumping-well name and associated drawdown (feet)										
	ER-20-4 main	ER-20-7	ER-20-8 main upper and lower zones	ER-20-8-2 main	ER-20-11 main	ER-EC-11 main	ER-EC-12 main upper and lower zones	ER-EC-13 main upper zone	ER-EC-13 main lower zone	ER-EC-14 main upper and lower zones	ER-EC-15 main upper, intermediate, and lower zones
ER-EC-14 *deep (main lower zone)*	—	—	—	—	(0.04)	—	—	—	0.08	[1,3]1.1–12	[8](0.03)
ER-EC-14 *shallow (main upper zone)*	—	—	—	—	(0.01)	—	—	—	0.07	[1,3]2.2–137	[8](0.03)
ER-EC-15 *deep (main lower zone)*	—	—	U	—	—	—	(0.09)	(0.03)	[4](0.02)	[7]0.25	[1]90
ER-EC-15 *intermediate (main intermediate zone)*	—	—	U	—	[9]U	—	(0.05)	0.07	[4]U	[7]0.39	[1]146
ER-EC-15 *shallow (main upper zone)*	—	—	U	—	[4,9]U	—	(0.05)	0.08	0.08	[7]0.22	[1]94
UE-18r	—	—	—	—	—	—	—	—	—	U	—

[1] Drawdown is correlated with well losses.

[2] Drawdown is correlated with temperature-induced water-level change.

[3] Drawdown is correlated with leakage across packer or bridge plug.

[4] Transducer failed and was replaced near the start of or during the aquifer test. Estimate is uncertain because a step change between transducer measurements was applied.

[5] Drawdown is uncertain because analysis period began during the end of the constant-rate test and spanned only 14 days.

[6] Drawdown is uncertain because water levels are still influenced by drawdown response to ER-20-8 main pumping.

[7] Drawdown uncertain because analysis period began during aquifer testing.

[8] Drawdown from ER-EC-15 main pumping is obscured by large and prolonged drawdown from ER-20-11 main pumping.

[9] Drawdown uncertain because antecedent and recovery data are limited.

expansion. For example, measured water levels rose 15 ft in the pumping well during the *ER-EC-11 main* aquifer test (fig. 9). Temperatures near the static water level in *ER-EC-11 intermediate* rose from 41 to 51 °C during the constant-rate test. This equates to a water-level rise of 10 ft in a 2,000-ft column of water if temperatures did not change at the pumped interval (fig. 9*B*). Pumping rates declined from 318 to 300 gal/min, but this can only explain 6 ft of the observed rise. Actual temperature changes in long water columns below the transducers remain unknown, which is why transmissivity estimates from single-well pumping tests remain uncertain.

The transmissivity estimate in *ER-EC-14 main lower zone* was based on specific capacity because water levels inexplicably rose more than 2 ft during the constant-rate pumping test (fig. 8*C*). A pumping rate of 265 gal/min was sustained with little variation, so declining discharge could not explain the rise (fig. 8*C*). Water-level rise could not be explained easily by thermal expansion because the transducer was deployed next to the pumped interval, 1,185 ft below the static water level. The rise could reflect well development, heating below the pumped interval, or another unexplained factor. The unexplained signal obscured the drawdown, regardless of the cause, rendering the aquifer-test results inconclusive. A transmissivity of 30,000 ft^2/d was estimated for *ER-EC-14 main lower zone* by the local, power-law relation between specific capacity and transmissivity (table 5).

Transmissivity estimates from single-well aquifer test interpretations ranged from less than 1 ft^2/d at *ER-EC-12 intermediate* to about 100,000 ft^2/d at *ER-20-8 deep*. Although 9 of the 16 estimates were uncertain, the estimates represent a first approximation of formation hydraulic properties. Transmissivity estimates were less than 150 ft^2/d for *ER-EC-12 intermediate*, *ER-EC-15 intermediate*, and *ER-EC-15 deep*, which are open to the TCA, TCA, and TSA, respectively. Transmissivity estimates from wells screened in the TSA exhibited the most variation, ranging from 40 ft^2/d at *ER-EC-15* deep to 100,000 ft^2/d at *ER-20-8 deep*. The transmissivity of this unit appeared to decrease from the NTMMSZ toward the Timber

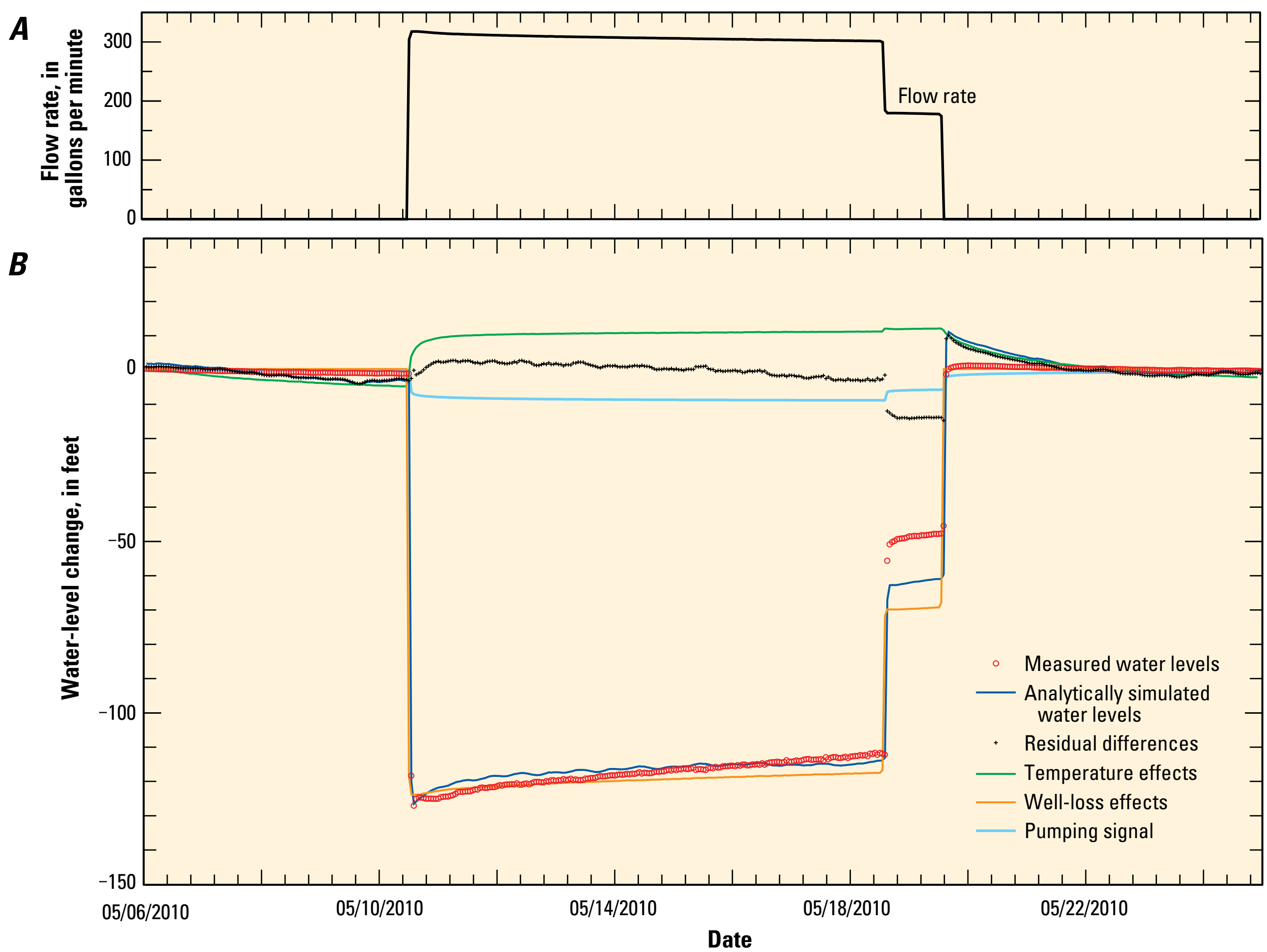

Figure 9. Well data for the Pahute Mesa, Nevada National Security Site, May 2010: *A*, discharge in *ER-EC-11 main* and *B*, the water-level response in *ER-EC-11 deep* to pumping *ER-EC-11 main*. Water-level responses in *ER-EC-11 deep* include well loss, temperature effects, and pumping.

Mountain caldera complex structural margin (TMCCSM). In the TMCC, transmissivities in the RMWTA ranged from a minimum of 700 ft^2/d at well *ER-EC-14 shallow* to roughly 30,000 ft^2/d at *ER-EC-14 deep*, indicating that this unit is highly heterogeneous.

Transmissivity trends by depth were inconclusive at the five well sites with multiple pumping wells (table 5). Estimates at well sites ER-EC-12, ER-EC-13, and ER-EC-15 generally decreased with depth, whereas estimates at well site ER-EC-14 increased. At well site ER-20-8, transmissivity estimates decreased from the SPA (*ER-20-8-2*) to the TCA (*ER-20-8 intermediate*) and increased from the TCA to the TSA (*ER-20-8 deep*).

Transmissivity estimates from single-well aquifer tests were affected minimally by choice of analytical method (table 5). Transmissivity estimates for any single well were within a factor of 2 for all analytical methods and aquifer tests evaluated, with the exception of the *ER-EC-15 intermediate* aquifer test. Estimates at well *ER-EC-15 intermediate* varied by a factor of 6, but were small regardless of the method used (from less than 20 ft^2/d using a water-level model to 130 ft^2/d using nSights software; table 5).

Multiple-Well Aquifer Tests

Multiple-well aquifer tests, where drawdowns were detected as much as 3 miles or more from pumped wells, greatly increased the volume of aquifers characterized (fig. 10). Drawdowns between 204 pumping- and observation-well pairs were estimated using water-level models. Drawdowns between pumping and observation wells investigated an area greater than 50 mi^2 (fig. 10).

The responses from pumping several wells at different depths beneath a well site typically were interpreted as one multiple-well aquifer test because resulting drawdowns in distant observation wells could not be differentiated easily. These well sites were pumped within a two month period, so recovery from pumping the first well was incomplete before pumping in the second well began. For example, pumping in *ER-20-8 main lower zone* began 18 days after pumping in *ER-20-8 main upper zone* ceased, and water levels in observation well *ER-EC-6 shallow* were still recovering from pumping the *upper zone* (fig. 11). The combined effect of pumping from multiple zones was simulated by superimposing Theis models for each pumping schedule. This approach produced a single combined-drawdown estimate.

Drawdown Detection

Drawdown detection was classified as undetected, detected, or ambiguous (table 6) on the basis of the signal-to-noise ratio (Garcia and others, 2013) and other factors. Signal and noise are defined as the analytically simulated maximum drawdown in a well during an aquifer test and the water-level model RMS error, respectively. Environmental (non-pumping) fluctuations in the water-level record often exceed maximum drawdown from pumping at distant observation wells. Drawdown detection becomes ambiguous when the signal-to-noise ratio is low or where correlation exists between environmental fluctuations and pumping signals. Drawdown was classified as undetected where the signal-to-noise ratio was less than two, indicating drawdown could not be reliably differentiated from the noise. Drawdown was classified as detected where the signal-to-noise ratio was greater than 10, drawdown was above a detection threshold of 0.05 ft, and correlation with environmental water-level fluctuations was unlikely. The detection threshold of 0.05 ft is subjective and conservative—likely greater than the actual detection limit. Correlation is unlikely where pumping signals are sharply defined (saw-tooth pattern) or a long period of recovery is observed. Drawdown was classified as ambiguous when the signal-to-noise ratio ranged between 2 and 10.

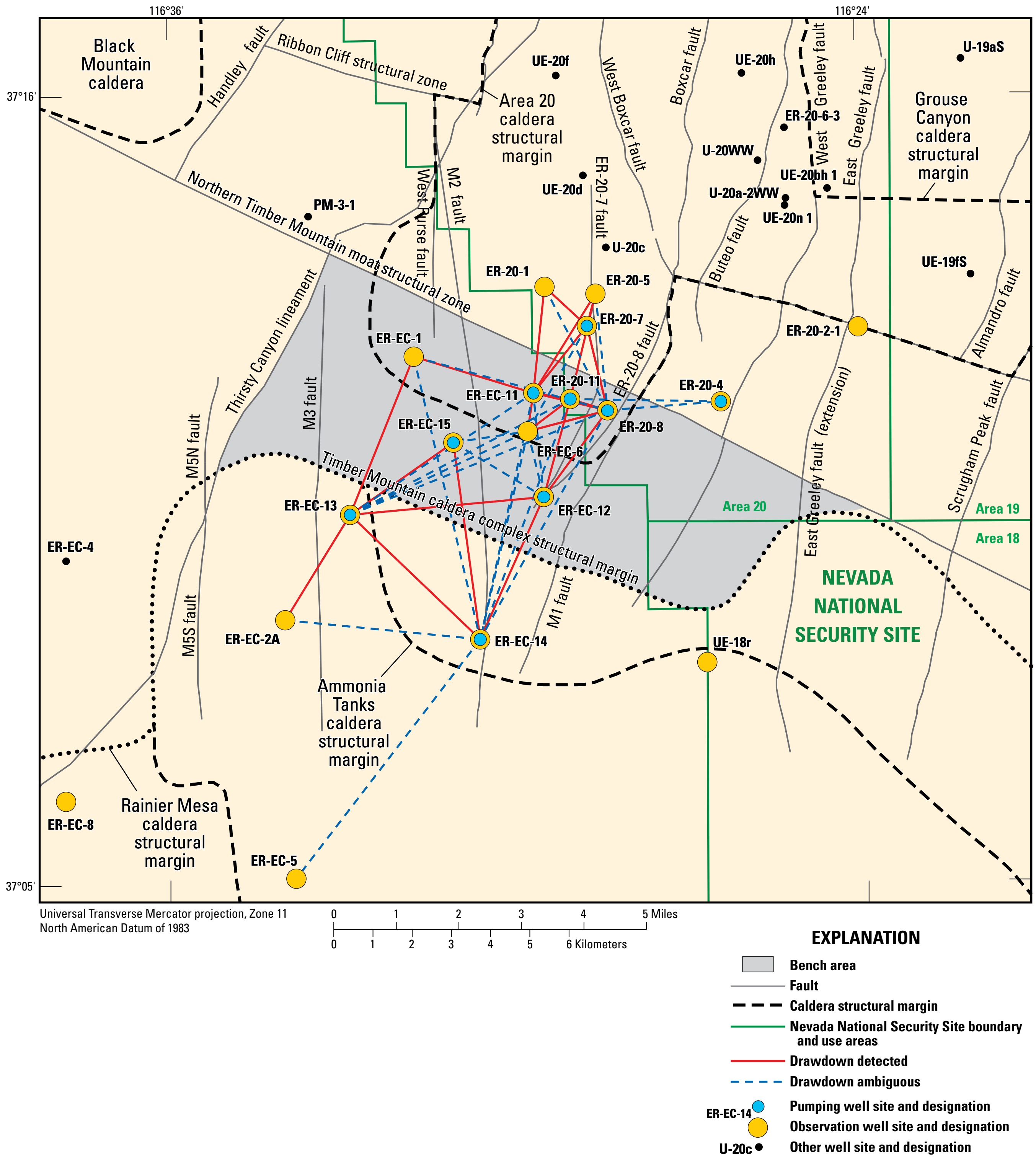

Figure 10. Hydraulic connections between pumping- and observation-well pairs, Pahute Mesa, Nevada National Security Site and vicinity.

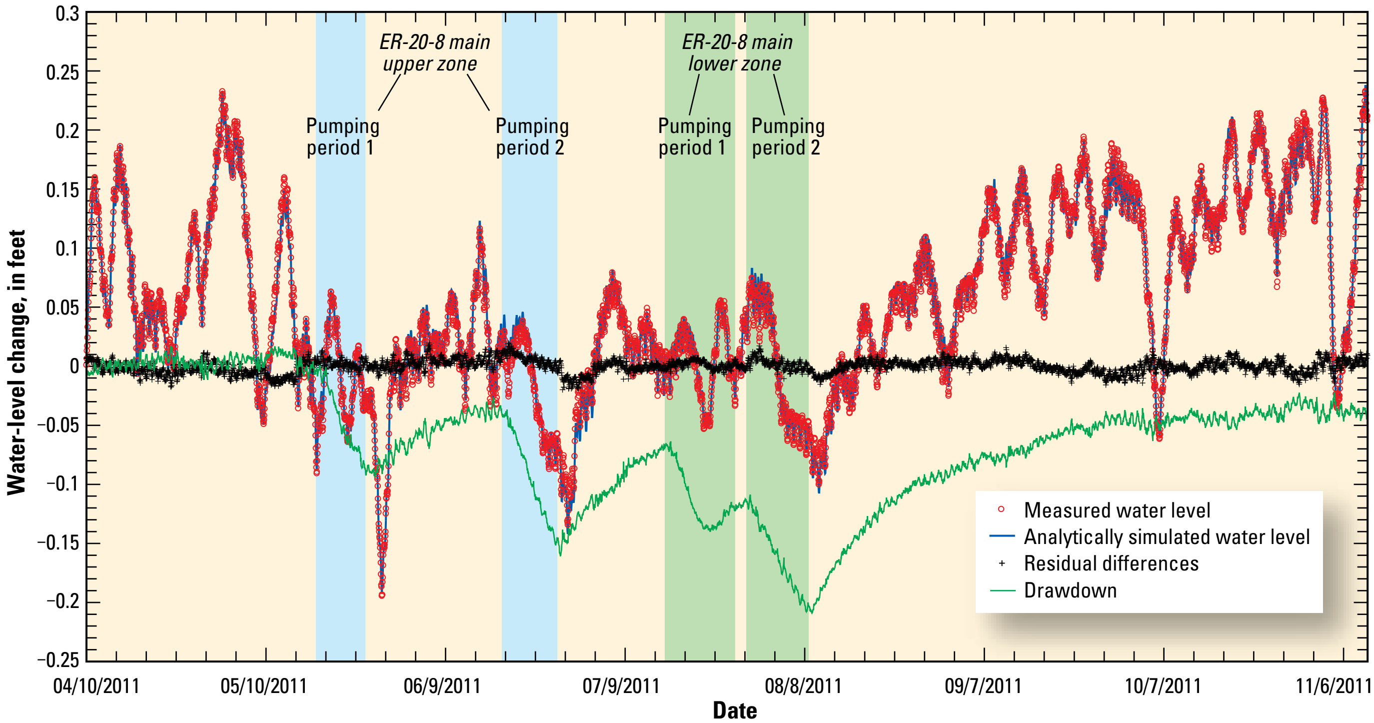

Figure 11. Drawdown in *ER-EC-6 shallow* in response to consecutive pumping in *ER-20-8 main upper and lower zones*, Pahute Mesa, Nevada National Security Site and vicinity, April–November 2011.

Analytically simulated water levels matched measured water levels in observation wells evaluated during the 16 multiple-well aquifer tests with root-mean-square errors between 0.002 and 0.05 ft (appendix 2). Similar root-mean-square errors were obtained for observation wells at pumping-well sites (0.004–0.05 ft) and at distant observation wells (0.002 and 0.02 ft; appendix 2). Drawdown in wells at pumping-well sites ranged from 0.22 ft (well *ER-20-8 intermediate* response to *ER-20-8 main lower zone* pumping) to 2.42 ft (*ER-20-4 shallow* response to *ER-20-4 main* pumping). Detected drawdown ranged from 0.05 to 0.87 ft at distant observation wells (table 6).

Despite the good fit among measured and analytically simulated water levels, drawdown estimates in observation wells at pumping-well sites were less certain than in wells beyond pumping-well sites because of well construction and proximity to the pumped well. Leakage across bridge plugs and packers affected drawdowns in *ER-EC-12 intermediat*e and *ER-EC-13 deep and intermediate*. Packer leakage is evident when most drawdown in the unpumped interval occurs during the first hour of aquifer testing, and there is very little additional drawdown during the remaining test period. For example, leakage rates of less than 0.01 gal/min across the packer could explain the observed drawdown in *ER-EC-12 intermediate* from pumping in *ER-EC-12 main upper zone* (adjacent to *ER-EC-12 shallow*; fig. 12). If simulated as a pumping signal, leakage rates as low as 0.006 gal/min from *ER-EC-12 main lower zone* (next to *ER-EC-12 intermediate*) into *ER-EC-12 main upper zone* would draw down water levels more than 8 ft, if transmissivity was 0.1 ft^2/d and the storage coefficient was 0.001 (dimensionless). There was also thermal heating and cooling of the water column because pumping and observation wells were in the same wellbore (table 6).

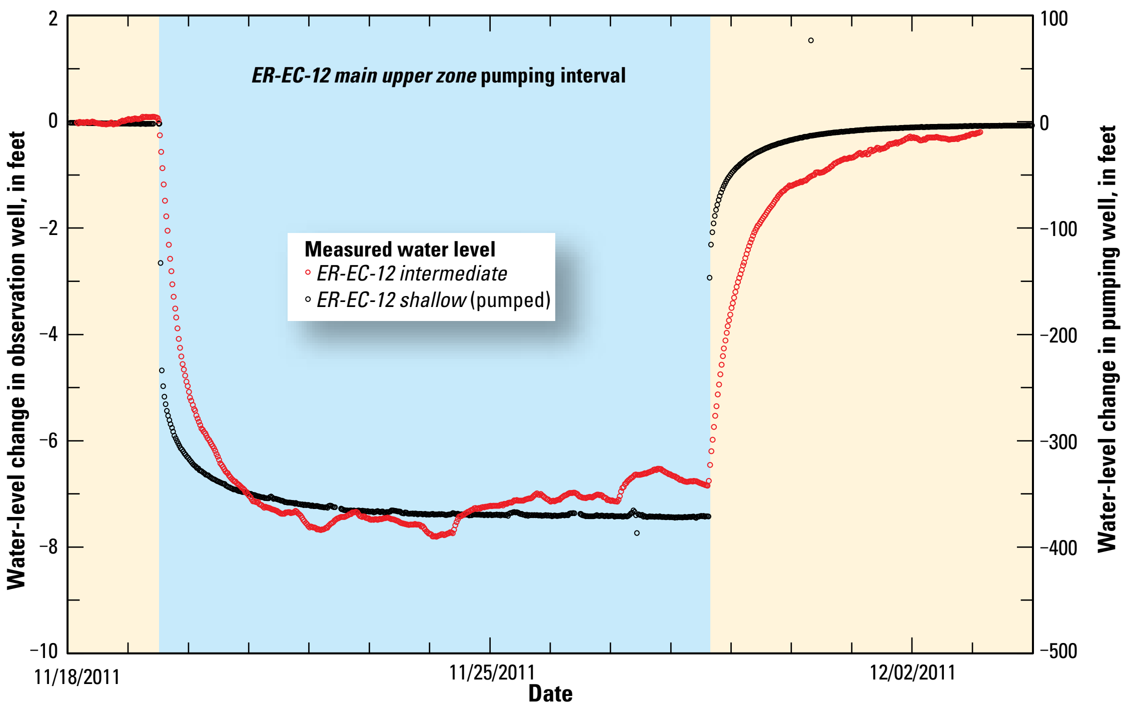

Figure 12. Water-level response in *ER-EC-12 intermediate* to pumping in *ER-EC-12 shallow* as a result of a leaky packer and bridge plug, Pahute Mesa, Nevada National Security Site and vicinity, November–December 2011.

Drawdown classifications shown in figure 13 exhibit detected and ambiguous drawdown responses to pumping. Water levels in *ER-EC-6 intermediate* declined about 0.8 ft during pumping in *ER-20-11 main*, which was about 0.9 mi away. Wells *ER-20-11 main* and *ER-EC-6 intermediate* penetrate the BA and are in the same structural block in the bench area (fig. 2; appendix 1). An ambiguous drawdown of 0.02 ft was observed in *ER-EC-11 intermediate* from pumping *ER-EC-13 main lower zone*, which is about 3.5 mi to the southwest (figs. 2, 13*B*).

Drawdowns were detected at distances of as much as 3.2 mi from pumping wells and across major faults and structural blocks. The maximum distance where drawdown was detected was between pumping-well *ER-EC-14 main* and observation-wells *ER-EC-15 deep*, *intermediate*, and *shallow* (fig. 10). These pumping and observation-well pairs penetrated distinct structural blocks that are separated by the TMCCSM and penetrated distinct HSUs (table 2; appendix 1).

Pumping signals from *ER-EC-14 main* were detected at a farther distance than those from any other aquifer test. Detected drawdown extended laterally 3.2 mi to *ER-EC-15 deep*, *intermediate*, and *shallow* (fig. 10). Drawdown from pumping *ER-EC-14 main* also was detected at *ER-EC-12 shallow* and *ER-EC-13 deep*, *intermediate*, and *shallow*. Despite signal-to-noise ratios of 10 or more at *ER-EC-1*, *ER-20-11 main*, and *ER-20-8 intermediate*, drawdown estimates were considered ambiguous because values were below a detection threshold of 0.05 ft and recovery was not observed (appendix 2). Water-level model RMS errors for these wells increased substantially when pumping signals were excluded from analyses, however, indicating that drawdown estimates below 0.05 ft could be real. An ambiguous drawdown estimate at *ER-EC-5* of 0.04 ft was below the detection limit and had a signal-to-noise ratio of 8, but the drawdown signal was well defined and clearly exhibited recovery (appendix 2). If drawdown at *ER-EC-5* was real, the pumping signal was

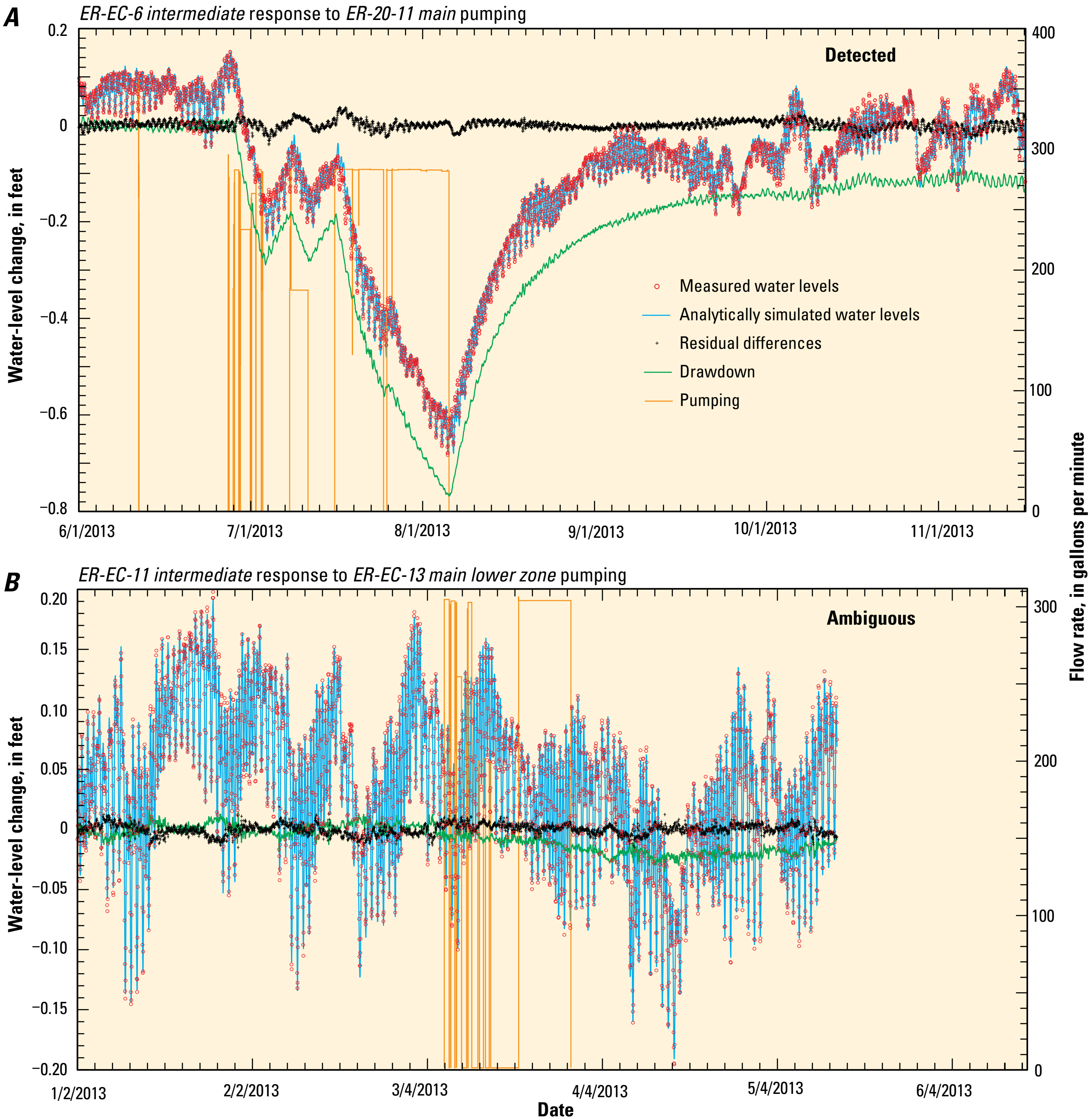

Figure 13. Measured and analytically simulated water levels, drawdown, and fitting residuals from water-level modeling in observation wells, Pahute Mesa, Nevada National Security Site and vicinity, January–November 2013: *A*, *ER-EC-6 intermediate* during pumping in *ER-20-11 main* and *B*, *ER-EC-11 intermediate* during pumping in *ER-EC-13 main lower zone*.

evident at a distance of nearly 5 mi from the RMWTA to the ATWTA. Considering that single-well aquifer-test transmissivity estimates from *ER-EC-5* and *ER-EC-14* aquifer tests were about 14,000 ft^2/d (U.S. Department of Energy, 2002c) and 30,000 ft^2/d (table 5), respectively, distant signal propagation is possible.

The *ER-20-11 main* aquifer test was the largest aquifer test during the study period, with a total of 10.8 Mgal of groundwater withdrawn from a single pumping well. Drawdown from pumping *ER-20-11 main* was detected at 15 observation wells, which was more than for any other multiple-well test (figs. 10, 14).

Drawdowns from the *ER-EC-15 main upper-zone* aquifer test were obscured because water levels were still recovering from the *ER-20-11 main* aquifer test. The *ER-20-11 main* constant-rate pumping test was done within 44 days of and discharged more than 3 times the volume discharged from the *ER-EC-15* aquifer test (table 3). Large, distant observation-well drawdowns from the *ER-20-11 main* aquifer test (up to 0.87 ft, table 6) and slow and prolonged recovery rates limited drawdown detection from testing at the ER-EC-15 well site, despite a moderate estimated transmissivity of 3,200 ft^2/d in *ER-EC-15 shallow* (Table 5).

Drawdown from pumping *ER-EC-13 main* was detected across the TMCCSM at *ER-EC-1*, *ER-EC-15 shallow* and *intermediate*, and *ER-EC-12 shallow* in the bench (fig. 10). Although drawdown was small in distant observation wells, a 6-month period between *upper* and *lower zone* pumping in *ER-EC-13 main* provided the opportunity for repeat analyses. Drawdown responses in *ER-EC-1* and *ER-EC-2A* from pumping *ER-EC-13 main upper* and *lower zones* were small and ambiguous, respectively, but similar responses observed from both *upper* and *lower zone* testing analyses confirmed drawdown detection and provided support for the drawdown estimation method (fig. 15; appendix 2).

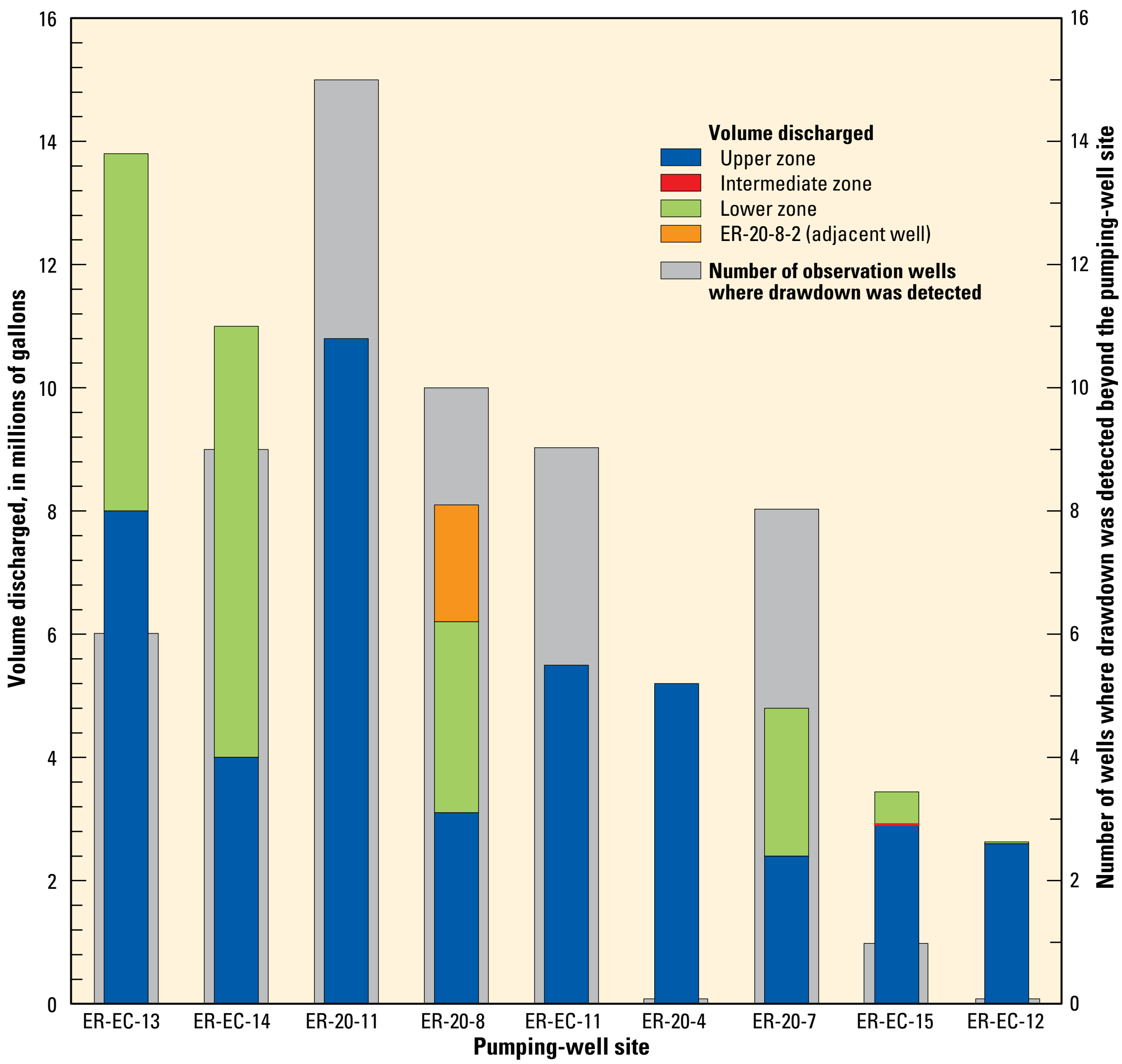

Figure 14. Drawdown detection in observation wells during the 16 multiple-well aquifer tests, and the volume of water discharged during each test, Pahute Mesa, Nevada National Security Site and vicinity, 2009–14.

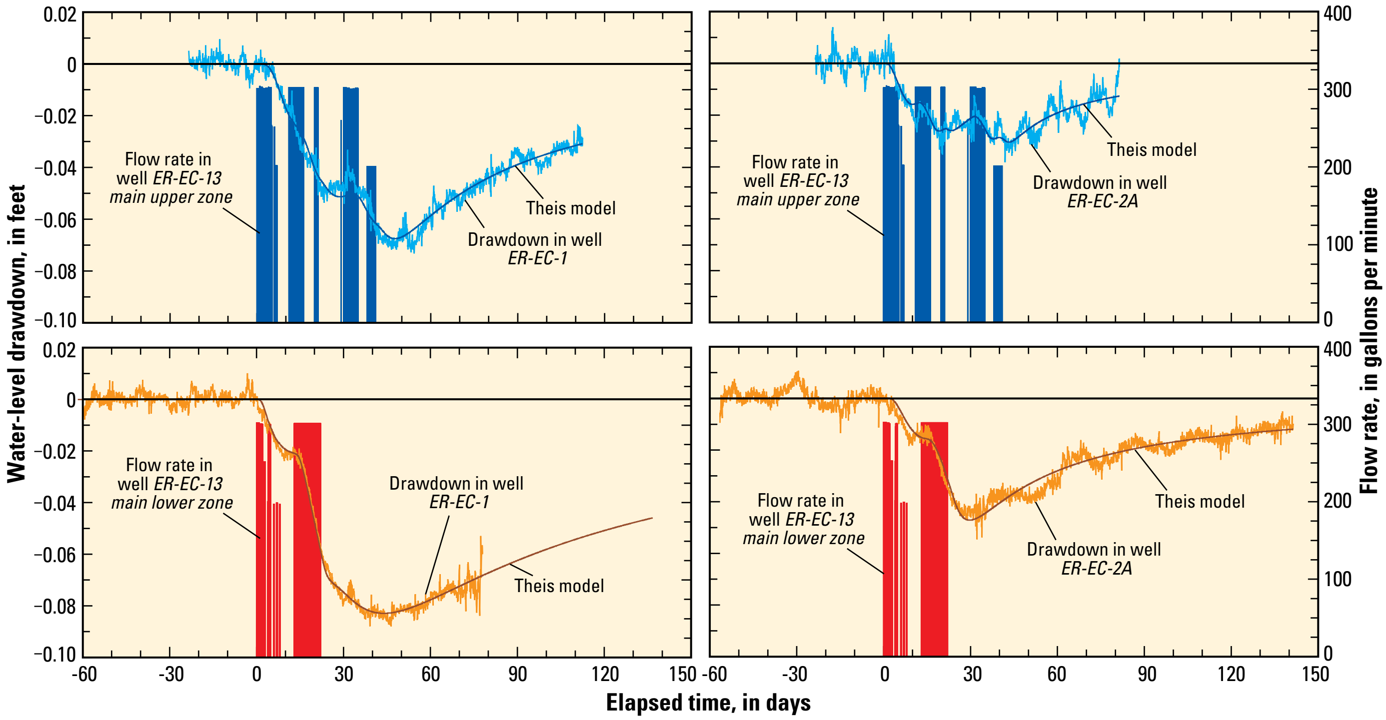

Figure 15. Distant drawdown responses in *ER-EC-1* and *ER-EC-2A* to pumping *ER-EC-13 main upper and lower zones*, Pahute Mesa, Nevada National Security Site and vicinity, April 2012–August 2013.

Drawdowns from pumping *ER-20-4 main* were undetected or ambiguous at distant observation wells, indicating the ER-20-4 well site is relatively isolated from other study-area wells (table 6; fig. 10). Ambiguous drawdowns were observed in *ER-20-8 deep* from pumping *ER-20-4 main* (0.07 ft, table 6); the ambiguity might be related to correlation between environmental fluctuations and the pumping signal indicated in the linear drawdown trend (appendix 2).

Hydraulic Connections

Hydraulic responses between pumping and observation wells at the pumping-well site provide insight into vertical heterogeneity in the HSUs. For example, drawdown observations at the ER-EC-13 well sites indicated a low-permeability unit likely separates pumping and observation wells. Wells *ER-EC-13 main lower* and *upper zone*s are completed in the same HSU (FCULFA4; table 2; appendix 1), but drawdowns were not observed in *ER-EC-13 main lower zone* while *ER-EC-13 main upper zone* was pumped, and vice versa. The spatial extent of this low-permeability unit is limited because similar drawdowns at the ER-EC-14 well site were observed from pumping either *ER-EC-13 main lower zone* or *ER-EC-13 main upper zone* (table 6).

Limited drawdown beyond ER-EC-12 and ER-EC-15 pumping-well sites and low-transmissivity estimates in most pumping-well completions at these sites indicated the presence of a low-transmissivity zone in the TCA and TSA HSUs in the south-central bench area. Transmissivities of 0.1–400 ft^2/d in *ER-EC-12 main upper* and *lower zones* and transmissivities below 50 ft^2/d in *ER-EC-15 intermediate* and *deep* (table 5) were estimated from single-well aquifer tests in the TCA and TSA HSUs. Low transmissivities limited the total volumes discharged from ER-EC-12 and ER-EC-15 well sites (2.3 and 3.5 Mgal, respectively) relative to volumes discharged in northern bench wells (table 3; fig. 2), despite similar HSUs tested (TCA and TSA; table 2). The small volumes pumped at these well sites and lack of signal propagation beyond the ER-EC-12 pumping-well site indicated that the TCA and TSA units near ER-EC-12 and ER-EC-15 well sites in the south-central bench are less permeable than are similar units near the NTMMSZ. The BA, TCA, and TSA units open to well *ER-EC-6*, within the central Bench area, also exhibit low transmissivity with respect to similar units near the NTMMSZ. A single-well aquifer-test analysis by U.S. Department of Energy (2002e) provided a transmissivity estimate of about 1,000 ft^2/d across all units penetrated by well *ER-EC-6*.

Detected drawdowns in distant observation wells indicated that pumping signals propagated across nearly all structural features between the pumping- and observation-well pairs (fig. 10). Drawdown propagated across the NTMMSZ and TMCCSM, which bound the bench, and Area 20 and Ammonia Tanks caldera structural margins. Drawdown also propagated across several faults, including ER-20-7, ER-20-8, M2, and M3 faults (fig. 10). Drawdown detection across eastern study-area faults, including the Boxcar, West Greeley, and East

Greeley faults, most likely was limited by distance between pumping- and observation-well pairs. Pumping-signal propagation across the Boxcar fault was ambiguous. Pumping-signal propagation was undetected across the West Greeley fault during these aquifer tests, but was detected previously from pumping well U-20WW (Garcia and others, 2011). The shortest lateral distance between pumping and observation wells straddling the Boxcar fault was nearly 2 mi, whereas the shortest distance between wells straddling the West Greeley fault was 2.6 mi.

Drawdown-detection patterns between pumping- and observation-well pairs reflected radial propagation of pumping signals, rather than propagation through preferred pathways. Detected drawdown from pumping ER-20-7, ER-20-8, ER-EC-11, and ER-20-11 well sites, north of the bench and in the bench, was observed to the north, west, south, and east (excluding the ER-20-8 well site). Drawdown from pumping in the TMCC also was detected in all cardinal directions when monitored within about 3 mi. Radial signal propagation across most layered and juxtaposed HSUs indicated that permeable zones exist throughout the volcanic rocks beneath Pahute Mesa.

Integrated Aquifer-Test Analysis

Aquifer test results were integrated by simultaneously interpreting observed drawdowns from all aquifer tests with multiple groundwater-flow models and a single hydrostratigraphic framework model. The integrated analysis ensured that hydraulic properties of volcanic rocks underlying Pahute Mesa were consistent with observed hydraulic connections among wells and across structural features for all aquifer tests. Hydraulic-property distributions in complexly layered and faulted volcanic rocks are three-dimensional and heterogeneous; therefore, numerical methods are required to solve the groundwater-flow equations. Hydrogeologic complexities precluded practical application of analytical solutions because of their inherent simplifying assumptions, for example those related to aquifer homogeneity and isotropy.

Integration of multiple groundwater-flow models allows for the simultaneous calibration and interpretation of the 16 multiple-well aquifer tests. Drawdowns from pumping in the complexly layered and faulted volcanic rocks were simulated with MODFLOW (Harbaugh and others, 2000). Multiple groundwater-flow models allowed grid refinement near each pumping well and different pumping schedules specific to each aquifer test. Multiple groundwater-flow models also facilitated independent aquifer-test assessments and provided assurance that simulated drawdowns and sensitivities were computed and extracted correctly.

The integrated analysis of multiple groundwater-flow models ensured that a single, consistent set of hydraulic properties was estimated for the study area. Inconsistent hydraulic-property distributions would be estimated if each aquifer test was interpreted individually because drawdown responses from multiple aquifer tests traverse similar volumes of rock. An integrated analysis of multiple aquifer tests also reduced hydraulic-property estimate uncertainty along the periphery of the spatial extent where drawdowns were detected, which was limited by the distribution of existing wells during early aquifer testing (2009–10).

Hydrostratigraphic Framework

The groundwater-flow models incorporate a single three-dimensional hydrostratigraphic framework model (HFM) to estimate consistent hydraulic-property distributions in volcanic rocks beneath Pahute Mesa. Many conceptual HFMs exist for distributing hydraulic properties of Pahute Mesa, including those where hydraulic properties of mapped faults and structural zones differ from hydraulic properties of the HSUs. The HFM used in this study does not incorporate distinct hydraulic properties of faults or structural zones, but simply juxtaposes HSUs affected by faults and structural zones accounting for vertical and horizontal offsets imposed by the features. This approach is consistent with observed pumping responses.

Phase II Hydrostratigraphic Framework Model

The HFM for this study was created by sampling the Phase II HFM of the Pahute Mesa-Oasis Valley area (Navarro, written commun., 2014) with a three-dimensional array of points, spaced 984 ft (300 m) in the X and Y directions and 164 ft (50 m) in the Z direction, and querying the Phase II HFM at each point for the hydrostratigraphic unit present at that location. The resultant array of points was built into a three-dimensional rectangular grid suitable for import into groundwater-flow models (fig. 16). The lateral extent of the rectangular grid was guided by hydraulic responses from aquifer testing. Horizontal- and vertical-grid spacing was selected to capture laterally extensive HSUs and both vertically massive HSUs and thin-permeable intervals embedded within. The Phase II HFM was constructed from wellbore data, refined cross-sections using data from newly drilled wells (Sigmund Drellack, National Security Technologies, LLC, written commun., 2011), and HSU designations from the Pahute Mesa Corrective Action Unit Phase I HFM (Bechtel Nevada, 2002; fig. 16). The Phase II HFM is a three-dimensional rectangular grid about 82,000-ft long from south to north and about 73,000-ft wide from west to east (fig. 1). The grid is about 8,700-ft thick, with a vertical extent ranging from the highest land surface at 6,972 ft above sea level to 1,722 ft below sea level. The numerical grid has uniform longitudinal, transverse, and vertical discretization with 83 columns, 74 rows, and 52 layers.

The three-dimensional Phase II HFM grid is composed of 55 HSUs in the aquifer-test study area (fig. 3). The block diagram shown in figure 16 is a subset of the entire Phase II HFM rectangular grid and shows the level of subsurface geologic detail contained in the Phase II HFM in the bench area. The

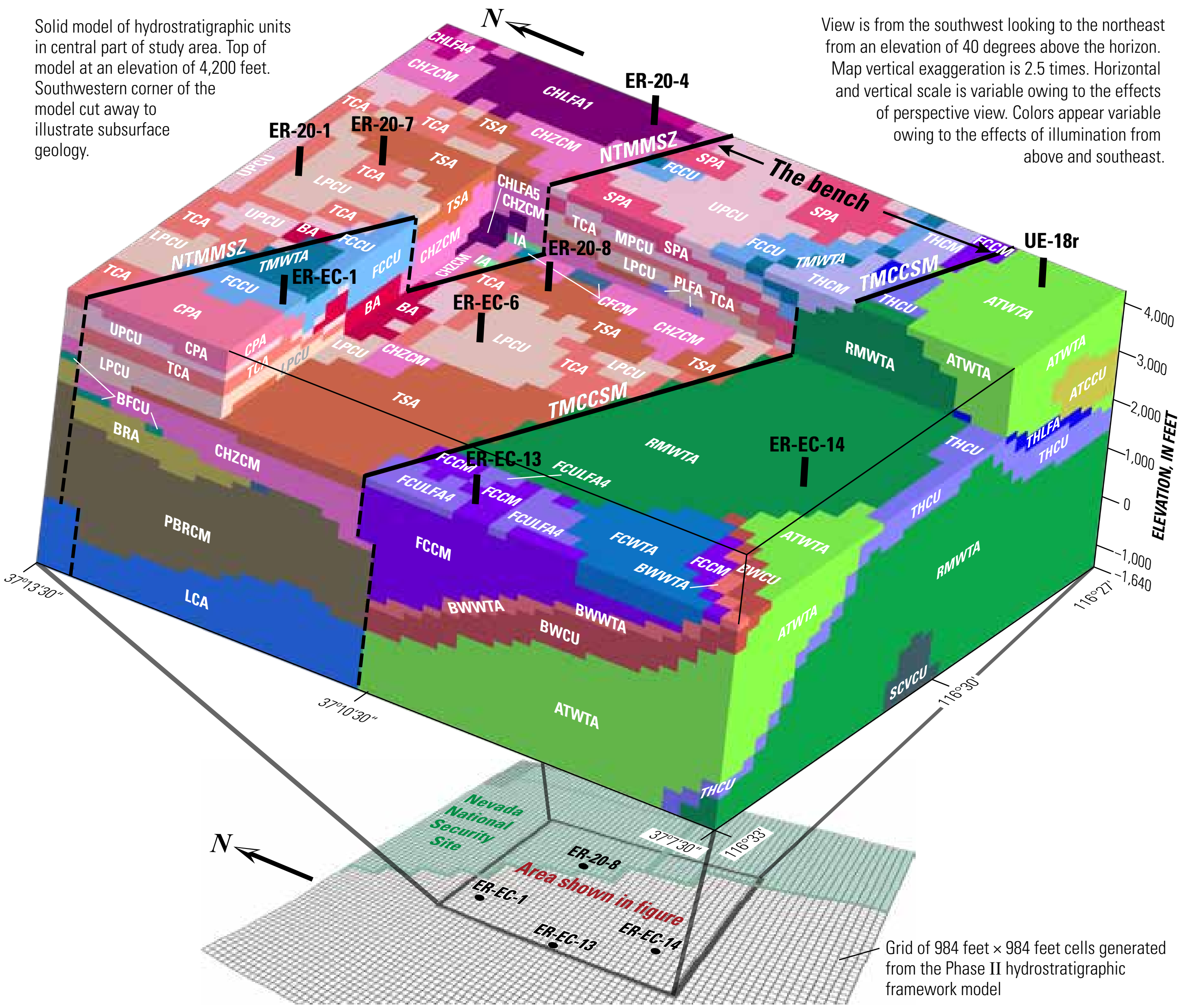

EXPLANATION

Hydrostratigraphic units

FCCM	Fortymile Canyon composite unit
FCULFA4	Fortymile Canyon upper lava-flow aquifer 4
FCWTA	Fortymile Canyon welded-tuff aquifer
BWWTA	Beatty Wash welded-tuff aquifer
BWCU	Beatty Wash confining unit
THLFA	Tannenbaum Hill lava-flow aquifer
THCM	Tannenbaum Hill composite unit
TMWTA	Timber Mountain welded-tuff aquifer
ATWTA	Ammonia Tanks welded-tuff aquifer
ATCCU	Ammonia Tanks caldera confining unit
THCU	Tannenbaum Hill confining unit
RMWTA	Rainier Mesa welded-tuff aquifer
FCCU	Fluorspar Canyon confining unit
CPA	Comb Peak aquifer
BA	Benham aquifer
UPCU	Upper Paintbrush confining unit
SPA	Scrugham Peak aquifer
MPCU	Middle Paintbrush confining unit
TCA	Tiva Canyon aquifer
LPCU	Lower Paintbrush confining unit
PLFA	Paintbrush lava-flow aquifer
TSA	Topopah Spring aquifer
CHZCM	Calico Hills zeolitic composite unit
CHLFA	Calico Hills lava-flow aquifer 1–5
IA	Inlet aquifer
CFCM	Crater Flat composite unit
BFCU	Bullfrog confining unit
BRA	Belted Range aquifer
PBRCM	Pre-Belted Range composite unit
LCA	Lower carbonate aquifer
SCVCU	Silent Canyon volcanic confining unit

ER-EC-14 • **Well site shown on base map**

ER-EC-14 ▌ **Well site shown on block diagram**

Fault on top surface of block

Fault shown on vertical panel of block diagram. The 984-foot grid results in local abrupt offsets in fault trace

Three lava flows within the Calico Hills lava-flow aquifer are shown: CHLFA1, CHLFA4, and CHLFA5

NTMMSZ, Northern Timber Mountain moat structural zone; TMCCSM, Timber Mountain caldera complex structural margin

Figure 16. Subsection of the three-dimensional Phase II hydrostratigraphic framework model.

164-ft (50-m) vertical discretization preserved stratigraphic layering of volcanic units (fig. 16), but north of the TMCCSM, stratigraphic detail near boreholes did not always match well intercepts explicitly. There was occasional misalignment between well intercepts and the resampled HFM where well screens were near or intersected by HSU contacts that were generalized with the coarser HFM discretization.

Modification of Phase II Hydrostratigraphic Framework Model

The existing 55 HSUs in the Phase II HFM were subdivided and grouped into 22 modified HSUs (table 7) so that groundwater-flow models could replicate observed hydraulic responses between pumping and observation wells. Hydrostratigraphic-unit modification was warranted because the original Phase II hydrostratigraphic discretization was inconsistent with observed hydraulic responses from multiple-well aquifer testing. The Phase II HFM was modified through an iterative process using observed drawdowns and hydraulic-property estimates from aquifer testing and insights from groundwater-flow model results. Here, HSU refers to original HSUs in the Phase II HFM (Navarro, written commun., 2014), and mHSU refers to modified HSUs that were developed for the modified Phase II HFM.

Timber Mountain Caldera Complex

The Timber Mountain caldera complex (TMCC) was grouped and divided into mHSUs on the basis of drawdown observations and single-well aquifer-test analyses. Groupings and divisions were largely guided by lithology and observed vertical heterogeneity at the three TMCC well sites where drawdowns were detected: ER-EC-2A, ER-EC-13, and ER-EC-14 (table 6). Groundwater-flow model simulations

Table 7. Existing and modified hydrostratigraphic units (HSUs) developed from the Phase II hydrostratigraphic framework model, Pahute Mesa, Nevada National Security Site.

[**Modified HSU:** formed by combining or splitting HSUs in the Phase II hydrostratigraphic framework model. **HSU:** Saturated HSUs from Phase II hydrostratigraphic framework model (Navarro, written communication, 2014) within each modified HSU. HSUs in bold type comprise the majority of the saturated thickness in each modified HSU. **Explanation for Modification:** justification for the combining or splitting of HSUs to form modified HSUs. **Abbreviations:** AA, Alluvial aquifer; ATCCU, Ammonia Tanks caldera confining unit; ATICU, Ammonia Tanks intrusive confining unit; ATWTA, Ammonia Tanks welded-tuff aquifer; BA, Benham aquifer; BFCU, Bullfrog confining unit; BMICU, Black Mountain intrusive confining unit; BRA, Belted Range aquifer; BWCU, Beatty Wash confining unit; BWWTA, Beatty Wash welded-tuff aquifer; CFCM, Crater Flat composite unit; CFCU, Crater Flat confining unit; CHLFA 1–5, Calico Hills lava-flow aquifers 1–5; CHVTA, Calico Hills vitric-tuff aquifer; CHZCM, Calico Hills zeolitic composite unit; CPA, Comb Peak aquifer; FCCM, Fortymile Canyon composite unit; FCCU, Fluorspar Canyon confining unit; FCLLFA, Fortymile Canyon lower lava-flow aquifer; FCULFA 1–4, Fortymile Canyon upper lava-flow aquifers 1–4; FCWTA, Fortymile Canyon welded-tuff aquifer; IA, Inlet aquifer; LCA, Lower carbonate aquifer; LCCU1, Lower clastic confining unit, thrusted; LPCU, Lower Paintbrush confining unit; MPCU, Middle Paintbrush confining unit; PBPCU, Post-Benham Paintbrush confining unit; PBRCM, Pre-Belted Range composite unit; RMICU, Rainier Mesa intrusive confining unit; RMWTA, Rainier Mesa welded-tuff aquifer; SCVCU, Silent Canyon volcanic confining unit; SPA, Scrugham Peak aquifer; TCA, Tiva Canyon aquifer; TCVA, Thirsty Canyon volcanic aquifer; THCM, Tannenbaum Hill composite unit; THCU, Tannenbaum Hill confining unit; THLFA, Tannenbaum Hill lava-flow aquifer; TMLVTA, Timber Mountain lower vitric-tuff aquifer; TMUWTA, Timber Mountain upper welded-tuff aquifer; TMWTA, Timber Mountain welded-tuff aquifer; TSA, Topopah Spring aquifer; UCCU, upper clastic confining unit; UPCU, Upper Paintbrush confining unit; WWA, Windy Wash aquifer; YVCU, Younger volcanic confining unit]

Modified HSU	Modified HSU name	HSU	Explanation for modification
Timber Mountain caldera complex			
mFCCM1	modified Fortymile Canyon composite unit 1	**FCCM**, FCULFA1, FCULFA2, FCULFA4	Combined FCCM above an elevation of 3,940 ft with shallow interbedded aquifers to form a horizontal, laterally extensive unit. Unit justified by observed vertical heterogeneity in ER-EC-13 aquifer-test results.
mFCCU1	modified Fortymile Canyon confining unit 1	FCCM, **FCULFA4**	Local confining unit between elevations of 3,940 and 3,280 ft. Unit is a circular disk with a 1-mi radius centered at the ER-EC-13 well site.
mFCCM2	modified Fortymile Canyon composite unit 2	FCCM, **FCULFA4**, FCWTA1	Combined FCCM between elevations of 3,280 and 2,950 ft with interbedded aquifers to form a horizontal, laterally extensive unit. Unit justified by observed vertical heterogeneity in ER-EC-13 aquifer-test results.
mFCCU2	modified Fortymile Canyon confining unit 2	FCCM, **FCULFA4**	Local confining unit between elevations of 2,950 and 2,625 ft. Unit is a circular disk with a 1-mi radius centered at the ER-EC-13 well site.
mFCCM3	modified Fortymile Canyon composite unit 3	FCCM, **FCULFA4**, FCWTA1	Combined FCCM between elevations of 2,625 and 2,300 ft with interbedded aquifers to form a horizontal, laterally extensive unit. Unit justified by observed vertical heterogeneity in ER-EC-13 aquifer-test results.
mFCCU3	modified Fortymile Canyon confining unit 3	**FCCM**	FCCM below an elevation of 2,300 ft, which is below all well screens in the FCCM. Forms a horizontal, laterally extensive confining unit.
mRMWTA1	modified Rainier Mesa welded tuff aquifer 1	FCCM, FCULFA3, FCWTA, BWWTA, BWCU, ATWTA, THCU, **RMWTA**	Combined units above an elevation of 3,445 ft to form a horizontal, laterally extensive unit. Unit justified by observed vertical heterogeneity in ER-EC-14 aquifer test results.
mRMWTA2	modified Rainier Mesa welded tuff aquifer 2	FCWTA, FCLLFA, BWWTA, BWCU, ATWTA, ATCCU, THCU, **RMWTA**	Combined caldera units between elevations of 3,445 and 2,300 ft to form a horizontal, laterally extensive unit. Unit justified by oberved vertical heterogeneity in ER-EC-14 aquifer test results.
mRMCM	modified Rainier Mesa composite unit	BWWTA, BWCU, ATWTA, ATCCU, THCU, **RMWTA**	Combined caldera units below an elevation of 2,300 ft, which is below the screened intervals of pumping and observation wells.
mICU	modified Intrusive confining unit	**SCVCU**, RMICU, ATICU	Combined intrusive confining units, which are deeper than the screened intervals of pumping and observation wells.

Table 7. Existing and modified hydrostratigraphic units developed from the Phase II hydrostratigraphic framework model, Pahute Mesa, Nevada National Security Site.—Continued

[**Modified HSU:** formed by combining or splitting HSUs in the Phase II hydrostratigraphic framework model. **HSU:** Saturated HSUs from Phase II hydrostratigraphic framework model (Navarro, written communication, 2014) within each modified HSU. HSUs in bold type comprise the majority of the saturated thickness in each modified HSU. **Explanation for Modification:** justification for the combining or splitting of HSUs to form modified HSUs. **Abbreviations:** AA, Alluvial aquifer; ATCCU, Ammonia Tanks caldera confining unit; ATICU, Ammonia Tanks intrusive confining unit; ATWTA, Ammonia Tanks welded-tuff aquifer; BA, Benham aquifer; BFCU, Bullfrog confining unit; BMICU, Black Mountain intrusive confining unit; BRA, Belted Range aquifer; BWCU, Beatty Wash confining unit; BWWTA, Beatty Wash welded-tuff aquifer; CFCM, Crater Flat composite unit; CFCU, Crater Flat confining unit; CHLFA 1–5, Calico Hills lava-flow aquifers 1–5; CHVTA, Calico Hills vitric-tuff aquifer; CHZCM, Calico Hills zeolitic composite unit; CPA, Comb Peak aquifer; FCCM, Fortymile Canyon composite unit; FCCU, Fluorspar Canyon confining unit; FCLLFA, Fortymile Canyon lower lava-flow aquifer; FCULFA 1–4, Fortymile Canyon upper lava-flow aquifers 1–4; FCWTA, Fortymile Canyon welded-tuff aquifer; IA, Inlet aquifer; LCA, Lower carbonate aquifer; LCCU1, Lower clastic confining unit, thrusted; LPCU, Lower Paintbrush confining unit; MPCU, Middle Paintbrush confining unit; PBPCU, Post-Benham Paintbrush confining unit; PBRCM, Pre-Belted Range composite unit; RMICU, Rainier Mesa intrusive confining unit; RMWTA, Rainier Mesa welded-tuff aquifer; SCVCU, Silent Canyon volcanic confining unit; SPA, Scrugham Peak aquifer; TCA, Tiva Canyon aquifer; TCVA, Thirsty Canyon volcanic aquifer; THCM, Tannenbaum Hill composite unit; THCU, Tannenbaum Hill confining unit; THLFA, Tannenbaum Hill lava-flow aquifer; TMLVTA, Timber Mountain lower vitric-tuff aquifer; TMUWTA, Timber Mountain upper welded-tuff aquifer; TMWTA, Timber Mountain welded-tuff aquifer; TSA, Topopah Spring aquifer; UCCU, upper clastic confining unit; UPCU, Upper Paintbrush confining unit; WWA, Windy Wash aquifer; YVCU, Younger volcanic confining unit]

Modified HSU	Modified HSU name	HSU	Explanation for modification
North of Timber Mountain caldera complex			
mFCCU	modified Fluorspar Canyon confining unit	AA, YVCU, TCVA, TMUWTA, TMWTA, THLFA, THCM, **FCCU**	Combined shallow HSUs north of TMCC. HSUs are contiguous and shallower than screened intervals of pumping and observation wells.
mCPA	modified Comb Peak aquifer	WWA, **CPA**, BA, SPA	Combined major shallow water-producing HSUs. HSUs are continguous.
mUPCU	modified Upper Paintbrush confining unit	PBPCU, **UPCU**	Combined contiguous confining units.
mMPCU	modified Middle Paintbrush confining unit	**MPCU**	
mTCA	modified Tiva Canyon aquifer	TMLVTA, **TCA**, PVTA	Combined contiguous water-producing HSUs.
mLPCU	modified Lower Paintbrush confining unit	**LPCU**	
mTSA	modified Topopah Spring aquifer	PLFA, **TSA**	Combined contiguous water-producing HSUs.
mCHLFA1	modified Calico Hills lava flow aquifer 1	**CHLFA1**	
mCHLFA5	modified Calico Hills lava flow aquifer 5	CHZCM, CHLFA2, CHLFA3, CHLFA4, **CHLFA5**	Combined thin aquifers interbedded in CHZCM with shallow part of CHZCM to provide transmissive flow paths north of Bench.
mCHZCM	modified Calico Hills zeolitic composite unit	CHVTA, **CHZCM**, IA	Combined deep part of CHZCM with contiguous HSUs north of TMCC.
mCFCM	modified Crater Flat composite unit	**CFCM**, CFCU, BFCU	Combined all Crater Flat Group units.
mCCU	modified Clastic confining unit	BRA, **PBRCM**, LCCU1, UCCU, LCA, BMICU	Combined all deep HSUs north of TMCC. HSUs are contiguous and deeper than screened intervals of pumping and observation wells. HSUs also are below the volume of aquifer material investigated as pumping signals did not propagate to deep depths.

using the Phase II HFM could not adequately simulate drawdown observations at ER-EC-13 and ER-EC-14 well sites. In the Phase II HFM, *ER-EC-13 shallow* is screened in the massive (that is, 1,000 ft to more than 3,000 ft thick) FCCM, and *ER-EC-13 intermediate* and *deep* are screened in the FCULFA4, which is interpreted as a localized disk-shaped lava-flow aquifer in the FCCM, approximately centered at the ER-EC-13 well site (fig. 17). Observed drawdown in *ER-EC-13* observation wells indicated that less permeable, localized confining units must separate the three observation wells (see “Drawdown Observations” section). Localized confining units were not distinguished from FCCM and FCULFA4 units in the Phase II HFM, but can be supported by alternating lithologic units between well completions. Wells *ER-EC-13 shallow* and *intermediate* are separated by nonwelded tuff and nonwelded block and ash-flow deposits embedded in the FCCM. In the FCULFA4, stoney lavas intersecting wells *ER-EC-13 intermediate* and *deep* are separated by vitrophyric and pumiceous lava that could restrict vertical flow between wells.

The HSUs in the TMCC were differentiated vertically at the ER-EC-13 well site into six distinct mHSUs (table 7; fig. 17). Divisions were based primarily on drawdown responses observed at the ER-EC-13 well site from pumping *ER-EC-13 main* and *ER-EC-14 main* and on lithologic distinctions. The upper composite unit (mFCCM1) extends upward from the base of the *ER-EC-13 shallow* well screen, the middle composite unit (mFCCM2) intersects the *ER-EC-13 intermediate* well screen, and the lower composite unit (mFCCM3) intersects the *ER-EC-13 deep* well screen. Two localized confining units with a 1-mile radius centered at the *ER-EC-13* well site separate the well screens: modified Fortymile Canyon confining unit 1, between *ER-EC-13 shallow* and *intermediate*, and modified Fortymile Canyon confining unit 2, between *ER-EC-13 intermediate* and *deep*. A deeper, laterally extensive confining unit, modified Fortymile Canyon confining unit 3 (mFCCU3), underlies the lower composite unit (mFCCM3).

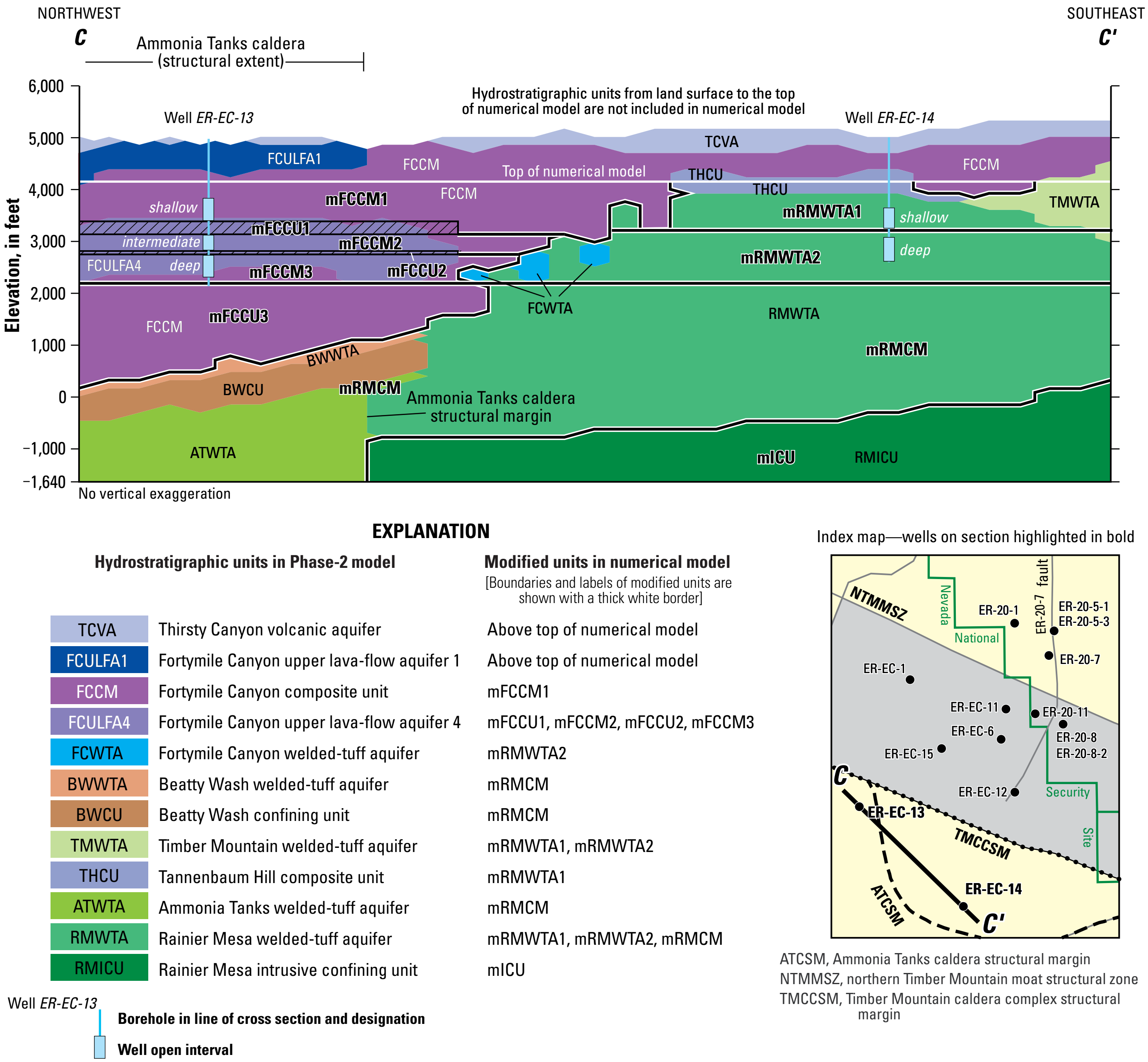

Figure 17. Northwest-southeast geologic cross section across the Timber Mountain caldera complex showing faults, hydrostratigraphic units from the Phase II hydrostratigraphic framework model, modified hydrostratigraphic units, and key boreholes, Pahute Mesa, Nevada National Security Site and vicinity.

The RMWTA intersecting the *ER-EC-14* well screens and nine surrounding Fortymile Canyon and Timber Mountain Group HSUs were grouped and divided into three mHSUs (mRMWTA1, mRMWTA2, and mRMCM; table 7; fig. 17). The Phase II HFM positioned *ER-EC-14 shallow* and *deep* in the massive and undifferentiated RMWTA; however, single-well aquifer-test analyses indicated *ER-EC-14 deep* is 10 to 100 times more transmissive than *ER-EC-14 shallow* (table 5). Based on the *ER-EC-14* aquifer test results, the mHSUs consist of two laterally extensive welded-tuff aquifers and one laterally extensive composite unit. The upper welded-tuff aquifer (mRMWTA1) intersects the *ER-EC-14 shallow* well screen, and the lower welded-tuff aquifer (mRMWTA2) intersects the *ER-EC-14 deep* well screen. The RMWTA composes the majority of the saturated thickness of each aquifer. The composite unit mRMCM underlies the *ER-EC-14 deep* well screen and is deeper than observation wells screened in Ammonia Tanks and Rainier Mesa caldera units (table 7). A modified intrusive confining unit (mICU) underlies modified Fortymile Canyon and Timber Mountain HSUs in the TMCC (table 7).

North of the Timber Mountain Caldera Complex

Calico Hills Formation

Hydrostratigraphic units of the Calico Hills Formation were grouped and divided to adequately represent observed hydraulic connections between pumping and observation wells north of the TMCC. Calico Hills lava-flow aquifers in the Phase II HFM provide hydraulic connections between wells north of the bench. However, because these aquifers are interbedded within the 4,500-ft-thick CHZCM, when compared with observed drawdowns during aquifer testing simulated hydraulic connections are attenuated and disrupted. Modifications to the Calico Hills Formation HSUs improved simulations, while mostly retaining consistency with the Phase II HFM.

North of the NTMMSZ, lava-flow aquifers interbedded in the CHZCM (CHLFA2 through CHLFA5) were combined with the overlying CHZCM to provide transmissive-flow paths between wells (fig. 18). For example, pumping well *ER-20-7* is screened predominantly in the TSA, but a small portion of the screened interval is in the CHZCM, which overlies the CHLFA5. At well sites ER-20-5 and ER-20-8, the deepest wells exhibited the greatest drawdown responses to pumping at *ER-20-7*. The deep well at well site ER-20-5, *ER-20-5-3,* is screened primarily in the CHLFA5, which is underlain and overlain by the CHZCM. Well *ER-20-8 deep* is screened across the same HSUs as *ER-20-7*, but is offset more than 1,000 ft by the NTMMSZ, such that the two wells are hydraulically connected by the CHLFA5 and the overlying CHZCM north of the NTMMSZ and the TSA south of the NTMMSZ. Greater drawdown responses in deeper wells indicated the *ER-20-7* pumping signal propagated downward through the CHZCM overlying the CHLFA5 and laterally through the CHLFA5. The unmodified Phase II HFM grouped the CHZCM overlying and underlying the CHLFA5 into a single, 2,000-ft-thick, homogeneous unit, which disrupted hydraulic connections between pumping well *ER-20-7* and observation wells at the ER-20-5 and ER-20-8 well sites.

Timber Mountain, Paintbrush, Crater Flat, and Belted Range Groups

North of the TMCC, mHSUs represent a combination of individual, grouped, and divided HSUs. Grouped units represent either (1) HSUs with similar hydraulic properties or (2) HSUs above or below the screened intervals of wells, where no information exists to differentiate hydraulic properties of individual HSUs. The modified Fluorspar Canyon confining unit (mFCCU) includes laterally continuous Timber Mountain, Thirsty Canyon, and younger volcanic and alluvial units, where the FCCU composes the majority of the saturated thickness (table 7). These HSUs lie above the screened intervals of all pumping and observation wells; therefore, variations in hydraulic properties among units cannot be differentiated in a groundwater-flow model. Paintbrush Group HSUs were aggregated into six mHSUs, based on contiguous lava-flow aquifers and confining units. Paintbrush Group mHSUs included the modified Comb Peak aquifer (mCPA), the modified Upper Paintbrush confining unit (mUPCU), the modified Tiva Canyon aquifer (mTCA), and the modified Topopah Spring aquifer (table 7). The Middle Paintbrush confining unit and Lower Paintbrush confining unit (LPCU) were kept as separate units. The modified Crater Flat composite unit (mCFCM) aggregated all Crater Flat Group units, and the modified clastic confining unit (mCCU) aggregated Belted Range Group HSUs with other basement units below the well screens of all pumping and observation wells and beyond the area of investigation.

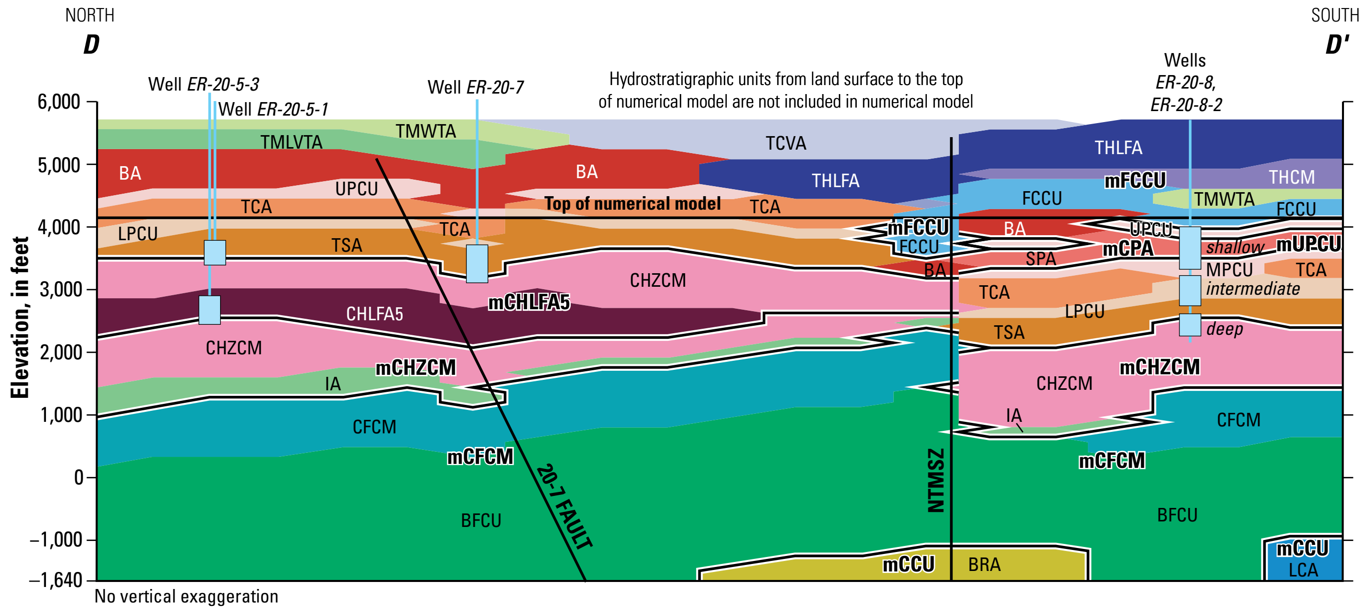

EXPLANATION

Hydrostratigraphic units in Phase-2 model		Modified units in numerical model [Boundaries and labels of modified units are shown with a thick, white border]
TCVA	Thirsty Canyon volcanic aquifer	Above top of numerical model
TMWTA	Timber Mountain welded-tuff aquifer	Above top of numerical model
TMLVTA	Timber Mountain lower vitric-tuff aquifer	Above top of numerical model
THLFA	Tannenbaum Hill lava-flow aquifer	Above top of numerical model
THCM	Tannenbaum Hill composite unit	Above top of numerical model
FCCU	Fluorspar Canyon confining unit	mFCCU
UPCU	Upper Paintbrush confining unit	mUPCU (same area in figure as UPCU)
BA	Benham aquifer	mCPA
SPA	Scrugham Peak aquifer	mCPA
MPCU	Middle Paintbrush confining unit	mMPCU (same area in figure as MPCU)
TCA	Tiva Canyon aquifer	mTCA (same area in figure as TCA)
LPCU	Lower Paintbrush confining unit	mLPCU (same area in figure as LPCU)
TSA	Topopah Spring aquifer	mTSA (same area in figure as TSA)
CHZCM	Calico Hills zeolitic composite unit	mCHZCM, mCHLFA5
CHLFA5	Calico Hills lava-flow aquifer 5	mCHLFA5
IA	Inlet aquifer	mCHZCM
CFCM	Crater Flat composite unit	mCFCM
BFCU	Bullfrog confining unit	mCFCM
BRA	Belted Range aquifer	mCCU
LCA	Lower carbonate aquifer	mCCU

Well ER-20-7 — **Borehole in line of cross section and designation**

Well open interval

Index map—wells on section highlighted in bold

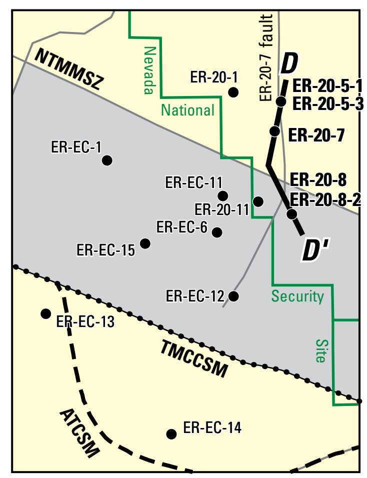

ATCSM, Ammonia Tanks caldera structural margin
NTMMSZ, northern Timber Mountain moat structural zone
TMCCSM, Timber Mountain caldera complex structural margin

Figure 18. North-south geologic cross section across the northern Timber Mountain moat structural zone, showing faults, hydrostratigraphic units from the Phase II hydrostratigraphic framework model, modified hydrostratigraphic units, and key boreholes, Pahute Mesa, Nevada National Security Site.

Groundwater-Flow Models

The integrated groundwater-flow model is composed of 11 MODFLOW models (Harbaugh and others, 2000), which simulated drawdowns from pumping one to three wells at a well site. Each of these 11 groundwater-flow models are referred to as a “well-site model.” Multiple-well aquifer tests and corresponding well-site models are reported in table 8.

All 11 well-site models shared a common lateral extent (fig. 1) of about 400,000 ft (76-mi) on a side, where model columns were oriented north-south. All well-site models were discretized into 119 rows of 128 columns that largely coincided with the 984-ft sided grid of the Phase II HFM, where models overlapped. Grids of the 11 well-site models differed because each was locally refined to a 33-ft (10-m) sided cell at each pumping well (fig. 19). Well-site model grids laterally extended about 160,000 ft beyond the Phase II HFM edge to avoid the influence of boundary effects at pumping and observation wells. All the external model boundaries were specified no-flow boundaries.

All 11 well-site models were discretized vertically from 1,700 ft below sea level to 4,200 ft above sea level, which approximated the water table. All well-site models were discretized identically into 29 layers to avoid inconsistent hydraulic-property estimates and to correspond with delineated HSUs in the modified Phase II HFM that were within and just beyond the volume investigated by the 16 multiple-well aquifer tests (fig. 19). The upper model boundaries were the water table, where aquifer storage is represented by the specific yield defined as the volume of water available for gravity drainage per unit head decline per area of aquifer. Uppermost model layers were specified as 1-foot thick. Changes in saturated thickness were not simulated because maximum drawdowns near the water table were small. Vertical discretization was made finer between 2,300 and 3,700 ft above sea level (layers 5–20) because most wells were completed between these depths where transient responses to pumping stresses are greatest. The well-site models extended vertically from 1,700 ft below sea level to 2,300 ft above sea level (layers 21–29) to avoid boundary effects with the specified no-flow boundary along the base of the model.

Pumping during well development and aquifer testing was simulated with the Multi-Node Well (MNW) MODFLOW Package (Halford and Hanson, 2002) to more realistically simulate the multiple completions screened in different mHSUs. Variable discharge rates were simulated using between 6 and 12 stress periods, as determined from simplified pumping schedules (fig. 8). More stress periods were specified

Table 8. Number of stress periods, observation wells, and drawdown observations used in each of the 11 well-site models, Pahute Mesa, Nevada National Security Site.

[**Pumping well names** are listed in alphabetical order. Bold part of name is well site as shown on figure 1. **Stress periods:** the number of transient stress periods used to simulate well development, pumping, and recovery periods. **Total number of observation wells:** number of wells used to calibrate the groundwater-flow models. **Number of reliable observation wells:** number of wells with drawdown observations weighted greater than or equal to 0.5. Reliable wells for model calibration were those with drawdown observations unaffected by frictional well loss, thermal effects, abridged records, leaking packers or bridge plugs, considerable background noise, water-level step changes owing to transducer failure and replacement, or signal obscurement by previous aquifer tests. **Number of observation wells with root-mean square error (RMSE) below best fit:** the number of wells with RMSE below the best-fit RMSE (0.02 ft) for all groundwater-flow models. **Total number of drawdown observations:** number of observations used to calibrate each groundwater-flow model. Drawdown observations were reduced to 6-hour averages. **Number of reliable drawdown observations:** number of reliable observations with assigned weights greater than or equal to 0.5. ft, feet]

Well-site model	Pumping-well name	Stress periods	Number of observation wells			Number of drawdown observations	
			Total	Reliable	RMSE below best fit	Total	Reliable
ER-20-4m	***ER-20-4*** *main*	6	6	5	3	1,480	1,137
ER-20-7	***ER-20-7***	6	13	12	10	1,076	845
ER-20-8m	***ER-20-8*** *main upper* ***ER-20-8*** *main lower*	12	27	18	18	13,308	9,772
ER-20-8-2m	***ER-20-8-2*** *main*	9	14	13	10	2,015	1,925
ER-20-11m	***ER-20-11*** *main*	8	27	26	19	12,482	9,695
ER-EC-11m	***ER-EC-11*** *main*	6	13	10	8	1,554	1,317
ER-EC-12m	***ER-EC-12*** *main upper* ***ER-EC-12*** *main lower*	8	13	11	6	6,884	6,739
ER-EC-13mUZ	***ER-EC-13*** *main upper*	10	[1]20	15	17	5,526	4,593
ER-EC-13mLZ	***ER-EC-13*** *main lower*	8	[1]23	20	18	5,716	4,914
ER-EC-14m	***ER-EC-14*** *main upper* ***ER-EC-14*** *main lower*	10	25	19	19	9,979	7,774
ER-EC-15m	***ER-EC-15*** *main intermediate* ***E-EC-15*** *main lower*	11	27	16	18	13,576	6,133
Total			208	165	146	73,596	54,842

[1] Values exceed the number of observation wells shown in table 6. Wells ER-EC-4 and UE-18r were included to constrain the maximum simulated drawdown extent during ER-EC-13 pumping. Drawdown observations at these wells were assigned values of zero.

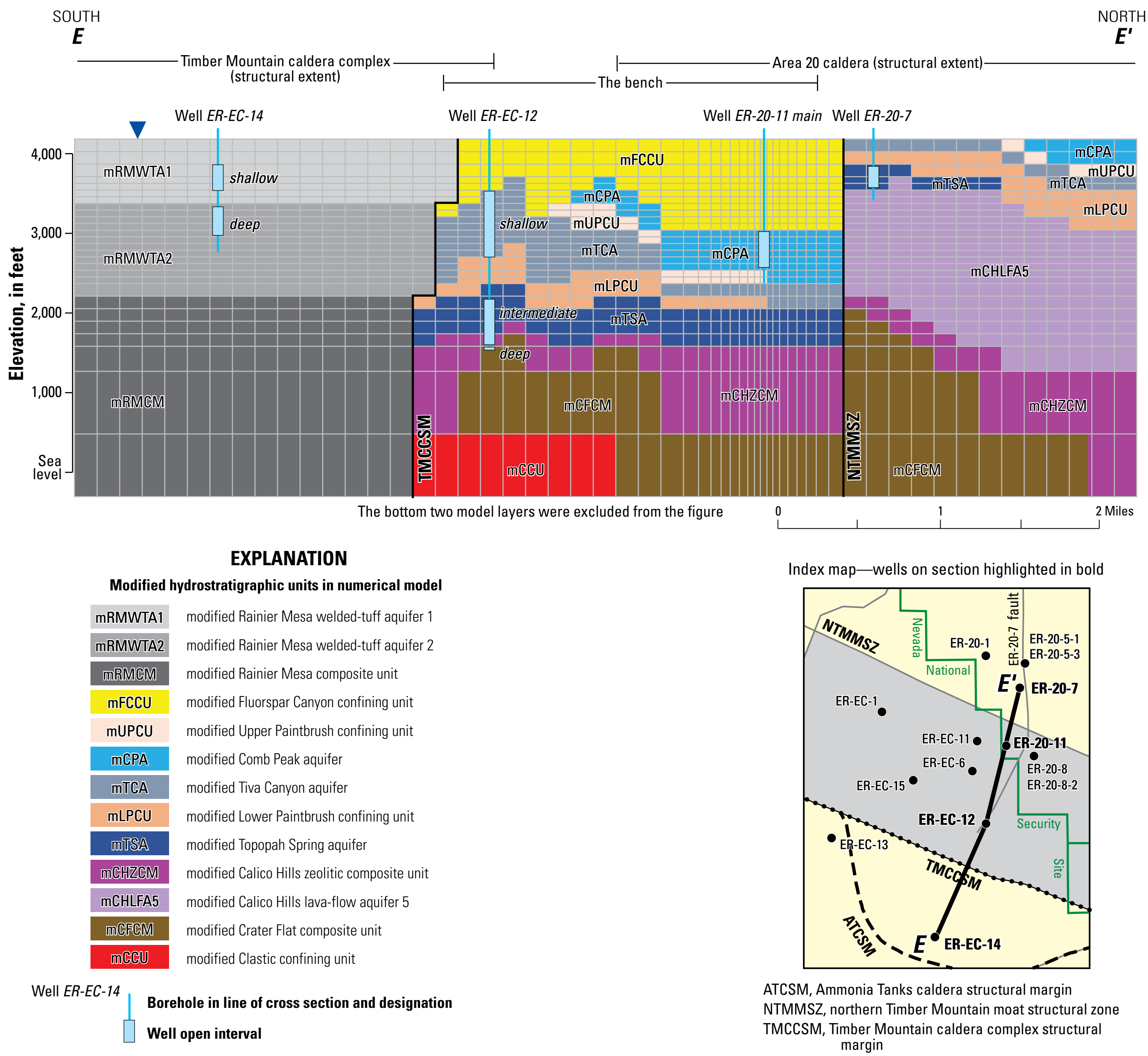

Figure 19. Diagram showing the ER-20-11m well-site model discretization.

in well-site models that simulated multiple aquifer tests (table 8). All stress periods were subdivided into 25 time steps that successively increased by a factor of 1.25. Initial heads of 0 ft were specified to indicate initial conditions of no drawdown.

Distributing Hydraulic Properties

Hydraulic properties in each mHSU were estimated and distributed with "pilot points". Pilot points are user-specified locations in an mHSU where hydraulic properties are estimated (RamaRao and others, 1995). Pilot points were assigned to mHSUs at 117 mapped locations, with denser spacing of pilot points near pumping and observation wells (fig. 20). Fewer than 117 pilot point locations were used in any given mHSU, because no mHSU spanned the entire model extent. Multiple pilot points were assigned at the same mapped location so that hydraulic properties could vary vertically, corresponding to different mHSUs. For example, a pilot point was assigned to each of the four mHSUs at the ER-EC-14 well site.

Hydraulic conductivity was distributed with 709 pilot points. Values were estimated at pilot points in the aquifer-system volume investigated by the 16 aquifer tests where drawdown was detected. Hydraulic-conductivity estimates were constrained during parameter estimation between 1×10^{-5} and 500 ft/d, which is the expected range for fractured

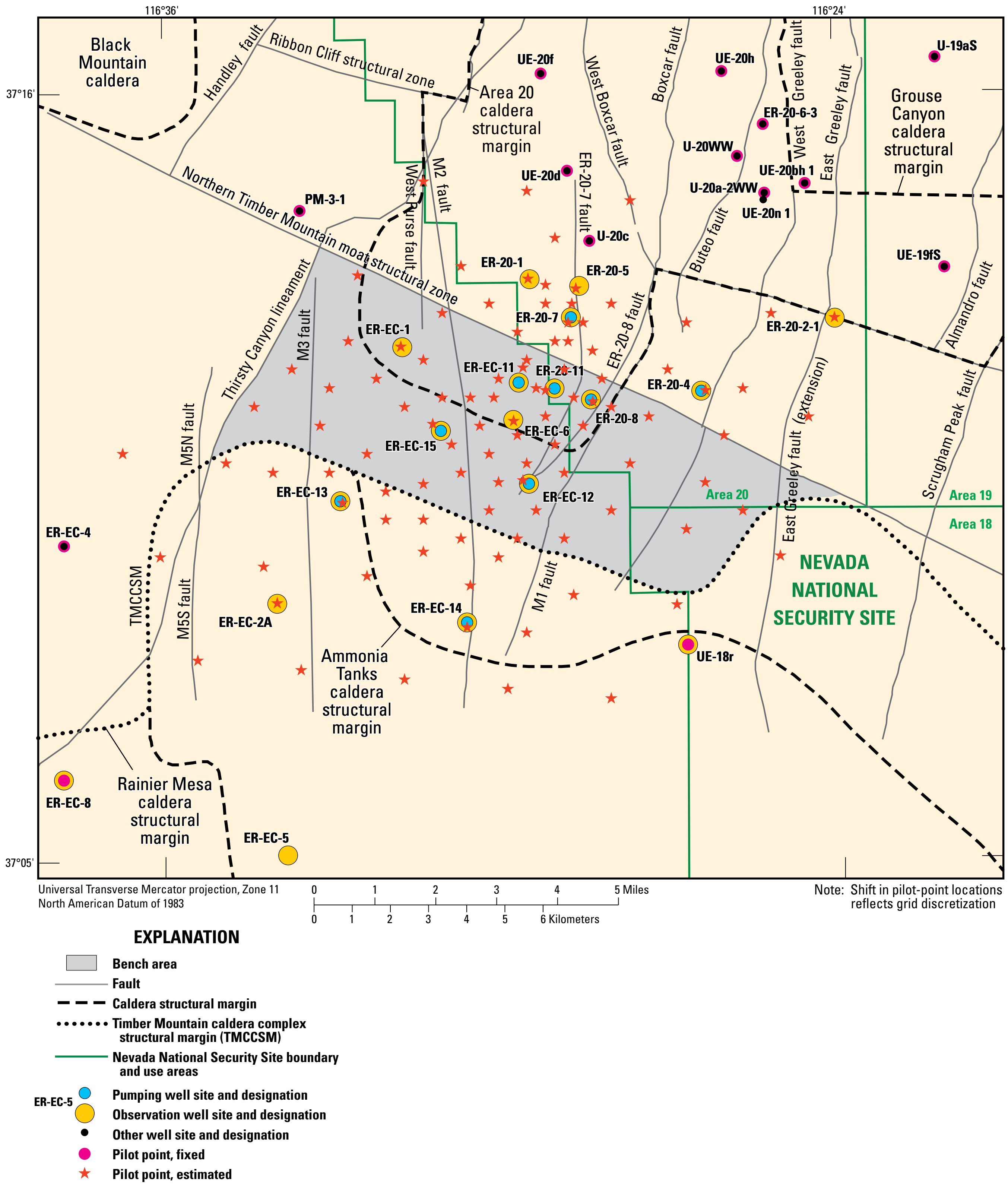

Figure 20. Pilot-point distribution in the hydrostratigraphic framework model domain.

rocks typical of the study area (Belcher and others, 2002). Hydraulic conductivities were specified at pilot points located beyond the volume investigated by the 16 aquifer tests, for example where drawdown was not detected. Pilot points with specified hydraulic-conductivity values were laterally distant from pumping wells or at depths above and below pumping intervals. These hydraulic-conductivity values represent "prior information" derived from previous investigations (table 9) and varied by depth, where depth-dependent completions or flow logs were available (Garcia and others, 2010). Multiple-depth aquifer and slug tests reported by R.K. Blankennagel, R.A. Young, J.B. Cooper, and H.A. Whitcomb, USGS (written commun., 1964), Blankennagel and Weir (1973), and Oberlander and others (2007) indicated that shallow, saturated rocks (less than 2,000 ft below the water table) generally are more permeable than deep, saturated rocks. Therefore, hydraulic conductivities of 0.0001 ft/d were specified at pilot points below the pumping intervals in mFCCU3, mRMCM, mCCU, and mICU.

Specific storage was estimated at most of the 709 hydraulic-conductivity pilot points. Specific-storage pilot points were constrained between 1×10^{-8} and 2×10^{-5} 1/ft during calibration. This range was greater than the expected range in fractured rocks, but was permitted to compensate for thin, undifferentiated transmissive intervals within thick rock sequences. For example, a 1,000-ft-thick mHSU with a specific storage of 2×10^{-6} 1/ft could contain a transmissive interval that is only 100-ft thick. To compensate for a permeable interval that is one-tenth the thickness of the mHSU, the specific-storage estimate is reduced by a factor of 10 to 2×10^{-7} 1/ft.

Specific yield was not estimated for each mHSU because expected specific yields were similar for all mHSUs. Specific yield was distributed and estimated at all 117 mapped pilot points at the water table (layer 1). Initial specific-yield values of 0.01 were constrained between 0.001 and 0.05, which is the expected range for fractured rock (Morris and Johnson, 1967).

Log-transformed hydraulic conductivity, specific yield, and specific-storage estimates at pilot-point locations were interpolated laterally in the well-site models by kriging (Doherty, 2015). Spatial variability of log-transformed hydraulic properties was defined with an isotropic, exponential variogram and no nugget. A range of 3 mi was specified so that hydraulic properties were interpolated smoothly among pilot points (fig. 20).

Parameter Estimation

Hydraulic-conductivity, specific-yield, and specific-storage values at pilot points were estimated by minimizing a weighted, composite, sum-of-squares objective function using the parameter estimation program PEST (Doherty, 2016). Differences between observed and simulated drawdowns

Table 9. Transmissivity values derived from previous aquifer tests at Pahute Mesa, Nevada National Security Site.

Pumping well site	Transmissivity, (feet-squared per day)	Testing method	Analysis method	Reference
ER-18-2	2	Constant-rate test	Cooper and Jacob (1946); Moench (1984)	U.S. Department of Energy (2002d)
ER-20-6-3	2,000–4,000	Multiple-well aquifer test	Numerical Model	Garcia and others (2011)
ER-EC-1	7,000	Constant-rate test	Cooper and Jacob (1946)	Garcia and others (2010)
ER-EC-2A	200	Constant-rate test	Borehole flowmeter	U.S. Department of Energy (2002f)
ER-EC-4	50,000	Constant-rate test	Cooper and Jacob (1946)	Garcia and others (2010)
ER-EC-5	14,000	Constant-rate test	Borehole flowmeter	U.S. Department of Energy (2002c)
ER-EC-6	1,000	Constant-rate test	Cooper and Jacob (1946)	U.S. Department of Energy (2002e)
ER-EC-7	10,000	Constant-rate test	Cooper and Jacob (1946)[2]	Determined in this study [2]
ER-EC-8	3,700	Constant-rate test	Moench (1984)	U.S. Department of Energy (2002b)
PM-3	50	Constant-rate test	Neuman (1975)	Kilroy and Savard (1995); Belcher and others (2001)
U-19aS	[1]2	Slug-injection recovery test	Specific Capacity	Elliot and Fenelon (2010)
U-20WW	3,000	Multiple-well aquifer test	Numerical Model	Garcia and others (2011)
U-20a-2WW	2,400	Slug-injection recovery test	Cooper and Jacob (1946)	Graves (2002a)
U-20c	1	Slug-injection recovery test	Specific Capacity	Fenelon and others (2016)
UE-18r	3,000	Constant-rate test	Cooper and Jacob (1946)	Belcher and others (2001)
UE-19fS	1,000	Constant-rate test	Cooper and Jacob (1946)	Graves (2002b)
UE-20bh1	1,200	Multiple-well aquifer test	Numerical Model	Garcia and others (2011)
UE-20d	5,900	Constant-rate test	Cooper and Jacob (1946)	Belcher and others (2001)
UE-20f	100	Constant-rate test	Cooper and Jacob (1946)	Graves (2002c)
UE-20h	1,400	Constant-rate test	Theis (1935) recovery	Belcher and others (2001)

[1] Interpreted from reported hydraulic test data.

[2] Determined from U.S. Department of Energy (2002g) data.

defined the goodness-of-fit or improvement of calibration. The sum-of-squares objective function (Φ) represents the sum of weighted and squared differences or residuals:

$$\Phi(x) = \sum_{i=1}^{nobs} \left[\left(\hat{o}_i - o_i \right) w_i \right]^2 \tag{1}$$

where

x is the vector of parameters being estimated,
nobs is the number of observations compared,
$(\hat{o}_i)$ is the i[th] simulated observation,
(o_i) is the i[th] measurement or regularization observation, and
w_i is the i[th] weight.

Although model calibration relied upon the sum-of-squares objective function, the RMS error was reported because RMS error more intuitively compares differences between observed and simulated drawdowns. Root-mean-square error is defined as follows:

$$RMS = \sqrt{\Phi / \sum_{i=1}^{nobs} w_i^2} \tag{2}$$

The integrated groundwater-flow model was calibrated to drawdown and regularization observations. Drawdown observations represent aquifer-system responses to pumping that were differentiated analytically from environmental fluctuations with water-level models. Regularization observations guided hydraulic conductivity, specific yield, and specific-storage estimates toward preferred conditions in mHSUs and in areas where drawdown observations were limited. This regularization approach is "Tikhonov regularization" (Doherty, 2016).

Drawdown observations were averaged (6-hour intervals) to minimize high-frequency noise and were weighted to improve model calibration. Drawdown averaging reduced measurement observations from more than 870,000 to about 74,000. More than 70 percent of drawdown observations were unaffected by confounding factors, classified as reliable, and assigned a weight of 1.0 (table 8). Unreliable drawdowns were affected by one or more confounding factors, such as well loss or thermal effects (table 5; appendix 3), and were assigned weights less than 0.5 to minimize their influence on the objective function.

Weights also were reduced where similar drawdowns were observed in multiple wells at a well site. Weights of 0.5 were assigned to reduce the clustering effect that would artificially skew calibration toward a well site. For example, similar drawdown responses in *ER-EC-6 shallow*, *ER-EC-6 intermediate*, and *ER-EC-6 deep* to the *ER-EC-11 main* aquifer test were assigned weights of 0.5 in the ER-EC-11m well-site model.

Drawdown in observation wells at the pumping-well site often were uncertain because of frictional well loss, thermal effects, packer or bridge-plug leakage, or a combination of these factors (table 5). Model calibration can be skewed toward fitting uncertain observations, especially if drawdown exceeds 100 ft and transmissivity of the pumped interval is less than 1,000 ft²/d, because hydraulic-property sensitivity is proportional to the magnitude of simulated drawdown. To reduce hydraulic-property sensitivity to uncertain drawdown observations and improve model calibration, compromised drawdown observations at pumping-well sites were assigned weights between 0.01 and 0.3. The effects of weighting are reported with unweighted and weighted sum-of-squares errors for each hydrograph (see the integrated grounwater-flow model online data release at *https://doi.org/10.5066/F76H4FJQ*).

Tikhonov regularization limited sharp changes in hydraulic properties and ensured relatively smooth hydraulic conductivity, specific-yield, and specific-storage distributions. Preferred homogeneity was specified by log differences in hydraulic conductivity, specific yield, or specific-storage estimates. About 29,000 regularization observations were specified and primarily informed hydraulic-property estimates within the drawdown extent where drawdown observations were limited.

Unrealistic hydraulic conductivity, specific yield, and specific-storage distributions were avoided by limiting the fit between observed and simulated drawdowns (Fienen and others, 2009). The expected measurement (drawdown observation) error specifies irreducible measurement and numerical errors as a weighted, sum-of-squares error. This term is specified by the variable PHIMLIM in PEST (Doherty, 2016). An RMS error of about 0.02 ft, which equals a PHIMLIM of 22 ft², was considered reasonable to preserve drawdown observations and hydraulic-property homogeneity in the mHSUs. The integrated groundwater-flow model with the best fit between observed and simulated drawdown had a PHIMLIM of 32 ft², which equates to an RMS error of about 0.025 ft.

Well-site model integration comprised simultaneous calibration of all models to a single set of parameters using PEST. A conceptual diagram of well-site model integration is shown in figure 21. PEST compares observed and simulated drawdowns from all 208 observation wells to estimate a consistent set of hydraulic properties at pilot points. Drawdowns in the 208 observation wells were simulated with the 11 well-site models that collectively were the model calibrated by PEST. Simulated results from all models simultaneously inform PEST, and parameter changes are estimated iteratively until the objective function has been minimized.

Simulated Drawdown

Simulated and observed drawdowns compared well, with an RMS error of 0.025 ft, which is similar to the expected error from water-level model results. The RMS error represents the best fit across the integrated groundwater-flow model. Drawdown observations were reliable at 165 of 208 pumping- and observation-well pairs (table 8) where drawdown was unaffected by confounding factors, such as frictional well loss or thermal effects (table 6). Simulated

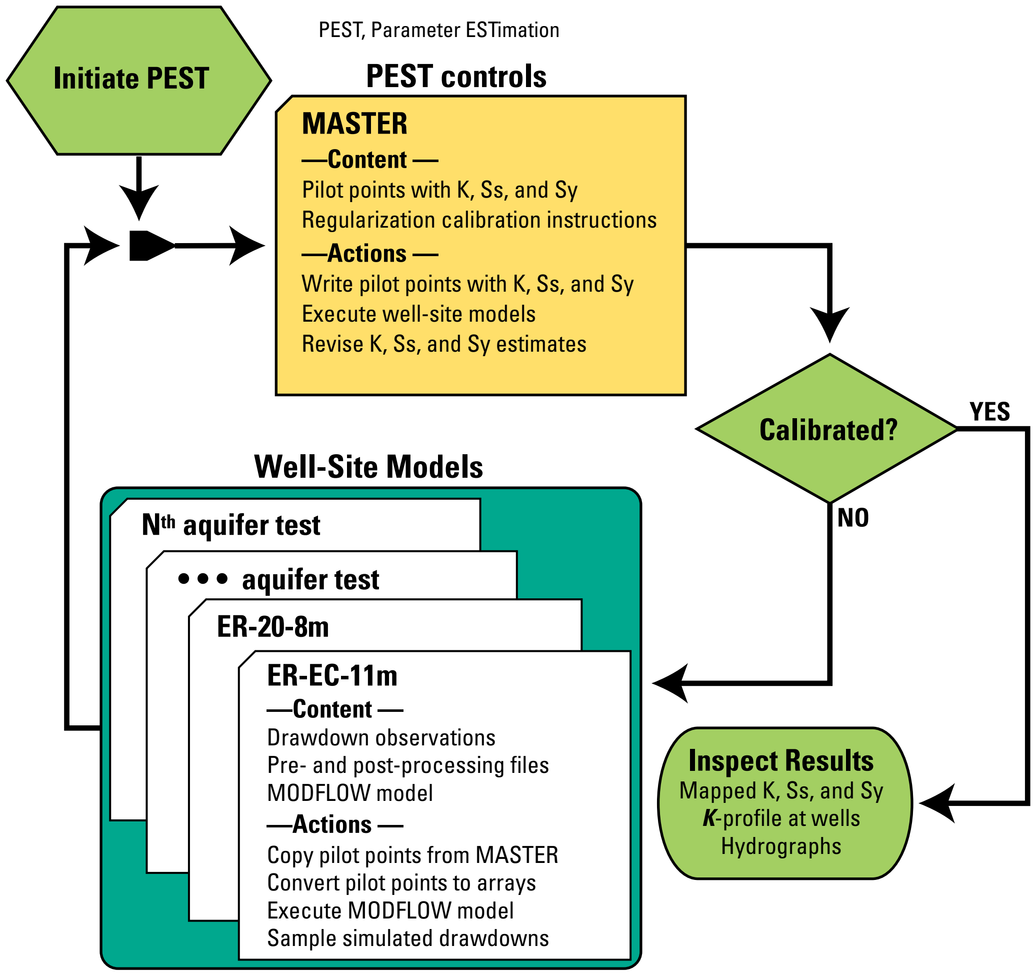

Figure 21. Conceptual diagram showing well-site model integration, where *K* is hydraulic conductivity, *Ss* is specific storage, and *Sy* is specific yield.

drawdowns matched 88 percent of reliable observations, with RMS errors of less than 0.02 ft (table 8).

Simulated and observed drawdowns agreed far north of the NTMMSZ, in the bench, and in the TMCC. For example, in the central bench area, simulated drawdown in *ER-EC-6 intermediate* matched observed drawdown from 10 well-site aquifer tests to within 0.04 ft (fig. 22). Drawdowns in *ER-EC-6 intermediate* were simulated in 10 of the 11 well-site models and agreed with observed drawdowns (fig. 22).

The area and aquifer volume investigated in the model domain was defined using the maximum simulated drawdown from any of the 16 multiple-well aquifer tests. For example, maximum simulated drawdown in *ER-EC-6 intermediate* was 0.76 ft, which was observed during day 10 of the *ER-20-11main* aquifer test (fig. 22). A maximum simulated-drawdown threshold of 0.05 ft defined the lateral area and thickness of the aquifer investigated. This threshold corresponds with a maximum drawdown-estimation error of 0.05, determined from water-level modeling by Garcia and others (2013). The two-dimensional area investigated was defined by the maximum simulated drawdown at any depth (fig. 23). The area investigated totaled 60 mi^2 and was greater than 12 mi across at its widest extent. The aquifer volume investigated exceeded 30 cubic miles (mi^3). The average thickness of the investigated volume exceeded 1 mi. In the aquifer volume investigated, 15 of the 22 mHSUs evaluated had volumes greater than 0.5 mi^3.

Of the 34 observation wells, 29 were in the 0.05 ft drawdown area (fig. 23). These wells are predominantly within the bench area. Fewer observation wells (*ER-EC-13 shallow, intermediate, and deep* and *ER-EC-14 shallow and deep*) are southwest of the bench in the TMCC and northeast of the NTMMSZ (*ER-20-1*, *ER-20-4 shallow and deep*, *ER-20-5-1*, *ER-20-5-3*, and *ER-20-7*; fig. 23). Observation wells *ER-20-2-1*, *ER-EC-2A*, *ER-EC-5*, *ER-EC-8*, and *UE-18r* are outside the 0.05 ft drawdown area.

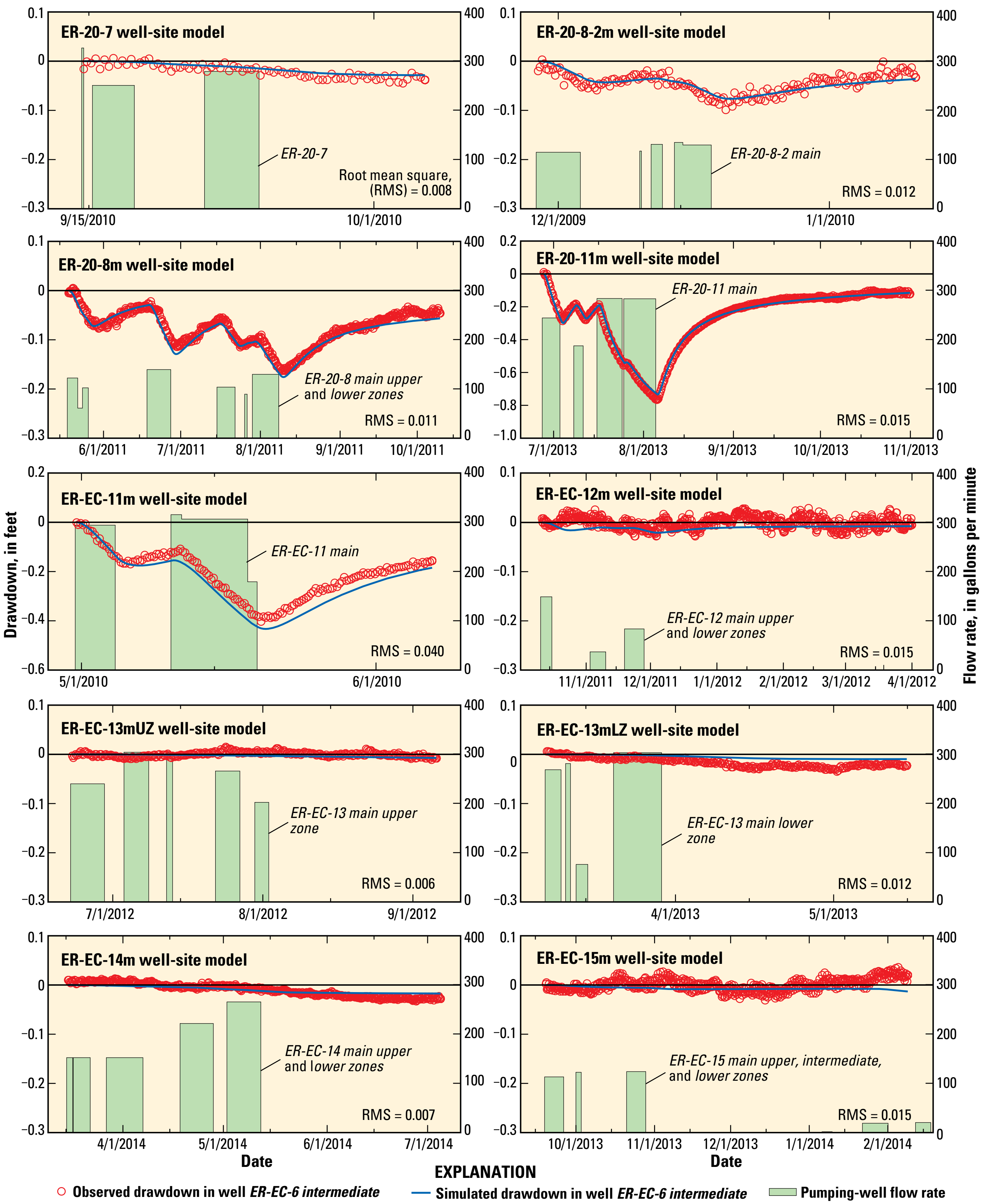

Figure 22. Comparisons of simulated and observed drawdowns in *ER-EC-6 intermediate* as determined from 10 well-site models and 12 aquifer tests, Pahute Mesa, Nevada National Security Site, 2009–14.

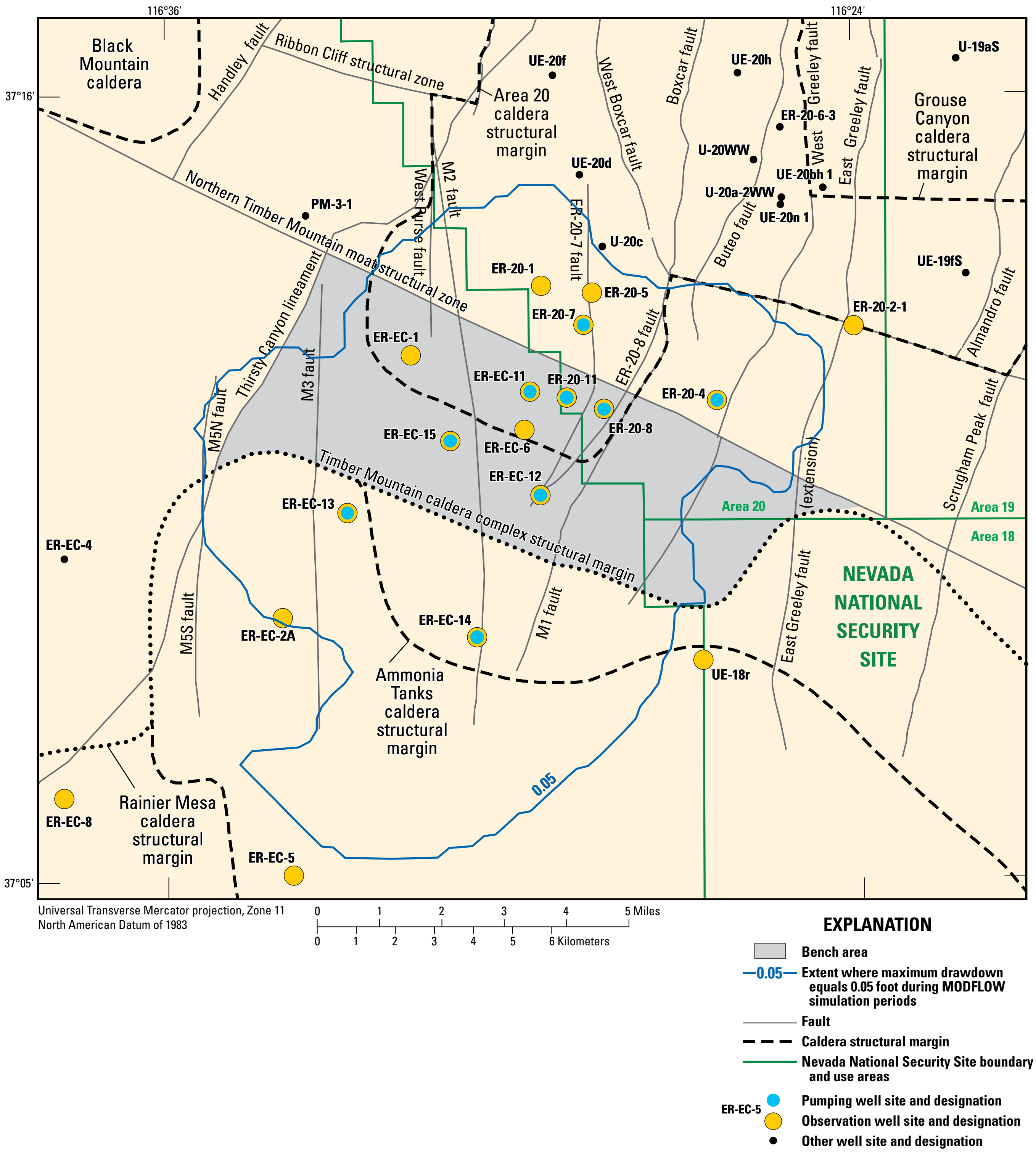

Figure 23. Area investigated by the 11 well-site models and 16 multiple-well aquifer tests. Area investigated represents the extent where maximum drawdown equaled or exceeded 0.05 feet during simulation periods.

Hydraulic-Property Estimates

Hydraulic Conductivity

Hydraulic-conductivity geometric mean estimates for the mHSUs in the investigated volume averaged 0.6 ft/d (table 10) and ranged between 1×10^{-4} ft/d and 230 ft/d within the 5th to 95th percentiles of the mHSU distributions. Of the 15 mHSUs that had more than 0.5 mi^3 in the area investigated and geometric-mean hydraulic conductivities greater than 0.001 ft/d (table 10), the most permeable were the mCPA and mRMWTA2, located in the bench area and the TMCC, respectively (table 7), with geometric-mean hydraulic conductivities of 2 ft/d or more. The mCCU was the least permeable of the 15 mHSUs shown in figure 24, with a geometric mean hydraulic conductivity of 0.002 ft/d. Other extensive and less permeable mHSUs in the area investigated include the mUPCU and mLPCU in the bench area, which underlie the mCPA and mTCA (fig. 18), and the mRMWTA1 in the TMCC, which underlies the mRMWTA2 (fig. 17). Of the 15 mHSUs shown in figure 24, 10 were hydraulically similar, having geometric-mean hydraulic conductivities that differed by an order of magnitude or less. These are small differences relative to the variability within individual mHSUs; hydraulic conductivities of individual mHSUs shown in figure 24 varied by more than 2 to more than 4 orders of magnitude between the 5th to 95th percentiles.

The large variability in hydraulic-conductivity values indicated most mHSUs in the area investigated are heterogeneous. The mFCCM3 and FCCU are the least heterogeneous units shown in figure 24, with estimates that span fewer than 3 orders of magnitude. The mFCCU, however lies predominantly above pumping and observation wells (figs. 18 and 19). The minimal variability primarily was the result of few pumping signals interfering with the assumed homogeneity imposed by Tikhonov regularization.

Table 10. Mean and standard deviation of simulated hydraulic-conductivity estimates for modified hydrostratigraphic units (HSUs), number of observation, background wells, and prior-information wells intersecting each unit; and volume of each modified HSU within the aquifer volume investigated by the 16 multiple-well aquifer tests, Pahute Mesa, Nevada National Security Site and vicinity.

[**Geometric mean** refers to the the geometric mean of hydraulic conductivity values for a given modified HSU. **Standard deviation** refers to the standard deviation of hydraulic conductivity values for a given modified HSU. **Prior-information wells** include those other than observation and background wells. **Volume investigated:** modified HSU volume investigated by the 16 multiple-well aquifer tests. **Abbreviations:** mCCU, modified clastic confining unit; mCFCM, modified Calico Hills composite unit; mCHLFA1-5, modified Calico Hills lava-flow aquifers 1 and 5; mCHZCM, modified Calico Hills zeolitic composite unit; mCPA, modified Comb Peak aquifer; mFCCM1–3, modified Fortymile Canyon composite units 1–3; mFCCU, modified Fluorspar Canyon confining unit; mFCCU1-3, modified Fortymile Canyon confining units 1–3; mLPCU, modified Lower Paintbrush confining unit; mMPCU, modified Middle Paintbrush confining unit; mRMCM, modified Rainier Mesa Composite Unit; mRMWTA1–2, modified Rainier Mesa welded tuff aquifers1–2; mTCA, modified Tiva Canyon aquifer; mTSA, modified Topopah Spring aquifer; mUPCU, modified Upper Paintbrush confining unit; <, less than]

Modified HSU	Hydraulic conductivity (feet per day)		Number of wells screened in modified HSUs			Volume investigated (cubic miles)
	Geometric mean	Standard deviation	Observation wells	Background wells	Prior-information wells	
mFCCM1	0.2	8	1	0	0	2
mFCCU1	<0.002	98	0	0	0	0.1
mFCCM2	0.5	14	2	0	0	1
mFCCU2	<0.001	87	0	0	0	0.1
mFCCM3	0.3	5	1	0	0	0.6
mFCCU3	<0.001	15	0	0	0	0.3
mRMWTA1	0.07	8	1	0	2	3
mRMWTA2	2	9	4	0	1	5
mRMCM	<0.001	11	0	0	0	0.6
mFCCU	0.2	5	0	0	1	1
mCPA	3	9	7	0	0	1
mUPCU	0.1	7	0	0	1	0.5
mMPCU	0.2	9	0	0	0	0.2
mTCA	0.3	8	6	1	1	1
mLPCU	0.07	5	0	0	1	1
mTSA	0.2	6	6	0	0	1
mCHLFA1	3	4	1	0	0	0.1
mCHLFA5	0.9	12	3	3	5	3
mCHZCM	1	6	2	0	3	5
mCFCM	0.4	5	0	0	4	9
mCCU	0.002	12	0	0	0	1
Total			34	4	19	37

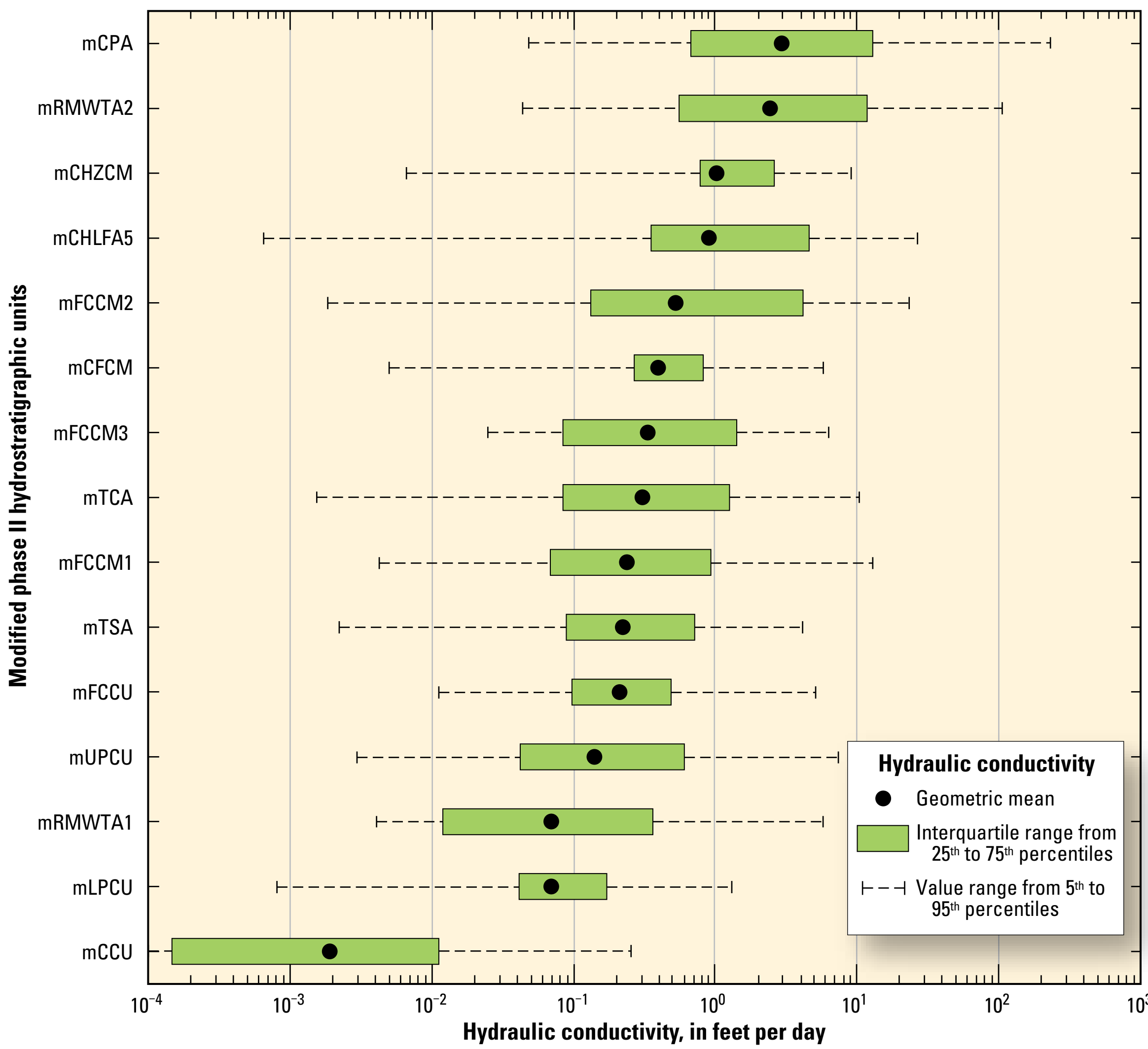

mCPA: modified Comb Peak aquifer
mRMWTA2: modified Rainier Mesa welded-tuff aquifer 2
mCHZCM: modified Calico Hills zeolotic composite unit
mCHLFA5: modified Calico Hills lava-flow aquifer 5
mFCCM2: modified Fortymile Canyon composite unit 2
mCFCM: modified Crater Flat composite unit
mFCCM3: modified Fortymile Canyon composite unit 3
mTCA: modified Tiva Canyon aquifer
mFCCM1: modified Fortymile Canyon composite unit 1
mTSA: modified Topopah Spring aquifer
mFCCU: modified Fluorspar Canyon confining unit
mUPCU: modified Upper Paintbrush confining unit
mRMWTA1: modified Rainier Mesa welded-tuff aquifer 1
mLPCU: modified Lower Paintbrush confining unit
mCCU: modified clastic confining unit

Figure 24. Estimated hydraulic-conductivity distributions for modified hydrostratigraphic units in the area investigated by the 16 multiple-well aquifer tests, Pahute Mesa, Nevada National Security Site and vicinity.

Specific Yield and Specific Storage

The geometric mean of specific-yield estimates was 0.02 (table 11), and 70 percent ranged between 0.002 and 0.05. Specific-yields that were estimated as less than 0.02 were predominantly outside the area investigated; however, all estimated values were within the expected range for fractured rock (0.001–0.05; Morris and Johnson, 1967).

The specific-storage geometric mean estimates across all mHSUs averaged 8×10^{-7} 1/ft (table 11). About 60 percent of the specific-storage estimates were less than 1×10^{-6} 1/ft, which is typically the lower bound for fractured rocks (Domenico and Miffin, 1965). This indicates that the permeable thicknesses in most mHSUs were less than the mapped thickness. Specific-storage estimates less than 1×10^{-6} 1/ft resulted from compensating errors, where too great a thickness was assigned to an mHSU.

Transmissivity

The total transmissivity distribution (fig. 25) was derived as the sum of the hydraulic-conductivity × thickness product at a location in each mHSU. Total transmissivity is a more robust estimate than the multiple hydraulic-conductivity distributions (by mHSU) and is less sensitive to a particular HFM

Table 11. Mean and standard deviation of simulated specific-yield and specific-storage estimates for modified hydrostratigraphic units (HSUs), and the number of observation, background, and prior-information wells intersecting each unit, Pahute Mesa, Nevada National Security Site and vicinity.

[**Geometric mean** refers to the the geometric mean of specific yield (layer 1) or specific storage values for a given modified HSU. **Standard deviation** refers to the standard deviation of specific yield (layer 1) or specific storage values for a given modified HSU. **Prior-information wells** include those other than observation and background wells. **Abbreviations:** HSU, hydrostratigraphic unit; mCCU, modified clastic confining unit; mCFCM, modified Calico Hills confining unit; mCHLFA1-5, modified Calico Hills lava-flow aquifers 1 and 5; mCHZCM, modified Calico Hills zeolitic composite unit; mCPA, modified Comb Peak aquifer; mFCCM1-3, modified Fortymile Canyon composite units 1–3; mFCCU, modified Fluorspar Canyon confining unit; mFCCU1-3, modified Fortymile Canyon confining units 1–3; mLPCU, modified Lower Paintbrush confining unit; mMPCU, modified Middle Paintbrush confining unit; mRMCM, modified Rainier Mesa composite unit; mRMWTA1–2, modified Rainier Mesa welded-tuff aquifers1–2; mTCA, modified Tiva Canyon aquifer; mTSA, modified Topopah Spring aquifer; mUPCU, modified Upper Paintbrush confining unit; ft, foot; <, less than]

Modified HSU	Specific yield/Specific storage		Number of wells screened in modified HSUs		
	Geometric mean	Standard deviation	Observation wells	Background wells	Prior-information wells
Specific yield					
Layer 1[1]	0.02	0.01	0	0	0
Specific storage (1/10^6 feet)					
mFCCM1	0.04	0.4	1	0	0
mFCCU1	1	0.3	0	0	0
mFCCM2	0.7	0.6	2	0	0
mFCCU2	1	0.3	0	0	0
mFCCM3	0.06	0.2	1	0	0
mFCCU3	1	0.2	0	0	0
mRMWTA1	0.02	0.1	1	0	2
mRMWTA2	0.6	0.4	4	0	0
mRMCM	1	0.2	0	0	0
mFCCU	1	0.1	0	0	1
mCPA	1	2	7	0	0
mUPCU	0.03	0.1	0	0	1
mMPCU	0.5	0.4	0	0	0
mTCA	0.9	1	6	1	1
mLPCU	0.04	0.1	0	0	1
mTSA	1	2	6	0	0
mCHLFA1	1	0.4	1	0	0
mCHLFA5	0.1	0.5	3	3	5
mCHZCM	1	1	2	0	3
mCFCM	0.08	0.1	0	0	4
mCCU	1	0.2	0	0	0
Total			34	4	18

[1] Specific yield (fraction) was estimated for all model cells in layer 1, regardless of modified HSU.

than hydraulic-conductivity distributions. Similarities among pumping-well transmissivity estimates from the integrated groundwater-flow model and single-well aquifer tests provided support for the simulated-transmissivity distribution (fig. 26; tables 5, 12). Simulated-transmissivity estimates at the pumping well were determined by sampling a representative radial volume of the aquifer around the pumping well. The volume of aquifer sampled in the integrated groundwater-flow model affected transmissivity estimates, but not greatly. For example, a test of scale-dependence of transmissivity estimates around the ER-20-8 well site showed computed estimates ranged between 68,000 and 35,000 ft^2/d for sampling radii between 500 and 2,000 ft (fig. 27). The simulated range in transmissivity estimates around the *ER-20-8* well and the single-well aquifer-test estimate of 100,000 ft^2/d (table 5) differed by less than a factor of 3. These are relatively small differences for hydraulic-property estimates.

Transmissivity estimates from the integrated groundwater-flow model (table 12) and single-well aquifer tests (table 5) agreed within an average factor of 2 and had a coefficient of determination of 0.92 (fig. 26). At *ER-20-11 main*, integrated groundwater-flow model-based transmissivity was more than twice that estimated by the single-well aquifer-test analysis (11,000 and 5,000 ft^2/d, respectively; tables 5, 12). The

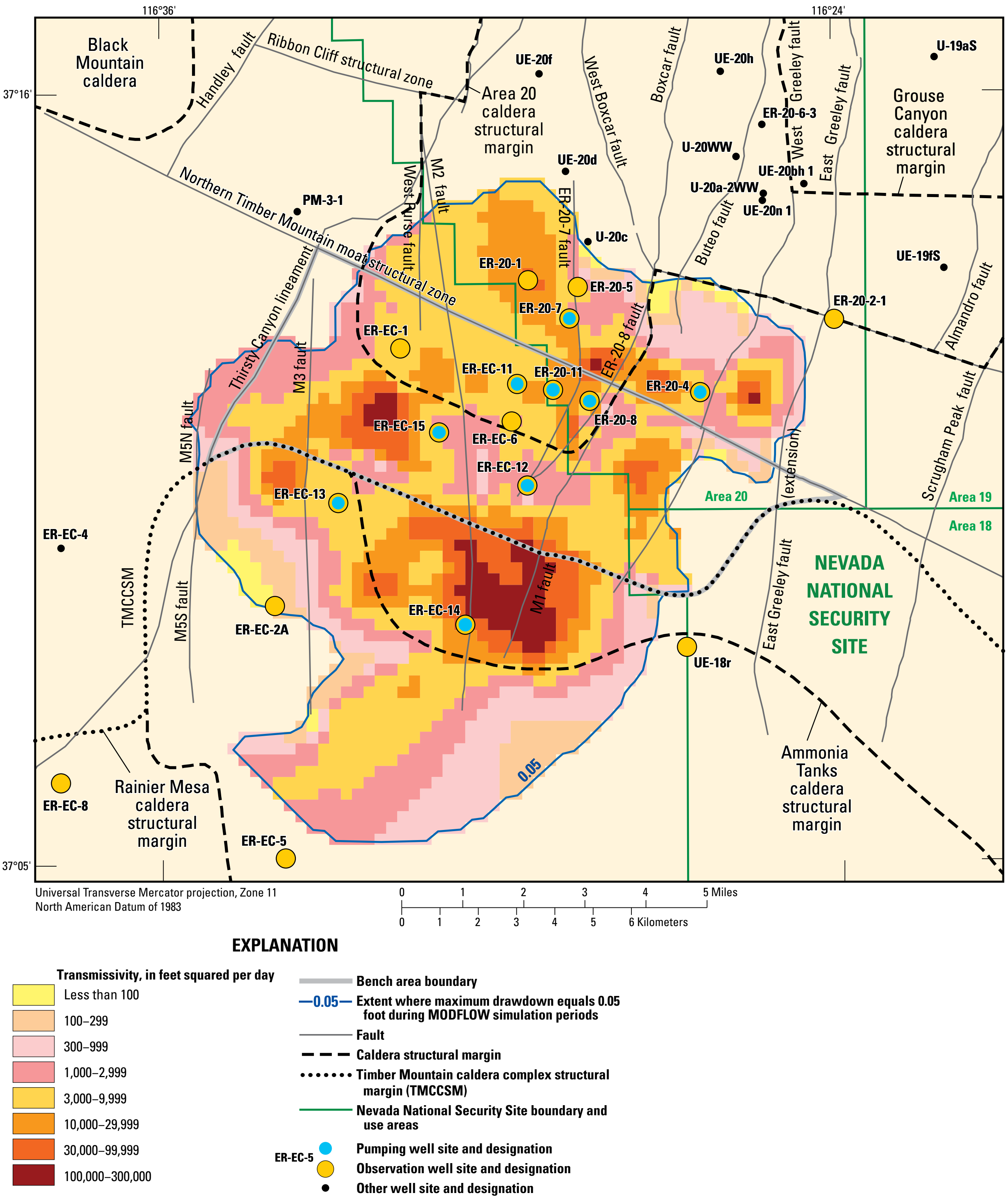

Figure 25. Simulated-transmissivity distribution from the integrated groundwater-flow model in the area investigated by the 16 multiple-well aquifer tests, Pahute Mesa, Nevada National Security Site and vicinity.

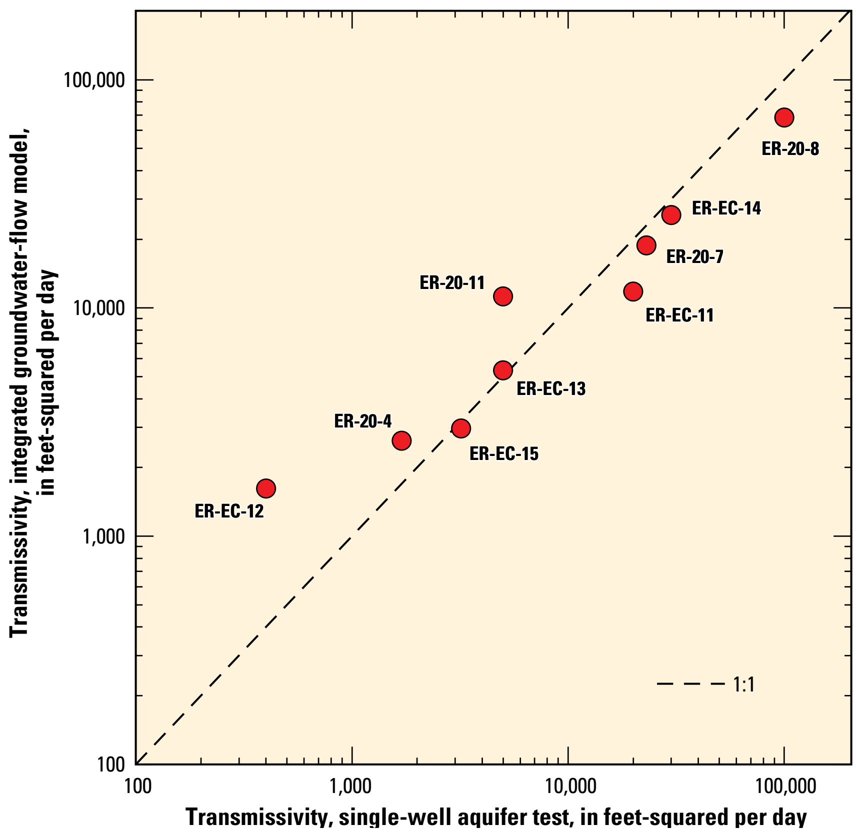

Figure 26. Comparison between transmissivity estimates determined from single-well aquifer tests and the integrated groundwater-flow model within a sampling radius of 500 feet, Pahute Mesa, Nevada National Security Site and vicinity.

single-well aquifer-test analysis assumed a homogeneous cynlindrical volume of aquifer was sampled during aquifer testing (Cooper and Jacob, 1946), whereas the simulated multiple-well aquifer-test analysis incorporated a heterogeneous distribution of transmissivity across the entire depth distribution of the HSUs surrounding the ER-20-11 well site. The method used to numerically compute transmissivity could bias estimates high if deeper HSUs (sufficiently below the well) are transmissive.

Transmissivity estimates in the area investigated (greater than or equal to 0.05 ft of drawdown) varied spatially from less than 100 to 250,000 ft^2/d (fig. 25). Transmissivity estimates were greatest north of the ER-EC-14 well site near the TMCCSM that borders the southern end of the bench (fig. 25). Just north of the TMCCSM, faulted and displaced rhyolitic lava flows, ash-flow tuffs, and welded tuffs in the bench abut the TMCCSM to the south. High-transmissivity estimates in the TMCC could be the result of highly fractured rock along the structural margins of the Rainier Mesa and Ammonia Tanks caldera complexes (fig. 2), where collapse of the structural dome formed steep, unstable slopes and rubble zones along the structural margin.

High-transmissivity zones are also in and just north of the bench area. In the northeast part of the bench near ER-20-8 and ER-20-11 well sites and north of the bench near the ER-20-7 well site, transmissivities ranged from about 5,000 to 100,000 ft^2/d. Bench well sites and *ER-20-7* are separated by the NTMMSZ, where rhyolitic lava flows, ash-flow tuffs, and welded tuffs in the bench have vertical displacements of more than 1,000 ft from their respective bedding planes north of the NTMMSZ. High-transmissivity estimates could be the result of rubble zones along the structural margin.

Transmissivity estimates around well sites (fig. 25) that are hydraulically connected to multiple pumping wells (fig. 10) are the most reliable. Model-estimated transmissivities at ER-20-7 and ER-20-5 well sites north of the NTMMSZ, at all well sites between the NTMMSZ and TMCCSM, and at ER-EC-13 and ER-EC-14 well sites in the TMCC are considered reliable and representative of multiple-well aquifer tests. Transmissivity around well site ER-EC-11 totaled 12,000 ft^2/d (table 12) and distributions among mHSUs near the well site likely are reliable because drawdown was detected in that area during 11 of the 16 aquifer tests (tables 6, 12; fig. 10).

Estimated transmissivities surrounding well sites were greatest near the NTMMSZ south of the ER-20-7 well site and in the TMCC near the ER-EC-14 well site (table 12; fig. 25). The mCHLFA5 contributes to the bulk of the transmissivity estimated near the NTMMSZ, whereas the mRMWTA exclusively contributes to the transmissivity estimated at the ER-EC-14 well site.

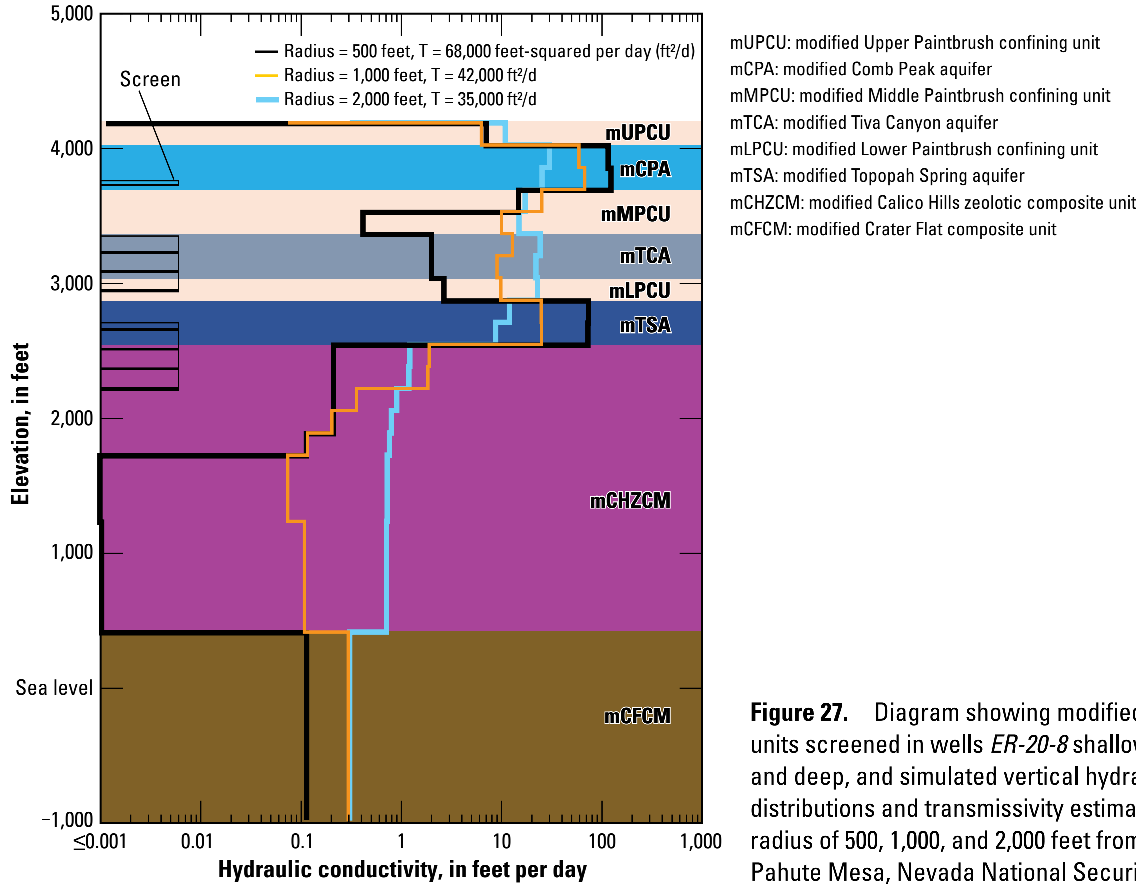

Figure 27. Diagram showing modified hydrostratigraphic units screened in wells *ER-20-8* shallow, intermediate, and deep, and simulated vertical hydraulic-conductivity distributions and transmissivity estimates within a sampling radius of 500, 1,000, and 2,000 feet from the ER-20-8 well site, Pahute Mesa, Nevada National Security Site.

Table 12. Simulated transmissivity estimates for modified hydrostratigraphic units within a 500-foot radius observation- and pumping-well sites.

[**mCFCM**, modified Calico Hills composite unit; **mCHLFA1,5**, comprises modified Calico Hills lava-flow aquifers 1 and 2 (mCHLFA1 and mCHLFA5); **mCHZCM**, modified Calico Hills zeolitic composite unit; **mCPA**, modified Comb Peak aquifer; **mFCCM**, comprises all modified Fortymile Canyon composite (mFCCM1-3) and confining units (mFCCU1-3); **mFCCU**, modified Fluorspar Canyon confining unit; **mLPCU**, modified Lower Paintbrush confining unit; **mMPCU**, modified Middle Paintbrush confining unit; **mRMWTA**, comprises all modified Rainier Mesa welded-tuff aquifers (mRMWTA1-2); **mTCA**, modified Tiva Canyon aquifer; **mTSA**, modified Topopah Spring aquifer; **mUPCU**, modified Upper Paintbrush confining unit; ft²/d, feet-squared per day; <, less than]

Well sites	Modified hydrostratigraphic units and associated transmissivity (ft²/d)												Total transmissivity (ft²/d)
	mFCCM	mRMWTA	mFCCU	mCPA	mUPCU	mMPCU	mTCA	mLPCU	mTSA	mCHLFA1,5	mCHZCM	mCFCM	
ER-20-1	—	—	—	—	100	—	200	1,100	—	36,000	3,700	1,200	42,000
ER-20-4	—	—	—	—	—	—	—	—	—	1,600	—	1,000	2,600
ER-20-5	—	—	—	—	—	—	—	100	200	3,400	1,200	200	5,100
ER-20-7	—	—	—	—	—	—	—	300	5,300	11,000	1,000	1,100	19,000
ER-20-8	—	—	—	39,000	1,200	2,500	700	400	24,000	—	200	200	68,000
ER-20-8-2	—	—	—	39,000	100	2,100	5,000	2,200	25,000	—	900	800	75,000
ER-20-11	—	—	1,100	1,400	500	—	1,200	200	1,200	—	4,600	1,100	11,000
ER-EC-1	—	—	<100	500	<100	—	300	100	100	—	3,700	3,000	7,700
ER-EC-2A	200	—	—	—	—	—	—	—	—	—	—	—	200
ER-EC-6	—	—	<100	12,000	<100	—	100	<100	100	—	400	300	13,000
ER-EC-11	—	—	100	1,100	100	—	1,000	700	3,700	—	3,600	1,400	12,000
ER-EC-12	—	—	200	—	—	—	400	100	<100	—	100	800	1,600
ER-EC-13	5,300	—	—	—	—	—	—	—	—	—	—	—	5,300
ER-EC-14	—	26,000	—	—	—	—	—	—	—	—	—	—	26,000
ER-EC-15	—	—	400	1,500	100	—	100	<100	<100	—	400	500	3,000

Heterogeneity in the estimated transmissivity distribution reflects observed drawdown responses between pumping- and observation-well pairs during aquifer testing. The transmissivity distribution in the area defined by ER-EC-11, ER-20-11, ER-20-8, and ER-EC-6 well sites likely is the most certain, because drawdown from at least seven aquifer tests was detected in this area, and wells are separated by 0.6–1.2 mi (figs. 10, 25; table 6). In the area defined by ER-EC-1, ER-EC-12, ER-EC-13, ER-EC-14, and ER-EC-15 well sites that fall along the TMCCSM, the transmissivity distribution was less certain because fewer wells were in close proximity to one another. Hydraulic connections identified between TMCC and bench area wells indicated transmissive pathways occur across the TMCCSM; however, the wide separation of pumping- and observation-well pairs (1.7–4.7 mi) precluded identification of a definitive transmissivity distribution across the TMCCSM. Because few pumping- and observation-well pairs exist, additional pairs could yield similar model results with different distributions of the more transmissive areas.

Hydraulic Characterization of Volcanic Rocks

Single- and multiple-well aquifer-test analyses in combination with the Phase II HFM provided a comprehensive dataset for hydraulically characterizing volcanic rocks beneath Pahute Mesa. Hydraulic connections across structural features indicated structures neither impede nor divert flow. Pumping signals propagated across nearly all structural features between pumping- and observation-well pairs, including the NTMMSZ; TMCCSM; Area 20 and Ammonia Tanks caldera structural margins; and ER-20-7, ER-20-8, M2, and M3 faults (fig. 10). Distances of 2 mi or more separated pumping and observation wells straddling the Boxcar, West Greeley, and East Greeley faults and limited hydraulic interpretation of these structures.

Inconsistencies between mapped extents of HSUs defined in the Phase II HFM and hydraulic responses from aquifer testing in the TMCC indicate undifferentiated HSU hydraulic properties are vertically heterogeneous. The massive FCCM and RMWTA units of the Phase II HFM were divided into multiple, laterally extensive mHSUs to enable accurate simulation of observed responses from aquifer testing and to differentiate hydraulic properties among shallow and deep intervals. Furthermore, the CHZCM HSU in the Phase II HFM was divided into shallow and deep units (mCHLFA5 and mCHZCM), where the shallow part of the CHZCM was combined with CHLFA2–5 to provide a laterally continuous transmissive unit (mCHLFA5). The mHSUs markedly improved simulation results by allowing the integrated model to simulate high- and low-permeability intervals at depth. Unrealistically low specific-storage estimates in mFCCM1, mFCCM2, and mFCCM3 units (3×10^{-9}–1×10^{-6} 1/ft) indicated that thin, permeable intervals likely exist within some of the thick mHSUs.

Heterogeneous hydraulic-property distributions and radial signal propagation from aquifer tests indicated that hydraulic distinctions among most mHSUs are limited. Estimated ranges of hydraulic conductivities in mHSUs characterized as aquifers, composite units, and confining units frequently overlapped and typically spanned 2 or more orders of magnitude. Geometric-mean hydraulic-conductivity estimates for 10 mHSUs in the area investigated were within an order of magnitude, from 0.2 to 2 ft/d, indicating that most mHSUs characterized by the integrated groundwater-flow model were hydraulically similar. Exceptions included the permeable and laterally extensive mCPA and mRMWTA2, where the estimated geometric-mean hydraulic conductivities were 2 ft/d or more, and the less-permeable mCCU, where the estimated geometric-mean hydraulic conductivity was 0.002 ft/d (fig. 24). Overlapping hydraulic-conductivity distributions among mHSUs support radial signal propagation observed from multiple-well aquifer tests, rather than preferential signal propagation through more permeable units or structures. Hydraulic-property estimates and observed drawdowns between pumping- and observation-well pairs indicated that regions with significant variability of hydraulic conductivity exist throughout most mHSUs beneath Pahute Mesa.

Simulated total transmissivities were largely insensitive to the differences between HSUs and modified HSUs constituting the Phase II HFM and the modified HFM, which made transmissivity estimates relatively unique with respect to hydraulic-conductivity estimates. Distinct areas of lower and higher than average transmissivity were identified in the area investigated, where simulated drawdown exceeded 0.05 ft. The simulated geometric-mean transmissivity was 500 ft^2/d in the investigated area. Low transmissivities of less than 1,000 ft^2/d were simulated between well sites ER-EC-6, ER-EC-12, and ER-EC-15. A relatively transmissive feature was simulated between well sites ER-EC-1 and ER-EC-13, where transmissivities generally exceeded 10,000 ft^2/d.

Although structures do not attenuate flow, rubble zones along structural features, such as the NTMMSZ or TMCCSM, could have increased volcanic-rock transmissivities near the structure. Transmissivity estimates from single-well aquifer tests and the integrated groundwater-flow model ranged from about 6,000 to 250,000 ft^2/d within about 5 miles of the NTMMSZ (tables 5, 9, 12; fig. 25), whereas estimates more than 7 miles south of the NTMMSZ ranged from less than 20 to about 3,000 ft^2/d. Transmissivity estimates along the TMCCSM commonly ranged from 10,000 to 250,000 ft^2/d. Greater transmissivities near the NTMMSZ and TMCCSM could indicate that volcanic rocks have more secondary porosity and permeability in the vicinity of these structures due to large rubble zones formed by more than 1,000 ft of vertical rock displacement.

More than 90 percent of the transmissivity in the area investigated was within 2,000 ft of the water table. Transmissive intervals, locally, can be deeper, such as at the ER-EC-11 well site, where 70 percent of the transmissivity was between 1,000 and 3,000 ft below the water table.

Summary

Accurate hydraulic characterization of volcanic rocks beneath Pahute Mesa is needed to constrain hydraulic properties used in groundwater-flow and contaminant-transport models at the Nevada National Security Site. An integrated analysis of 16 multiple-well aquifer tests was used to estimate hydraulic properties of volcanic rocks beneath Pahute Mesa, Nevada National Security Site. A cumulative volume of 63 million gallons was pumped during these aquifer tests, and drawdown was observed in a network of 34 wells. Transmissivity estimates from single-well aquifer-test analyses at the 16 pumped wells and water-level drawdown observations from more than 200 pumping- and observation-well pairs were interpreted numerically to obtain hydraulic-property estimates across a well network composed of pumping, observation, and background wells. The integrated, numerical analysis of multiple aquifer tests provides a consistent set of hydraulic-property estimates where investigated areas of individual tests overlap.

Transmissivity estimates from single-well aquifer-test interpretations ranged from 0.1 ft^2/d at *ER-EC-12 intermediate* to about 100,000 ft^2/d at *ER-20-8 deep*. Several analysis methods were applied to obtain transmissivity estimates, the most common of which was the Cooper and Jacob (1946) approach. Transmissivities of 10,000 ft^2/d or greater were estimated in five wells, but all estimates are uncertain because drawdowns were small and unclear relative to water-level changes owing to thermal expansion of the water column, barometric-pressure fluctuations, and tidal effects. Despite the uncertainties, single-well aquifer-test derived transmissivity estimates represent a first approximation of formation hydraulic properties.

Water-level drawdowns (greater than 0.05 ft) in observation wells were detected at lateral distances of up to 3.2 miles from pumping wells. Pumping signals propagated across major faults, caldera structural margins, and within and between structural blocks, indicating that structures in the study area neither impede nor divert groundwater flow. Drawdown observations between pumping- and observation-well pairs were estimated using analytical water-level models, where measured water levels in observation wells were simulated using environmental water-level fluctuations and Theis (1935) models of aquifer-test pumping signals. Drawdown was computed as the summation of all Theis models and residuals of measured and analytically simulated water levels. Observed drawdown ranged from 0.05 ft in distant observation wells to 2.42 ft in observation wells at the pumping-well site. A 0.05 ft drawdown detection limit was applied to characterize drawdown as detected or ambiguous.

Pumping signals from *ER-EC-14 main* were detected farther than any other aquifer test. The greatest distance at which drawdown was detected was between *ER-EC-14 main* and observation wells *ER-EC-15 deep*, *intermediate*, and *shallow*. These pumping- and observation-well pairs penetrate distinct structural blocks that are separated by the northern margin of the TMCC. A small (within 0.04 ft), but well-defined drawdown signal was observed at *ER-EC-5* in response to pumping in *ER-EC-14 main*, indicating the *ER-EC-14 main* pumping signal might have been detected for nearly 5 miles in the TMCC.

Consistent hydraulic properties were estimated by simultaneously calibrating an integrated groundwater-flow model (MODFLOW) to responses from all 16 aquifer tests using the PEST parameter estimation program. Simultaneous interpretation was necessitated because many aquifer tests interfered with and interrogated the same volumes of aquifer. The integrated groundwater-flow model is composed of 11 groundwater-flow models—1 model for each aquifer-test well site. A modified version of the Phase II Pahute Mesa-Oasis Valley hydrostratigraphic framework model (HFM) comprising individual modified hydrostratigraphic units (mHSUs) was used in each groundwater-flow model to distribute hydraulic properties. The integrated model was calibrated to analytically derived drawdown observations obtained from water-level models, and hydraulic-property estimates were constrained by transmissivity estimates obtained from single-well aquifer-test analyses.

Most mHSUs evaluated were hydraulically similar in the area investigated by the 16 multiple-well aquifer tests, where simulated drawdown exceeded 0.05 ft. Hydraulic-conductivity distributions in the mHSUs typically spanned between more than 2 and more than 4 orders of magnitude. Ranges of hydraulic conductivity in mHSUs overlapped greatly among many mHSUs. The mCPA and mRMWTA2 were the most permeable mHSUs and had geometric-mean hydraulic conductivities of 2 ft/d or more. The least permeable mHSUs included the mCCU, mLPCU, mRMWTA1, and mUPCU, where geometric-mean hydraulic conductivities were 0.1 ft/d or less.

Transmissivities geometrically averaged 1,000 ft^2/d in the area investigated, and the distribution was characterized by distinct areas of lower and higher than average transmissivity. An area of lower transmissivity is in the central bench, where transmissivities were less than 1,000 ft^2/d between well sites ER-EC-6, ER-EC-12, and ER-EC-15. Zones of greater transmissivity bound this area in all directions, most notably to the west and east. Relatively high transmissive features exist along the NTMMSZ, TMCCSM, and between ER-EC-1 and ER-EC-13 well sites, which have transmissivities generally exceeding 10,000 ft^2/d. Greater transmissivities along the NTMMSZ and TMCCSM indicated that rubble zones near the structural margins likely contribute to increased permeability of the formations. The simulated-transmissivity distribution was largely insensitive to the differences between HSUs and modified HSUs constituting the Phase II HFM and the modified HFM; therefore, transmissivity estimates are considered more robust than hydraulic-conductivity estimates. The most reliable transmissivity estimates were those derived near well sites that are hydraulically connected to multiple pumping wells.

References Cited

Barker, J.A., 1988, A generalized radial flow model for hydraulic tests in fractured rock: Water Resources Research, v. 24, no. 10, p. 1796–1804.

Bechtel Nevada, 2002, A hydrostratigraphic model and alternatives for the groundwater flow and contaminant transport model of Corrective Action Units 101 and 102—Central and western Pahute Mesa, Nye County, Nevada: U.S. Department of Energy Report DOE/NV/11718—706, 383 p.

Belcher, W.R., Elliott, P.E., and Geldon, A.L., 2001, Hydraulic-property estimates for use with a transient ground-water flow model of the Death Valley regional ground-water flow system, Nevada and California: U.S. Geological Survey Water-Resources Investigations Report 01–4210, 34 p., *http://pubs.er.usgs.gov/publication/wri014210*.

Belcher, W.R., Sweetkind, D.S., and Elliott, P.E., 2002, Probability distributions of hydraulic conductivity for the hydrogeologic units of the Death Valley regional groundwater flow system, Nevada and California: U.S. Geological Survey Water-Resources Investigations Report 02–4212, 24 p., *http://pubs.usgs.gov/wri/wrir024212/*.

Blankennagel, R.K., and Weir, J.E., Jr., 1973, Geohydrology of the eastern part of Pahute Mesa, Nevada Test Site, Nye County, Nevada: U.S. Geological Survey Professional Paper 712–B, 35 p., *http://pubs.usgs.gov/pp/0712b/report.pdf*.

Bouwer, H., and Rice, R.C., 1976, A slug test method for determining hydraulic conductivity of unconfined aquifers with completely or partially penetrating wells: Water Resources Research, v. 12, no. 3, p. 423–428.

Byers, F.M., Jr., Carr, W.J., Christiansen, R.L., Lipman, P.W., Orkild, P.P., and Quinlivan, W.D., 1976a, Geologic map of the Timber Mountain caldera area, Nye County, Nevada: U.S. Geological Survey Miscellaneous Investigations Series Map I–891, scale 1:48,000, 10-p. text.

Byers, F.M., Jr., Carr, W.J., Orkild, P.P., Quinlivan, W.D., and Sargent, K.A., 1976b, Volcanic suites and related cauldrons of the Timber Mountain-Oasis Valley caldera complex, southern Nevada: U.S. Geological Survey Professional Paper 919, 70 p.

Byers, F.M., Jr., Carr, W.J., and Orkild, P.P., 1989, Volcanic centers of southwestern Nevada— Evolution of understanding, 1960–1988: Journal of Geophysical Research, v. 94, no. B5, p. 5,908–5,924.

Carr, W.J., Byers, F.J., Jr., and Orkild, P.P., 1986, Stratigraphic and volcano-tectonic relations of Crater Flat Tuff and some older volcanic units, Nye County, Nevada: U.S. Geological Survey Professional Paper 1323, 28 p.

Cooper, H.H., and Jacob, C.E., 1946, A generalized graphical method for evaluating formation constants and summarizing well field history: American Geophysical Union Transactions, v. 27, p. 526–534.

Day, W.C., Dickerson, R.P., Potter, C.J., Sweetkind, D.S., San Juan, C.A., Drake, R.M., II, and Fridrich, C.J., 1998, Bedrock geologic map of the Yucca Mountain area, Nye County, Nevada: U.S. Geological Survey Geologic Investigations Series I–2627, scale 1:24,000, 1 pl., 21 p.

Dickerson, R.P., and Drake, R.M., II, 1998, Geologic map of the Paintbrush Canyon area, Yucca Mountain, Nevada: U.S. Geological Survey Open-File Report 97–783, scale 1:6,000, 2 pl., 25 p.

Doherty, J., 2016, PEST: Model-independent parameter estimation, User Manual Part I: PEST, SENSAN, and Global Optimisers (6th ed.): Brisbane, Australia, Watermark Numerical Computing, 366 p., *http://www.pesthomepage.org/Downloads.php*.

Doherty, J., 2015, Groundwater Data Utilities, Part A: Overview: Brisbane, Australia, Watermark Numerical Computing, 68 p., *http://www.pesthomepage.org/Downloads.php*.

Domenico, P.A., and Mifflin, M.D., 1965, Water from low-permeability sediments and land subsidence: Water Resources Research, v. 1, no. 4, p. 563–576.

Dougherty, D.E., and Babu, D.K., 1984, Flow to a partially penetrating well in a double-porosity reservoir: Water Resources Research, v. 20, no. 8, p. 1116–1122.

Elliot, P.E., and Fenelon, J.M., 2010, Database of groundwater levels and hydrograph descriptions for the Nevada Test Site area, Nye County, Nevada, 1941–2010: U.S. Geological Survey Data Series 533, 16 p., *http://pubs.usgs.gov/ds/533/*.

Fenelon, J.M., 2000, Quality assurance and analysis of water levels in wells on Pahute Mesa and vicinity, Nevada Test Site, Nye County, Nevada: U.S. Geological Survey Water-Resources Investigations Report 00–4014, 68 p., *http://pubs.usgs.gov/wri/WRIR00-4014/*.

Fenelon, J.M., Sweetkind, D.S., and Laczniak, R.J., 2010, Groundwater flow systems at the Nevada Test Site, Nevada: A synthesis of potentiometric contours, hydrostratigraphy, and geologic structures: U.S. Geological Survey Professional Paper 1771, 54 p., 6 pls.

Fenelon, J.M., Halford, K.J., and Moreo, M.T. 2016, Delineation of the Pahute Mesa–Oasis Valley groundwater basin, Nevada: U.S. Geological Survey Scientific Investigations Report 2015–5175, 40 p., *http://doi.org/10.3133/sir20155175*.

Ferguson, J.F., Cogbill, A.H., and Warren, R.G., 1994, A geophysical-geological transect of the Silent Canyon caldera complex, Pahute Mesa, Nevada: Journal of Geophysical Research, v. 99, no. B3, p. 4,323–4,339.

Fienen, M.N., Muffels, C.T., and Hunt, R.J., 2009, On constraining pilot point calibration with regularization in PEST: Ground Water, v. 47, no. 6, p. 835–844.

Garcia, C.A., Halford, K.J., and Laczniak, R.J., 2010, Interpretation of flow logs from Nevada Test Site boreholes to estimate hydraulic conductivity using numerical simulations constrained by single-well aquifer tests: U.S. Geological Survey Scientific Investigations Report 2010–5004, 28 p.

Garcia, C.A., Fenelon, J.M., Halford, K.J., Reiner, S.R., and Laczniak, R.J., 2011, Assessing hydraulic connections across a complex sequence of volcanic rocks—Analysis of U-20 WW multiple-well aquifer test, Pahute Mesa, Nevada National Security Site, Nevada: U.S. Geological Survey Scientific Investigations Report 2011–5173, 24 p.

Garcia, C.A., Halford, K.J., and Fenelon, J.M., 2013, Detecting drawdowns masked by environmental stresses with water-level models: Groundwater, v. 51, no. 3, p. 322–332.

Geofirma Engineering Ltd. and INTERA, Inc., 2011, nSIGHTS version 2.50 user manual, Austin, Tex: INTERA, Inc.

Grauch, V.J.S., Sawyer, D.A., Fridrich, C.J., and Hudson, M.R., 1999, Geophysical frame-work of the southwestern Nevada volcanic field and hydrogeologic implications: U.S. Geological Survey Professional Paper 1608, 39 p.

Graves, R., 2002a, Aquifer-test report for Test Well U-20a-2: U.S. Geological Survey Aquifer-Test Package, available at 'Nevada Water Science Center Aquifer Tests' webpage, accessed August 18, 2014, at *http://nevada.usgs.gov/water/aquifertests/nts_singlewell_U-20a-2.cfm?studyname=nts_singlewell_U-20a-2*.

Graves, R., 2002b, Aquifer-test report for Test Well *UE-19fS*: U.S. Geological Survey Aquifer-Test Package, available at 'Nevada Water Science Center Aquifer Tests' webpage, accessed August 18, 2014, at *http://nevada.usgs.gov/water/aquifertests/nts_singlewell_UE-19fs.cfm?studyname=nts_singlewell_UE-19fs*.

Graves, R., 2002c, Aquifer-test report for Test Well *UE-20f*: U.S. Geological Survey Aquifer-Test Package, available at 'Nevada Water Science Center Aquifer Tests' webpage, accessed August 18, 2014, at *http://nevada.usgs.gov/water/aquifertests/nts_singlewell_UE-20f.cfm?studyname=nts_singlewell_UE-20f*.

Halford, K.J., 2006, Documentation of a spreadsheet for time-series analysis and drawdown estimation: U.S. Geological Survey Scientific Investigations Report 2006–5024, 48 p., *http://pubs.usgs.gov/sir/2006/5024/PDF/SIR2006-5024.pdf*.

Halford, K.J, and Hanson, R.T., 2002, User guide for the drawdown-limited, multi-node well (MNW) package for the U.S. Geological Survey's modular three-dimensional finite-difference ground-water flow model, versions MODFLOW-96 and MODFLOW-2000: Sacramento, Calif.: U.S. Geological Survey Open-File Report 02–293, 39 p.

Halford, K.J., and Yobbi, D.K., 2006, Estimating hydraulic properties using a moving-model approach and multiple aquifer tests: Groundwater, v. 44, no. 2, p. 284–291.

Halford, K.J., Garcia, C.A., Fenlon, J.M., and Mirus, B.B., 2012, Advanced methods for modeling water-levels and estimating drawdowns with SeriesSEE, an Excel add-in: U.S. Geological Survey Techniques and Methods Report, 4-F4. Reston, Virginia: USGS.

Hantush, M.S., and Jacob, C.E., 1955, Nonsteady radial flow in an infinite leaky aquifer: Eos Transactions American Geophysical Union, v. 36, no. 1, p. 95–100.

Harbaugh, A.W., Banta, E.R., Hill, M.C., and McDonald, M.G., 2000, MODFLOW–2000, the U.S. Geological Survey modular ground-water model—User guide to modularization concepts and the ground-water flow process: U.S. Geological Survey Open-File Report 00–92, 121 p.

Kilroy, K.C., and Savard, C.S., 1995, Geohydrology of Pahute Mesa-3 test well, Nye County, Nevada: U.S. Geological Survey Water Resources Investigations Report 95–4239, 37 p.

Laczniak, R.J., Cole, J.C., Sawyer, D.A., and Trudeau, D.A., 1996, Summary of hydrogeologic controls on ground-water flow at the Nevada test site: U.S. Geological Survey Water-Resources Investigations Report 96–4109, 59 p.

Lohman, S.W., 1972, Definitions of selected ground-water terms—Revisions and conceptual refinements: U.S. Geological Survey Water-Supply Paper 1988, 21 p., *http://pubs.usgs.gov/wsp/wsp_1988/*.

Mankinen, E.A., Hildenbrand, T.G., Dixon, G.L., McKee, E.H., Fridrich, C.J., and Laczniak, R.J., 1999, Gravity and magnetic study of the Pahute Mesa and Oasis Valley region, Nye County, Nevada: U.S. Geological Survey Open-File Report 99–303, 57 p.

McKee, E.H., Phelps, G.A., and Mankinen, E.A., 2001, The Silent Canyon Caldera—A three-dimensional model as part of a Pahute Mesa—Oasis Valley, Nevada, hydrogeologic model: U.S. Geological Survey Open-File Report 01–297, 23 p.

Moench, A.F., 1984, Double-porosity models for a fissured groundwater reservoir with fracture skin, Water Resources Research, v. 20, no. 7, p. 831–846.

Morris, D.A., and Johnson, A.I., 1967, Summary of hydrologic and physical properties of rock and soil materials as analyzed by the Hydrologic Laboratory of the U.S. Geological Survey, U.S. Geological Survey Water-Supply Paper 1839–D, 42 p.

National Oceanic and Atmospheric Administration, 2015, Nevada National Security Site Daily Precipitation Totals: Air Resources Laboratory/Special Operations and Research Division, January 8, 2014, accessed July 7, 2015, at *http://www.sord.nv.doe.gov/PrecipitationPage.php*.

Neuman, S.P., 1975, Analysis of pumping test data from anisotropic unconfined aquifers considering delayed gravity response: Water Resources Research, v. 11, no. 2, p. 329–342.

Oberlander, P.L, McGraw, D., and Russell, C.E., 2007, Final report, hydraulic conductivity with depth for underground test area (UGTA) wells: Desert Research Institute Publication 45228, 237 p.

Orkild, P.P., Sargent, K.A., and Snyder, R.P., 1969, Geologic map of Pahute Mesa, Nevada test site and vicinity, Nye County, Nevada: U.S. Geological Survey Miscellaneous Geologic Investigations Map I–567, scale 1:48,000.

Pawloski, G.A., Thompson, A.F.B., and Carle, S.F., 2001, Evaluation of the hydrologic source term from underground nuclear tests on Pahute Mesa at the Nevada test site—the CHESHIRE Test: Lawrence Livermore National Laboratory UCRL–ID–147023, 504 p.

Pawloski, G.A., Wurtz, J., Drellack, S.L., 2010, The Underground Test Area Project of the Nevada Test Site: building confidence in groundwater flow and transport models at Pahute Mesa through focused characterization studies: LLNL–CONF–422250, 14 p.

Prothro, L.B., and Drellack, S.L., Jr., 1997, Nature and extent of lava-flow aquifers beneath Pahute Mesa, Nevada Test Site: U.S. Department of Energy Report DOE/NV/11718–156, 50 p.

Prothro, L.B., Drellack, S.L., Jr., and Mercadante, J.M., 2009, A hydrostratigraphic system for modeling groundwater flow and radionuclide migration at the Corrective Action Unit scale, Nevada Test Site and surrounding areas, Clark, Lincoln, and Nye Counties, Nevada: U.S. Department of Energy Report DOE/NV/25946–630, 145 p.

Prudic, D.E., 1991, Estimates of hydraulic conductivity from aquifer-test analyses and specific-capacity data, Gulf Coast Regional Aquifer Systems, south-central United States: U.S. Geological Survey Water-Resources Investigations Report 90–4121, 38 p.

RamaRao, B.S., de Marsily, G., and Marietta, M.G., 1995, Pilot point methodology for automated calibration of an ensemble of conditionally simulated transmissivity fields: 1. Theory and computational experiments: Water Resources Research, v. 31, no. 3, p. 475–493.

Renard, P., 2005, The future of hydraulic tests: Hydrogeology Journal, v. 13, p. 259–262.

Risser, D.W., and Bird, P.H., 2003, Aquifer tests and simulation of ground-water flow in Triassic sedimentary rocks near Colmar, Bucks and Montgomery Counties, Pennsylvania: Reston, Va., U.S. Geological Survey Water-Resources Investigations Report 2003–4159, 73 p.

Sawyer, D.A., and Sargent, K.A., 1989, Petrologic evolution of divergent peralkaline magmas from the Silent Canyon caldera complex, southwestern Nevada volcanic field: Journal of Geophysical Research, v. 94, no. B5, p. 6,021–6,040.

Sawyer, D.A., Fleck, R.J., Lanphere, M.A., Warren, R.G., Broxton, D.E., and Hudson, M.R., 1994, Episodic caldera volcanism in the Miocene southwestern Nevada volcanic field—Revised stratigraphic framework, 40Ar/39Ar geochronology, and implications for magmatism and extension: Geological Society of America Bulletin, v. 106, p. 1,304–1,318.

Slate, J.L., Berry, M.E., Rowley, P.D., Fridrich, C.J., Morgan, K.S., Workman, J.B., Young, O.D., Dixon, G.L., Williams, V.S., McKee, E.H., Ponce, D.A., Hildenbrand, T.G., Swadley, W.C., Lundstrom, S.C., Ekren, E.B., Warren, R.G., Cole, J.C., Fleck, R.J., Lanphere, M.A., Sawyer, D.A., Minor, S.A., Grunwald, D.J., Laczniak, R.J., Menges, C.M., Yount, J.C., and Jayko, A.S., 1999, Digital geologic map of the Nevada Test Site and vicinity, Nye, Lincoln, and Clark Counties, Nevada, and Inyo County, California, Revision 4: U.S. Geological Survey Open-File Report 99–554–A, 53 p., scale 1:120,000.

Stoller-Navarro Joint Venture, 2009, Phase I transport model of Corrective Action Units 101 and 102: Central and Western Pahute Mesa, Nevada Test Site, Nye County, Nevada: Las Vegas, Nev. Stoller-Navarro Joint Venture, S-N/99205–111, Rev. 1, 643 p., *http://www.osti.gov/scitech/servlets/purl/948559*.

Theis, C.V., 1935, The relation between the lowering of the piezometric surface and the rate and duration of discharge of a well using groundwater storage: American Geophysical Union, v. 16, p. 519–524.

Thomasson, H.G., Jr., Olmsted, F.H., and LeRoux, E.F., 1960, Geology, water resources, and usable ground-water storage capacity of part of Solano County, California: U.S. Geological Survey Water-Supply Paper 1464, 693 p., *http://pubs.er.usgs.gov/publication/wsp1464*.

U.S. Department of Energy, Nevada Operations Office, 1997, Regional groundwater flow and tritium transport modeling and risk assessment of the Underground Test Area, Nevada Test Site, Nevada: LasVegas, Nev., U.S. Department of Energy Report DOE/NV–477. p.

U.S. Department of Energy, 2000, Completion report for well cluster *ER-EC-6*: U.S. Department of Energy Report DOE/NV/11718-360, 98 p., *http://www.osti.gov/scitech/servlets/purl/758400*.

U.S. Department of Energy, 2002a, Completion report for well *ER-EC-2A*: U.S. Department of Energy Report DOE/NV/11718–591. 18 p., *http://www.osti.gov/scitech/servlets/purl/793382*.

U.S. Department of Energy, 2002b, Analysis of well *ER-EC-8* testing, western Pahute Mesa—Oasis Valley FY 2000 Testing Program: U.S. Department of Energy Report DOE/NV/13052—179, 185 p., *http://www.osti.gov/scitech/servlets/purl/1184217*.

U.S. Department of Energy, 2002c, Analysis of well *ER-EC-5* testing, western Pahute Mesa—Oasis Valley FY 2000 Testing Program: U.S. Department of Energy Report DOE/NV/13052—848, 187 p., *http://www.osti.gov/scitech/servlets/purl/1186686*.

U.S. Department of Energy, 2002d, Analysis of Well *ER-18-2* testing, western Pahute Mesa—Oasis Valley FY 2000 Testing Program: U.S. Department of Energy Report DOE/NV/13052—845, 102 p., *http://www.osti.gov/scitech/servlets/purl/1184216*.

U.S. Department of Energy, 2002e, Analysis of well *ER-EC-6* testing, western Pahute Mesa—Oasis Valley FY 2000 Testing Program: U.S. Department of Energy Report DOE/NV/13052—849, 176 p., *http://www.osti.gov/scitech/servlets/purl/1186687*.

U.S. Department of Energy, 2002f, Analysis of well *ER-EC-2A* testing, western Pahute Mesa—Oasis Valley FY 2000 Testing Program: U.S. Department of Energy Report DOE/NV/13052—851, 185 p., *http://www.osti.gov/scitech/servlets/purl/1186783*.

U.S. Department of Energy, 2002g, Analysis of well *ER-EC-7* testing, western Pahute Mesa—Oasis Valley FY 2000 Testing Program: U.S. Department of Energy Report DOE/NV/13052—852, 175 p., *http://www.osti.gov/scitech/servlets/purl/1185231*.

U.S. Department of Energy, 2009, Phase II corrective action investigation plan for Corrective Action Units 101 and 102—Central and western Pahute Mesa, Nevada Test Site, Nye County, Nevada: U.S. Department of Energy Report DOE/NV–1312, Rev. 2, 255 p., *http://www.osti.gov/scitech/servlets/purl/968999-LMnj7f/*.

U.S. Department of Energy, 2010a, Completion report for well *ER-20-7*, Corrective Action Units 101 and 102—Central and Western Pahute Mesa: U.S. Department of Energy Report DOE/NV–1386, 126 p., *http://www.osti.gov/scitech/servlets/purl/977585*.

U.S. Department of Energy, 2010b, Completion report for well *ER-EC-11*, Corrective Action Units 101 and 102—Central and Western Pahute Mesa: U.S. Department of Energy Report DOE/NV–1435, 146 p., *http://www.osti.gov/scitech/servlets/purl/1003755*.

U.S. Department of Energy, 2011, Pahute Mesa well development and testing analyses for wells *ER-20-7*, *ER-20-8 #2*, and *ER-EC-11*: U.S. Department of Energy Report DOE/NV–Rev. 1, 163 p., *http://www.osti.gov/scitech/servlets/purl/1031914*.

U.S. Department of Energy, 2012, Pahute Mesa well development and testing analyses for wells *ER-20-8* and *ER-20-4*, Nevada National Security Site, Nye County, Nevada: U.S. Department of Energy Report DOE/NV–Final, Rev. 0, 170 p., *http://www.osti.gov/scitech/servlets/purl/1052206*.

U.S. Department of Energy, 2013, Completion report for well *ER-EC-14*, Corrective Action Units 101 and 102—Central and Western Pahute Mesa: U.S. Department of Energy Report DOE/NV–1448, 156 p., *http://www.osti.gov/scitech/servlets/purl/1067490*.

U.S. Department of Energy, 2015, Pahute Mesa well development and testing analyses for wells *ER-EC-14* and *ER-EC-15*, Nevada National Security Site, Nye County, Nevada: U.S. Department of Energy Report DOE/NV–Final, Rev. 0, 179 p.

U.S. Geological Survey, 2015, Aquifer tests: Carson City, Nev., U.S. Geological Survey, Nevada Water Science Center, accessed June 14, 2015, at *http://nevada.usgs.gov/water/aquifertests/index.htm*.

Vogel, T.A., Noble, D.C., and Younker, L.W., 1989, Evolution of a chemically zoned magma body—Black Mountain volcanic center, southwestern Nevada: Journal of Geophysical Research, v. 94, no. B5, p. 6,041–6,058.

Walton, W.C., 2008, Upgrading aquifer test analysis: Ground Water Technical Commentary, v. 46, no. 5, p. 660–662.

Warren, R.G., Cole, G.L., and Walther, D., 2000, A structural block model for the three-dimensional geology of the southwestern Nevada volcanic field: Los Alamos National Laboratory Report LA–UR–00–5866, 83 p.

Winograd, I.J., Thordarson, W., and Young, R.A., 1971, Hydrology of the Nevada Test Site and vicinity, southeastern Nevada: U.S. Geological Survey Open-file Report, 429 p.

Wolfsberg, A., Glascoe, L., Lu, G., Olson, A., Lichtner, P., McGraw, M., Cherry, T., and Roemer, G., 2002, TYBO/BENHAM—model analysis of groundwater flow and radionuclide migration from underground nuclear tests in southwestern Pahute Mesa, Nevada: Los Alamos National Laboratory Report LA–13977, 490 p.

Wood, D.B., 2009, Digitally available interval-specific rock-sample data compiled from historical records, Nevada Test Site and vicinity, Nye County, Nevada (ver. 2.0): U.S. Geological Survey Data Series 297, 56 p., 6 digital appendixes.

Yager, R.M., Maurer, D.K., and Mayers, C.J., 2012, Assessing potential effects of changes in water use with a numerical groundwater-flow model of Carson Valley, Douglas County, Nevada, and Alpine County, California: U.S. Geological Survey Scientific Investigations Report 2012–5262, 73 p.

Yobbi, D.K., and Halford, K.J., 2008, Numerical simulation of aquifer tests, west-central Florida (revised): U.S. Geological Survey Scientific Investigations Report 2005–5201, 85 p., *http://pubs.usgs.gov/sir/2005/5201/*.

Appendix 1. Well Construction of and Hydrostratigraphic Units Penetrated by Pumping and Observation Wells Monitored during Multiple-Well Aquifer Testing at Pahute Mesa, Nevada National Security Site, 2009–14

Appendix 2. Maximum Observed Drawdown Datasets and Observed Drawdown Hydrographs for each Pumping- and Observation-Well Pair for the 16 Multiple-Well Aquifer Tests at Pahute Mesa, 2009–2014

Maximum observed drawdown datasets including maximum observed drawdown, root-mean-square error (RMSE), signal-to-noise ratio, drawdown-detection classification, and associated remarks for pumping- and observation-well pairs are tabulated in a comma-separated values (.csv) file. Column headers are described in the workbook. Drawdown hydrographs include observed pumping-induced drawdown in observation wells, measured and analytically simulated water levels in observation wells and residual differences between the two, pumping-well discharge rates, and RMSE for all pumping- and observation-well pairs.

Appendix 2 data files are available for download at *https://doi.org/10.3133/sir20165151*.

Appendix 3. Hydrographs Comparing Simulated and Observed Drawdown for each Pumping- and Observation-Well Pair for the 16 Multiple-Well Aquifer Tests at Pahute Mesa, 2009–2014, and Mapped Hydraulic-Property Distributions for each Modified Hydrostratigraphic Unit

Drawdown hydrographs include simulated and observed pumping-induced drawdown in observation wells. Observed drawdowns are presented as raw observations and 6-hour averages of observations (denoted as “measured” in hydrographs). Hydrographs also include pumping-well discharge rates, sum of squares (ss) errors for weighted and unweighted drawdown observations in the objective function (see “Parameter Estimation” section), and root-mean square (rms) errors describing the fit between observed and simulated drawdown for all pumping- and observation-well pairs. Hydrographs are are organized as portable document format (.pdf) files by pumping well.

Hydraulic property distributions including hydraulic conductivity, specific yield and specific storage, and transmissivity are presented as maps (.pdf) and are provided for each modified hydrostratigraphic unit. Distributions are organized by hydraulic property.

Appendix 3 data files are available for download at *https://doi.org/10.3133/sir20165151*.

For additional information, contact:

Director, Nevada Water Science Center
U.S. Geological Survey
2730 N. Deer Run Rd.
Carson City, NV 89701

http://nevada.usgs.gov/

Garcia and others—**Hydraulic Characterization of Volcanic Rocks in Pahute Mesa Using an Integrated Analysis of 16 Multiple-Well Aquifer Tests, Nevada National Security Site, 2009–14**—SIR 2016-5151

ISSN 2328-0328 (online)
https://doi.org/10.3133/sir20165151